2

Combustion Fundamentals

To understand the formation of pollutants in combustion systems, we must first understand the nature of the fuels being burned, the thermodynamics of the combustion process, and some aspects of flame structure. In this chapter we discuss fundamental aspects of hydrocarbon fuel combustion that relate directly to the formation of pollutants or to the control of emissions. Questions of flame stability, detonations, and several other important aspects of combustion science are beyond the scope of the present discussion and will not be treated. Specific pollution control problems will be addressed in detail in later chapters.

2.1 FUELS

Of the spectrum of fuels currently in widespread use, the simplest in composition is natural gas, which consists primarily of methane but includes a number of other constituents as well. The compositions of other gaseous fuels are generally more complex, but they are, at least, readily determined. Table 2.1 illustrates the range of compositions encountered in gaseous fuels, both natural and synthetic.

Information on the composition of liquid or solid fuels is generally much more limited than that for gaseous fuels. Rarely is the molecular composition known since liquid fuels are usually complex mixtures of a large number of hydrocarbon species. The most commonly reported composition data are derived from the *ultimate analysis*, which consists of measurements of the elemental composition of the fuel, generally presented as mass fractions of carbon, hydrogen, sulfur, oxygen, nitrogen, and ash, where appro-

TABLE 2.1 PROPERTIES OF GASEOUS FUELS

	CH_4	C_2H_6	C_3H_8	Other hydrocarbons	CO	H_2	H_2S	N_2	CO_2	Heating value[a] (10^6 J m^{-3})
Natural gas										
No. 1	77.7	5.6	2.4	1.8	—	—	7.0	—	—	—
No. 2[b]	88.8	6.4	2.7	2.0	—	—	0.0004	—	0	41.9
No. 3	59.2	12.9	—	—	—	—	—	0.7	26.2	30.7
No. 4	99.2	—	—	—	—	—	—	0.6	0.2	36.3
Refinery gas										
No. 1	41.6	20.9	19.7	15.6	—	—	2.2	—	—	68.6
No. 2	4.3	82.7	13.0	—	—	—	—	—	—	67.1
No. 3	15.9	5.0	—	2.4	14.3	50.9	—	8.4	2.2	18.7
Coke oven gas	—	—	—	35.3	6.3	53.0	—	3.4	1.8	21.5
Blast furnace gas	—	—	—	—	26.2	3.2	—	57.6	13	3.4

[a] p, 101 kPa; T, 25°C.

[b] "Sweetened," H_2S removed.

TABLE 2.2 PROPERTIES OF TYPICAL LIQUID FUELS

Gasoline	Percent by weight					Ash	Specific gravity	Heating value (10^6 J kg^{-1})
	C	H	N	O	S			
Kerosene (No. 1)	86.5	13.2	0.1	0.1	0.1	Trace	0.825	46.4
Fuel oil								
No. 2	86.4	12.7	0.1	0.1	0.4–0.7	Trace	0.865	45.5
No. 4	85.6	11.7	0.3	0.4	<2	0.05	0.953	43.4
No. 6	85.7	10.5	0.5	0.4	<2.8	0.08	0.986	42.5

priate. The heating value, a measure of the heat release during complete combustion, is also reported with the ultimate analysis. Ultimate analyses of a number of liquid fuels are presented in Table 2.2.

In addition to the limited composition data given in Tables 2.1 and 2.2, physical properties that influence the handling and use of a particular fuel are frequently measured. For liquid fuels, the specific gravity or API gravity,* viscosity (possibly at several temperatures), flash point (a measure of the temperature at which the fuel is sufficiently volatile to ignite readily), and distillation profiles (fraction vaporized as a function of temperature) may be reported.

The properties of solid fuels vary even more widely than those of liquid fuels. The most common solid fuel is coal. Formed by biological decomposition and geological transformation of plant debris, coals are classified by rank, a measure of the degree to which the organic matter has been transformed from cellulose. Low-rank fuels such as peat or lignite have undergone relatively little change, whereas high-rank anthracite is nearly graphitic in structure. Low-rank fuels contain large amounts of volatile matter that are released upon heating. High-rank fuels contain much more *fixed carbon*, which remains after the volatiles are released.

Solid fuels are characterized by the ultimate analysis and by the so-called *proximate analysis*, which identifies the degree of coalifaction of a solid fuel (Table 2.3). Coal samples that have been air dried are subjected to a number of standardized tests to determine the amount of *moisture* inherent to the coal structure, the quantity of *volatile matter* released by the coal upon heating to 1200 K for several minutes, and the mass of *ash* or noncombustible inorganic (mineral) impurities that remains after low temperature (700 to 1050 K) oxidation. The difference between the initial mass of coal and the sum of masses of moisture, volatile matter, and ash is called *fixed carbon*. The conditions of these standardized tests differ markedly from typical combustion environments, and the values reported in the proximate analysis do not necessarily represent yields actually encountered in practical combustors. This point is discussed in more detail in the section on solid fuel combustion.

*Degrees API = [141.5/(specific gravity 16°C/water at 16°C) − 131.5].

TABLE 2.3 PROPERTIES OF SELECTED SOLID FUELS

Fuel (state)	Percent by weight									Heating value (10^6 J kg^{-1})
	Proximate analysis				Ultimate analysis					
	Carbon	Volatile matter	Moisture	Ash	C	H	N	O	S	
Meta-anthracite (RI)	65.3	2.5	13.3	18.9	64.2	0.4	0.2	2.7	0.3	21.7
Anthracite (PA)	77.1	3.8	5.4	13.7	76.1	1.8	0.6	1.8	0.6	27.8
Semianthracite (PA)	78.9	8.4	3.0	9.7	80.2	3.3	1.1	2.0	0.7	31.3
Bituminous (PA)	70.0	20.5	3.3	6.2	80.7	4.5	1.1	2.4	1.8	33.3
High-volatile bituminous										
(PA)	58.3	30.3	2.6	9.1	76.6	4.9	1.6	3.9	1.3	31.7
(CO)	54.3	32.6	1.4	11.7	73.4	5.1	1.3	6.5	0.6	30.7
(KY)	45.3	37.7	7.5	9.5	66.9	4.8	1.4	6.4	3.5	28.1
(IL)	39.1	40.2	12.1	8.6	12.8	4.6	1.0	6.6	4.3	26.7
Subbituminous (CO)	45.9	30.5	19.6	4.0	58.8	3.8	1.3	12.2	0.3	23.6
Lignite (ND)	30.8	28.2	34.8	6.2	42.4	2.8	0.7	12.4	0.7	16.8
Brown coal (Australia)	15.3	17.7	66.3	0.7					0.1	8.6
Wood (Douglas fir, as received)	17.2	82.0	35.9	0.8	52.3	6.3	0.1	40.5	0	21.0

2.2 COMBUSTION STOICHIOMETRY

Complete oxidation of simple hydrocarbon fuels forms carbon dioxide (CO_2) from all of the carbon and water (H_2O) from the hydrogen, that is, for a hydrocarbon fuel with the general composition C_nH_m,

$$C_nH_m + \left(n + \frac{m}{4}\right)O_2 \longrightarrow nCO_2 + \frac{m}{2}H_2O$$

Even in the idealized case of complete combustion, the accounting of all species present in combustion exhaust involves more than simply measuring the CO_2 and H_2O. Since fuels are burned in air rather than in pure oxygen, the nitrogen in the air may participate in the combustion process to produce nitrogen oxides. Also, many fuels contain elements other than carbon, and these elements may be transformed during combustion. Finally, combustion is not always complete, and the effluent gases contain unburned and partially burned products in addition to CO_2 and H_2O.

Air is composed of oxygen, nitrogen, and small amounts of carbon dioxide, argon, and other trace species. Since the vast majority of the diluent in air is nitrogen, for our purposes it is perfectly reasonable to consider air as a mixture of 20.9% (mole basis) O_2 and 79.1% (mole basis) N_2. Thus for every mole of oxygen required for combustion, 3.78 mol of nitrogen must be introduced as well. Although nitrogen may not significantly alter the oxygen balance, it does have a major impact on the thermodynamics, chemical kinetics, and formation of pollutants in combustion systems. For this reason it is useful to carry the "inert" species along in the combustion calculations. The stoichiometric relation for complete oxidation of a hydrocarbon fuel, C_nH_m, becomes

$$C_nH_m + \left(n + \frac{m}{4}\right)(O_2 + 3.78N_2) \longrightarrow nCO_2 + \frac{m}{2}H_2O + 3.78\left(n + \frac{m}{4}\right)N_2$$

Thus for every mole of fuel burned, $4.78(n + m/4)$ mol of air are required and $4.78(n + m/4) + m/4$ mol of combustion products are generated. The molar *fuel/air* ratio for stoichiometric combustion is $1/[4.78(n + m/4)]$.

Gas compositions are generally reported in terms of mole fractions since the mole fraction does not vary with temperature or pressure as does the concentration (moles/unit volume). The product mole fractions for complete combustion of this hydrocarbon fuel are

$$y_{CO_2} = \frac{n}{4.78(n + m/4) + m/4}$$

$$y_{H_2O} = \frac{m/2}{4.78(n + m/4) + m/4}$$

$$y_{N_2} = \frac{3.78(n + m/4)}{4.78(n + m/4) + m/4}$$

The large quantity of nitrogen diluent substantially reduces the mole fractions of the combustion products from the values they would have in its absence.

Example 2.1 ***Combustion of Octane in Air***

Determine the stoichiometric fuel/air mass ratio and product gas composition for combustion of octane (C_8H_{18}) in air.

The overall stoichiometry is

$$C_8H_{18} + 12.5(O_2 + 3.78N_2) \longrightarrow 8CO_2 + 9H_2O + 47.25N_2$$

For each mole of fuel burned, 59.75 mol of air is required. The molecular weight of octane is 114. The fuel/air mass ratio for stoichiometric combustion is, therefore,

$$\left(\frac{m_f}{m_a}\right)_s = \frac{114}{12.5(32 + 3.78 \times 28)} = \frac{114}{1723} = 0.0662$$

The total number of moles of combustion products generated is

$$8 + 9 + 47.25 = 64.25$$

Finally, the product gas composition is, on a mole fraction basis,

$$y_{CO_2} = \frac{8}{64.25} = 0.125 = 12.5\%$$

$$y_{H_2O} = \frac{9}{64.25} = 0.140 = 14.0\%$$

$$y_{N_2} = \frac{47.25}{64.25} = 0.735 = 73.5\%$$

Minor components and impurities in the fuel complicate our analysis of combustion products somewhat. Fuel sulfur is usually oxidized to form sulfur dioxide (SO_2). (Even though there are cases where sulfur compounds involving higher oxidation states of sulfur or reduced sulfur compounds are produced, it is a reasonable first approximation to assume that all of the fuel sulfur forms SO_2.) Upon combustion, organically bound fuel-nitrogen is converted to both N_2 and NO, with molecular nitrogen generally dominating. For the moment we shall assume that all of the fuel-nitrogen forms N_2. Ash, the noncombustible inorganic (mineral) impurities in the fuel, undergoes a number of transformations at combustion temperatures, which will also be neglected for the time being, so that the ash will be assumed to be inert.

For most common fuels, the only chemical information available is its elemental composition on a mass basis, as determined in the ultimate analysis. Before we can proceed with combustion calculations it is necessary to convert these data to an effective molar composition.

Example 2.2 ***Coal Composition***

Consider a Pittsburgh seam coal that contains 77.2% C, 5.2% H, 1.2% N, 2.6% S, 5.9% O, and 7.9% ash by weight. The ultimate analysis is generally reported on an "as received" basis, including the moisture in the chemical analysis. The molar composition may be de-

termined by dividing each of the mass percentages by the atomic weight of the constituent. For convenience in stoichiometric calculations, the composition is then normalized with respect to carbon:

Element	wt %	mol/100 g	mol/mol C
C	77.2 ÷ 12	= 6.43	÷ 6.43 = 1.00
H	5.2 ÷ 1	= 5.20	÷ 6.43 = 0.808
N	1.2 ÷ 14	= 0.0857	÷ 6.43 = 0.013
S	2.6 ÷ 32	= 0.0812	÷ 6.43 = 0.013
O	5.9 ÷ 16	= 0.369	÷ 6.43 = 0.057
Ash	7.9		÷ 6.43 = 1.23 g/mol C

The chemical formula that can be used to describe this particular coal is, thus,

$$CH_{0.808}N_{0.013}S_{0.013}O_{0.057}$$

The formula weight of the fuel, or, as written here, the mass per mole of carbon, including ash, is

$$M_f = \frac{100}{6.43}\frac{g}{\text{mol C}} = 15.55\,\frac{g}{\text{mol C}}$$

The combustion stoichiometry of this fuel must include the minor species, ash, and oxygen in the fuel. Making the simplifying assumptions described above, we may write the stoichiometry as

$$CH_{0.808}N_{0.013}S_{0.013}O_{0.057} + \alpha(O_2 + 3.78N_2) \longrightarrow CO_2 + 0.404H_2O + 0.013SO_2 + (3.78\alpha + 0.0065)N_2$$

where

$$\alpha = 1 + \frac{0.808}{4} + 0.013 - \frac{0.057}{2} = 1.19$$

The fuel/air mass ratio for stoichiometric combustion is

$$\left(\frac{m_f}{m_a}\right)_s = \frac{15.55\ \text{g/mol C}}{1.19(32 + 3.78 \times 28)\ \text{g/mol C}} = 0.0948$$

The total number of moles of gaseous combustion products per mole of C is

$$N_T = 1 + 0.404 + 0.013 + 4.504 = 5.921$$

The species mole fractions in the combustion products are, therefore,

$$y_{CO_2} = \frac{1}{5.921} = 0.169 = 16.9\%$$

$$y_{H_2O} = \frac{0.404}{5.921} = 0.068 = 6.82\%$$

$$y_{SO_2} = \frac{0.013}{5.921} = 0.00220 = 2200 \text{ ppm}$$

$$y_{N_2} = \frac{4.504}{5.921} = 0.761 = 76.1\%$$

where the SO_2 mole fraction has been expressed as parts per million (ppm) on a mole (or volume) basis, a common form for presenting data on minor species in the gas (recall Section 1.3).

Few combustion systems are operated precisely at the stoichiometric condition because of the difficulty of achieving such intimate mixing between fuel and air that perfect conversion is attained. More commonly, combustors are operated with a margin for error using more than the stoichiometric amount of air. The *fuel/air ratio* is used to define the operating conditions of a combustor. Comparison of the two examples presented above shows that the fuel/air ratio required for complete combustion varies with fuel composition. Values of the fuel/air and air/fuel mass ratios for stoichiometric combustion of a variety of fuels are presented in Table 2.4. Because the mass ratios vary widely with fuel composition, they are not a convenient base for comparison of systems burning different fuels.

The stoichiometric condition is a logical reference point for comparison of systems operating on different fuels. Several normalized ratios are used in the combustion literature to overcome the ambiguity of the mass ratio. The *equivalence ratio*, ϕ, is defined as the fuel/air ratio normalized with respect to the stoichiometric fuel/air ratio,

$$\phi = \frac{m_f/m_a}{(m_f/m_a)_s} \tag{2.1}$$

Alternatively, the stoichiometric ratio, λ, is the air/fuel ratio normalized with respect to stoichiometric, that is,

$$\lambda = \frac{m_a/m_f}{(m_a/m_f)_s} = \frac{1}{\phi} \tag{2.2}$$

Other ratios that appear in the literature include the percent excess air [$EA = (\lambda - 1) \times 100\%$] and the percent theoretical air ($TA = \lambda \times 100\%$). In reading the combustion

TABLE 2.4 MASS RATIOS FOR STOICHIOMETRIC COMBUSTION

Fuel	Molar H/C ratio	$(m_f/m_a)_s$	$(m_a/m_f)_s$
H_2	∞	0.029	34
CH_4	4	0.058	17
Kerosene C_nH_{2n}	2	0.068	15
Benzene (coke)	1	0.076	13
Char	0.5	0.081	12
Carbon	0	0.087	11
Methanol CH_3OH	4	0.093	10.8

literature, one should be careful to ascertain which of the various terms is being used since neither names nor symbols have been fully standardized. The fuel/air equivalence ratio, ϕ, will be used in this book unless otherwise stated.

The mix of combustion products varies with the equivalence ratio. Combustion may be complete under fuel-lean conditions (excess air, $\phi < 1$) with some oxygen remaining unreacted in the combustion products. The composition of the products of fuel-lean combustion is, to a good approximation, determined by atom balances alone. Consider, for example, the combustion of methane at $\phi = 0.85$,

$$CH_4 + \frac{2}{0.85}(O_2 + 3.78N_2) \longrightarrow CO_2 + 2H_2O + \left(\frac{2}{0.85} - 2\right)O_2 + \frac{2 \times 3.78}{0.85} N_2$$

$$\longrightarrow CO_2 + 2H_2O + 0.353O_2 + 8.89N_2$$

The composition of the combustion products now includes O_2:

$$y_{CO_2} = \frac{1}{12.24} = 0.0817 = 8.17\%$$

$$y_{H_2O} = \frac{2}{12.24} = 0.163 = 16.3\%$$

$$y_{O_2} = \frac{0.353}{12.24} = 0.0288 = 2.88\%$$

$$y_{N_2} = \frac{8.89}{12.24} = 0.726 = 72.6\%$$

In some references, the combustion condition is not stated in terms of a fuel/air ratio but, rather, in terms of the amount of oxygen in the combustion products (i.e., 2.9% O_2 in this case).

The problem of specifying the products of combustion is more complicated for fuel-rich combustion, $\phi > 1$, than for fuel-lean combustion. Since there is insufficient oxygen for complete combustion under fuel-rich conditions, some carbon monoxide, hydrogen, and possibly, unburned hydrocarbons remain in the combustion products. Thus there are at least five products present (CO, CO_2, H_2, H_2O, N_2), but only four elemental balances are possible. An auxiliary condition based on thermodynamics or kinetics is needed to determine the exhaust composition. We now turn our attention to combustion thermodynamics before returning to the question of product gas composition in fuel-rich combustion.

2.3 COMBUSTION THERMODYNAMICS

Substantial energy is released in a very short time when a fuel is burned, leading to a dramatic temperature increase of the combustion gases. Temperatures in excess of 2000 K are common in flames. It is the high temperature that allows rapid oxidation of hy-

drocarbons and carbon monoxide to carbon dioxide and water but also makes possible the oxidation of N_2 to form nitric oxide. The temperature in the flame must be known to consider the formation and control of pollutants.

Thermodynamics provides us with good estimates of the flame temperature that are needed not only to assess the combustion process itself but also to calculate the concentrations of the many chemical species that play a role in the formation and destruction of pollutants. We begin our study of the combustion process with a brief review of the relevant thermodynamics.

2.3.1 First Law of Thermodynamics

The first law of thermodynamics states that the change in the total energy of a closed system of fixed mass and identity is equal to the heat transfer to the system from its surroundings minus the work done by the system on its surroundings; that is, for an infinitesimal change of state,

$$dE = \delta Q - \delta W \tag{2.3}$$

The total energy of the system, E, includes the internal energy, U, the kinetic energy, and the potential energy. The energy is a property of the system that is independent of the path taken in going from one state to another. In contrast, the heat transfer, δQ, and the work transfer, δW, for any change in the state of the system depend on the manner in which the state of the system is changed. The change in the system energy is described by a total differential, dE. Since the work and heat transfer depend on the path followed by the system, the δ is used to indicate that these increments are not total differentials. For most systems of concern here, the kinetic and potential energy terms can be neglected, so we may express the system energy in terms of the internal energy, that is,

$$dU = \delta Q - \delta W \tag{2.4}$$

Integrating over a finite change of state from state 1 to state 2, the first law for a closed system becomes

$$U_2 - U_1 = Q_{12} - W_{12} \tag{2.5}$$

Only rarely in the consideration of combustion processes can we limit ourselves to a fixed mass in a closed system. More generally, the fuel and air enter the combustion zone across certain boundaries, and combustion products are exhausted across other boundaries. It is convenient, therefore, to derive an expression for the change in state of a fixed volume in space, called a *control volume*, rather than a fixed mass.

A control volume may be defined in terms of any volume in space in which one has interest for a particular analysis. Figure 2.1 illustrates a control volume that is prescribed by a surface, S. We would like to derive an equation that describes the change in the properties of the control volume when a small increment of mass, δm, crosses S and enters the control volume. To do this, we first define a closed system that includes both the material initially in the control volume, mass m, energy E_1, and the increment of mass to be added, δm. The initial state of the combined system consists of the control

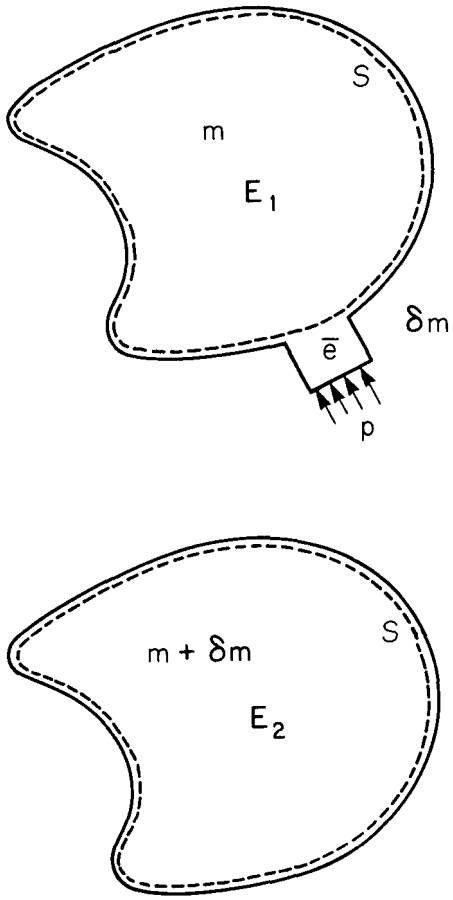

Figure 2.1 Schematic of mass addition to a control volume and related thermodynamic system. The control volume is enclosed by the dashed curve. The solid curve denotes the closed system.

volume with its initial mass and energy and the incremental mass. After δm is added, the mass in the control volume is $m + \delta m$, and the energy in the control volume is E_2. The first law for the change of state of the combined closed system may be written as

$$E_2 - (E_1 + \bar{e}\,\delta m) = Q_{12} + p\bar{v}\,\delta m - W_{x12}$$

where $\bar{e}$ denotes the energy/unit mass (called the mass specific energy) of δm, $\bar{v} = 1/\rho$ is the mass specific volume, $p\bar{v}\,\delta m$ is the work done on the combined system by the environment as the small volume is moved across the control volume surface, and W_x is any work other than that associated with that volume displacement. Overbars are used to denote mass specific properties. Rearranging, we find

$$E_2 - E_1 = \bar{e}\,\delta m + p\bar{v}\,\delta m + Q_{12} - W_{x12}$$

For a small increment of change of state, this becomes

$$dE = (\bar{e} + p\bar{v})\,\delta m + \delta Q - \delta W_x \tag{2.6}$$

The extension to a number of mass increments is straightforward: simply sum over all mass flows entering and leaving from the control volume, considering the relevant properties of each increment. The time rate of change of the energy in a control volume with a number of entering and exiting mass flows may then be written

$$\frac{dE}{dt} + \sum_{j,\text{out}} (\bar{e}_j + p\bar{v}_j)\bar{f}_j - \sum_{i,\text{in}} (\bar{e}_i + p\bar{v}_i)\bar{f}_i = Q - W_x \tag{2.7}$$

where $\bar{f}_j$ and $\bar{f}_i$ are the mass flow rates (mass per time) leaving or entering the control volume, Q is the rate of heat transfer to the system (energy per time), and W_x is the rate at which work is done by the system on its surroundings other than that associated with flows across the control volume boundary. As noted above, in the combustion applications of interest here we can generally neglect the kinetic and potential energy contributions to the total energy, giving

$$\frac{dU}{dt} = \sum_{i,\text{in}} \bar{f}_i\bar{h}_i - \sum_{j,\text{out}} \bar{f}_j\bar{h}_j + Q - W_x \tag{2.8}$$

where the mass specific enthalpy, $\bar{h}$, is defined as

$$\bar{h} = \bar{u} + p\bar{v} \tag{2.9}$$

The energy equation may also be written on a molar basis, that is,

$$\frac{du}{dt} = \sum_{i,\text{in}} f_i h_i - \sum_{j,\text{out}} f_j h_j + Q - W_x \tag{2.10}$$

where $h = u + pv$ denotes the molar specific enthalpy, and f_i is the molar flow rate of species i. We shall generally use the molar specific properties in our treatment of combustion systems.

Let us apply the foregoing to analyze the chemical reaction

$$aA + bB \longrightarrow cC + dD$$

occurring at steady state and constant pressure in the isothermal flow reactor illustrated in Figure 2.2. The feed and effluent flows are at their stoichiometric values.

Applying the steady-state form of (2.10) to this system gives

$$cfh_C(T_1) + dfh_D(T_1) - afh_A(T_1) - bfh_B(T_1) = Q$$

where no work is done by the combustion gases except that due to flows across the boundary, so $W_x = 0$. (The expansion work is already accounted for in the enthalpy.) The molar flow of A into the control volume is af, that of C is cf, and so on, and the temperature is T_1. Dividing through by f yields

$$ch_C(T_1) + dh_D(T_1) - ah_A(T_1) - bh_B(T_1) = \frac{Q}{f}$$

The heat transfer per mole that is required to maintain the process at a constant temperature, $T = T_1$, is called the *enthalpy of reaction*, and is given the symbol $\Delta h_r(T_1)$, that

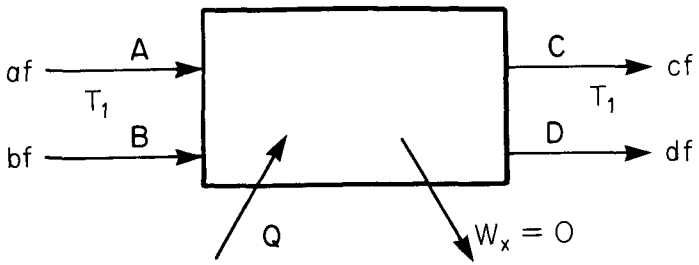

Figure 2.2 Isothermal steady flow reactor.

is,

$$\Delta h_r(T_1) = \frac{Q}{f} = ch_C(T_1) + dh_D(T_1) - ah_A(T_1) - bh_B(T_1) \qquad (2.11)$$

We see that the enthalpy of reaction is just the difference between the molar specific enthalpies of the products and reactants taking into account the stoichiometry of the reaction. To define the enthalpy of a species requires a reference state at which the enthalpy is taken to be zero. That reference state is arbitrary as long as a consistent reference state is used throughout the calculations. Generally, the reference temperature and pressure are taken to be $T_0 = 298$ K and $p_0 = 1$ atm $= 101$ kPa, respectively. It should be noted, however, that some sources report thermodynamic data relative to other reference temperatures or pressures. The chemical reference state is usually based on the pure elements in their predominant forms at T_0 and p_0, that is,

- C as solid graphite
- H as H_2 gas
- N as N_2 gas
- O as O_2 gas
- S as solid sulfur etc.

The enthalpy of a compound relative to the reference states of its constituent elements is the enthalpy of the reaction of these elemental species that form 1 mole of the compound. When evaluated for reactants and products at the same temperature, T, this quantity is called the *enthalpy of formation*. Thus the enthalpy of formation of water is the enthalpy of the reaction

$$H_2 + \tfrac{1}{2} O_2 \longrightarrow H_2O$$

namely

$$\Delta h^\circ_{f,H_2O}(T) = h_{H_2O}(T) - h_{H_2}(T) - \tfrac{1}{2} h_{O_2}(T)$$

The superscript $^\circ$ denotes evaluation with respect to the chemical reference state. By definition, the enthalpies of formation of the elemental reference compounds are zero,

that is,

$$\Delta h^\circ_{f,C_s} = \Delta h^\circ_{f,H_2} = \Delta h^\circ_{f,N_2} = \Delta h^\circ_{f,O_2} = 0$$

The enthalpy of a compound at any temperature may be written as the sum of the enthalpy of formation at the reference temperature and a sensible enthalpy term associated with the temperature change from the reference temperature to the desired temperature. Thus the enthalpy of species i at temperature T relative to the reference state is

$$h_i^\circ(T) = h_i(T) - h_i(T_0) + \Delta h_{fi}^\circ(T_0) \tag{2.12}$$

The sensible enthalpy term may be evaluated as an integral over temperature of the specific heat at constant pressure, $c_p = (\partial h/\partial T)_p$, that is,

$$h_i(T) - h_i(T_0) = \int_{T_0}^{T} c_{p,i}(T')\, dT' \tag{2.13}$$

The specific heat generally varies with temperature. If the range of temperature variation is large, as is commonly the case in combustion applications, one must account for the dependence of $c_{p,i}$ on temperature. For the present purposes, it is sufficient to approximate the specific heat as a linear function of temperature,

$$c_{p,i} \approx a_i + b_i T \tag{2.14}$$

This approximate form allows calculation of the sensible enthalpy over the range of temperatures commonly encountered in combustion calculations (i.e., 300 to 3000 K) within about 10%. Table 2.5 presents specific heats, enthalpies of formation, and additional data to which we shall refer later for species encountered in combustion problems. While the linear approximation to c_p is sufficient for present purposes, tabulations of thermodynamic data such as the *JANAF Thermochemical Tables* (Stull and Prophet, 1971) should be used, in general, for more precise calculations.

The first law of thermodynamics for a chemically reacting open system may now be written as

$$\frac{dU}{dt} + \sum_{j,\text{out}} f_j\left[h_j(T) - h_j(T_0) + \Delta h_{fj}^\circ(T_0)\right] - \sum_{i,\text{in}} f_i\left[h_i(T) - h_i(T_0) + \Delta h_{fi}^\circ(T_0)\right] = Q - W_x \tag{2.15}$$

If the chemical composition and thermodynamic properties of the fuel are known, (2.15) allows us to calculate temperature changes, heat transfer, or work performed in combustion systems.

As an example, consider a steady-flow furnace burning a stoichiometric methane–air mixture. The combustion reaction is

$$CH_4 + 2(O_2 + 3.78N_2) \longrightarrow CO_2 + 2H_2O + 7.56N_2$$

TABLE 2.5 APPROXIMATE THERMODYNAMIC DATA FOR SPECIES OF COMBUSTION INTEREST

Species	Name	$\Delta h_f°$(298 K) (J mol^{-1})	$s°$(298 K) (J mol^{-1} K^{-1})	$c_p = a + bT$ (J mol^{-1} K^{-1})	
				a	b
C	Carbon, monatomic	716,033	158.215	20.5994	0.00026
C(s)	Graphite (ref.)	0	5.694	14.926	0.00437
CH	Methylidine	594,983	183.187	27.6451	0.00521
CH_2	Methylene	385,775	181.302	35.5238	0.01000
CH_3	Methyl	145,896	194.337	42.8955	0.01388
CH_4	Methane	−74,980	186.413	44.2539	0.02273
CN	Cyano	435,762	202.838	28.2979	0.00469
CO	Carbon monoxide	−110,700	197.810	29.6127	0.00301
COS	Carbonyl sulfide	−138,605	231.804	47.6042	0.00659
CO_2	Carbon dioxide	−394,088	213.984	44.3191	0.00730
C_2H	CCH radical	447,662	207.615	40.4732	0.00880
C_2H_2	Acetylene	227,057	201.137	51.7853	0.01383
C_2H_4	Ethylene	52,543	219.540	60.2440	0.02637
C_2H_4O	Ethylene oxide	−52,710	243.272	70.1093	0.03319
C_2N_2	Cyanogen	309,517	241.810	63.7996	0.00913
H	Hydrogen, monatomic	218,300	114.773	20.7859	0
HCHO	Formaldehyde	−116,063	218.970	43.3037	0.01465
HCN	Hydrogen cyanide	135,338	202.000	38.9985	0.00885
HCO	Formyl	−12,151	245.882	37.3667	0.00766
HNO	Nitroxyl hydride	99,722	220.935	38.2143	0.00750
HNO_2	Nitrous acid, *cis*-	−76,845	249.666	54.0762	0.01100
HNO_2	Nitrous acid, *trans*-	−78,940	249.498	54.5058	0.01075
HNO_3	Nitric acid vapor	−134,499	266.749	68.1195	0.01549
HO_2	Hydroperoxyl	20,950	227.865	38.3843	0.00719
H_2	Hydrogen (ref.)	0	130.770	27.3198	0.00335
H_2O	Water vapor	−242,174	188.995	32.4766	0.00862
H_2O_2	Hydrogen peroxide	−136,301	232.965	41.6720	0.01952
H_2S	Hydrogen sulfide	−20,447	205.939	35.5142	0.00883
H_2SO_4	Sulfuric acid vapor	−741,633	289.530	101.7400	0.02143
H_2SO_4	Sulfuric acid liquid	−815,160	157.129	144.0230	0.02749
N	Nitrogen, monatomic	473,326	153.413	20.7440	0.00004
NH	Imidogen	339,392	181.427	28.0171	0.00349
NH_2	Amidogen	167,894	194.785	33.5349	0.00837
NH_3	Ammonia	−45,965	192.866	38.0331	0.01593
NO	Nitric oxide	90,421	210.954	30.5843	0.00278
NO_2	Nitrogen dioxide	33,143	240.255	43.7014	0.00575
NO_3	Nitrogen trioxide	71,230	253.077	61.1847	0.00932
N_2	Nitrogen (ref.)	0	191.777	29.2313	0.00307
N_2H	Diimide	213,272	218.719	43.2755	0.01466
N_2O	Nitrous oxide	82,166	220.185	44.9249	0.00693
N_2O_5	Dinitrogen pentoxide	11,313	346.933	122.4940	0.01018
O	Oxygen, monatomic	249,553	161.181	21.2424	−0.0002
OH	Hydroxyl	39,520	183.858	28.0743	0.00309
O_2	Oxygen (ref.)	0	205.310	30.5041	0.00349

TABLE 2.5 *(Continued)*

Species	Name	Δh_f°(298 K) (J mol^{-1})	s°(298 K) (J mol^{-1} K^{-1})	$c_p = a + bT$ (J mol^{-1} K^{-1})	
				a	b
O_3	Ozone	142,880	239.166	46.3802	0.00553
$S(g)$	Sulfur, gas	279,391	168.019	22.4619	−0.0004
$S(l)$	Sulfur, liquid	1,425	35.364	28.5005	0.00976
$S(s)$	Sulfur, solid (ref.)	0	31.970	13.9890	0.02191
SO_2	Sulfur dioxide	−297,269	248.468	45.8869	0.00574
SO_3	Sulfur trioxide	−396,333	256.990	62.1135	0.00877

The energy equation becomes

$$f_{CH_4}\Big\{\big[h(T_2) - h(T_0) + \Delta h_f^\circ(T_0)\big]_{CO_2} + 2\big[h(T_2) - h(T_0) + \Delta h_f^\circ(T_0)\big]_{H_2O} + 7.56\big[h(T_2) - h(T_0) + \Delta h_f^\circ(T_0)\big]_{N_2} - \big[h(T_1) - h(T_0) + \Delta h_f^\circ(T_0)\big]_{CH_4} - 2\big[h(T_1) - h(T_0) + \Delta h_f^\circ(T_0)\big]_{O_2} - 7.56\big[h(T_1) - h(T_0) + \Delta h_f^\circ(T_0)\big]_{N_2}\Big\} = Q - W_x = Q$$

where T_1 and T_2 are the temperatures of the reactants entering and the products leaving the furnace, respectively. W_x has been set equal to zero since we are dealing with a heat transfer system in which no work is performed. Using thermodynamic data for all of the chemical species involved, the heat transfer rate can readily be computed.

When the chemical composition of a fuel is not known, instead of using fundamental thermochemical data on the constituents, we must rely on the empirical characterization provided by the ultimate analysis. The enthalpy of the combustion reaction is readily measured using a calorimeter, such as the flow calorimeter illustrated schematically in Figure 2.3.

Fuel and air are introduced to the calorimeter at T_1 and p_1. The fuel is burned completely, and the products are cooled to T_1. The heat transfer required for this cooling is measured. Applying the first law, (2.8), at steady-state conditions in the absence of any work performed yields

$$\bar{f}_{\text{products}}\bar{h}^\circ_{\text{products}}(T_1) - \bar{f}_{\text{fuel}}\bar{h}^\circ_{\text{fuel}}(T_1) - \bar{f}_{\text{air}}\bar{h}^\circ_{\text{air}}(T_1) = Q_c - 0$$

We have used the first law on a mass rather than a molar basis to be consistent with the way enthalpies of combustion are commonly measured and reported, since if the molecular structure of the fuel is not known, we cannot uniquely define the enthalpy of reaction on a molar basis. The heat released per unit mass of fuel burned is, however, readily determined, so enthalpy of combustion data are commonly reported on a mass specific

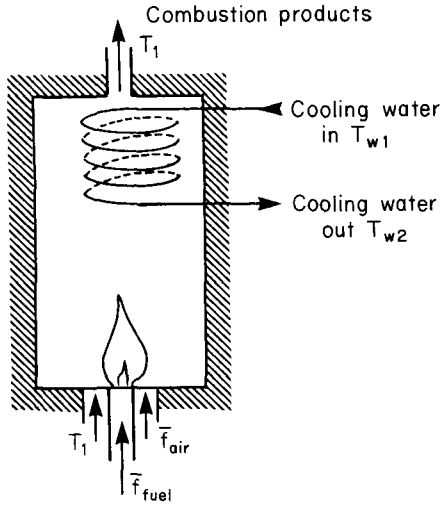

Figure 2.3 Flow calorimeter.

basis. We find the enthalpy of combustion of a unit mass of fuel

$$\Delta\bar{h}_c(T_1) = \frac{Q_c}{\bar{f}_{fuel}}$$

$$= \frac{\bar{f}_{products}}{\bar{f}_{fuel}} \bar{h}^\circ_{products}(T_1) - \bar{h}^\circ_{fuel}(T_1) - \frac{\bar{f}_{air}}{\bar{f}_{fuel}} \bar{h}^\circ_{air}(T_1) \qquad (2.16)$$

Since the combustion process is exothermic (releases heat), $\Delta\bar{h}_c(T_1)$ is negative. For combustion chemistry calculations, it is convenient to convert the mass specific enthalpy of combustion to a mole specific value using the formula weight, that is,

$$\Delta h_c(T_1) = M_f \Delta\bar{h}_c(T_1) \qquad (2.17)$$

Flow calorimeter measurements of the heating value are usually performed at temperatures in the range 288 to 298 K, introducing a problem in the interpretation of the enthalpy of combustion. The measurement requires complete combustion; that is, all carbon and hydrogen must be oxidized to form CO_2 and H_2O, respectively. If the calorimeter is operated near stoichiometric, the product gases may contain several percent H_2O, considerably more than the saturation vapor pressure of water at that temperature. Hence water will condense in the calorimeter, increasing the apparent heat release due to the latent heat of vaporization. The measured heating value thus depends on the phase of the product water.

The effect of this phase transition may be seen by examining the heat transfer required to generate vapor-phase water in the products and that needed for the condensation of that vapor. This analysis requires introduction of a second control volume in the thermodynamic model, as illustrated in Figure 2.4. The enthalpy of combustion as

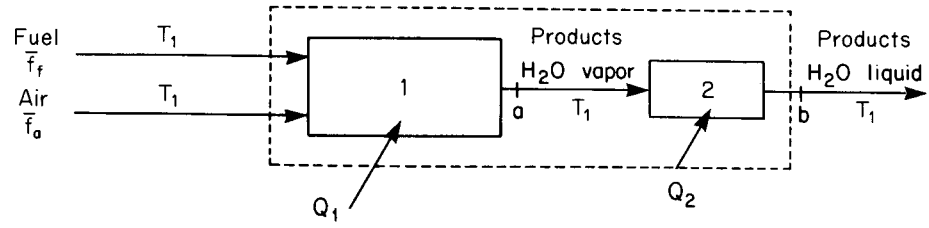

Figure 2.4 Thermodynamic model for calculating higher and lower enthalpies of combustion.

measured by reactor 1, $\Delta\bar{h}_c(T_1) = Q_1/\bar{f}_f$, is described above. The heat transfer to reactor 2 is that associated with the condensation of water.

$$\frac{Q_2}{\bar{f}_f} = \frac{\bar{f}_2}{\bar{f}_f}\left[\bar{h}^\circ_{w2}(T_1) - \bar{h}^\circ_{w1}(T_1)\right] = \frac{\bar{f}_w}{\bar{f}_f}\Delta\bar{h}_v(T_1)$$

where $\Delta\bar{h}_v(T_1)$ is the latent heat of vaporization of water at temperature T_1. At 298 K, $\Delta\bar{h}_v(298\text{ K}) = 2442\text{ J g}^{-1}$, or $\Delta h_v(298\text{ K}) = 44{,}000\text{ J mol}^{-1}$.* The enthalpy of combustion measured with H_2O present as liquid (reactors 1 and 2 combined) is, therefore,

$$\Delta\bar{h}_{c(1+2)}(T_1) = \Delta\bar{h}_{c1}(T_1) + \frac{\bar{f}_w}{\bar{f}_f}\Delta\bar{h}_v(T_1) \tag{2.18}$$

The term *heating value* is used to denote heat release due to combustion, $-\Delta\bar{h}_c(T_1)$. The two measures of the enthalpy of combustion are generally specified in terms of the heating value. The higher heating value, HHV, corresponds to the heat of reaction when the latent heat of condensation of water is recovered:

$$\text{HHV} = -\Delta\bar{h}_{c(1+2)}(T_1)$$

The lower heating value, LHV, corresponds to the case when the water is present as vapor:

$$\text{LHV} = -\Delta\bar{h}_{c1}(T_1)$$

While heating values in the U.S.A. are usually reported as higher heating values, lower heating values are often given in other parts of the world. Exhaust temperatures for most combustors are sufficiently high that the water is exhausted as vapor. At the temperatures of a flame, water is present only as vapor. Thus the lower heating value is more relevant. It is frequently necessary to compute lower heating values from the commonly reported higher heating value data.

The subscripts L and H will be used to indicate the enthalpies of combustion corresponding to the lower and higher heating values, respectively, that is,

$$\Delta\bar{h}_{cL}(T_1) = -\text{LHV}$$

$$\Delta\bar{h}_{cH}(T_1) = -\text{HHV}$$

*The units J mol^{-1} will, throughout this book, mean J g-mol^{-1}

Given the heating value of a fuel, an effective enthalpy of formation can readily be calculated. Working in terms of molar quantities, we may write

$$\Delta h_c(T_1) = \sum_{i,\text{prod}} \frac{f_i}{f_{\text{fuel}}} \Delta h_{fi}^{\circ}(T_1) - \frac{f_{O_2}}{f_{\text{fuel}}} \Delta h_{f,O_2}^{\circ}(T_1) - \Delta h_{f,\text{fuel}}^{\circ}(T_1)$$

where, if the molecular form of the fuel is not known, the molar flow rate of fuel may be expressed in terms of moles of carbon per second. Rearranging, we find the enthalpy of formation of the fuel

$$\Delta h_{f,\text{fuel}}^{\circ}(T_1) = \sum_{i,\text{prod}} \frac{f_i}{f_{\text{fuel}}} \Delta h_{fi}^{\circ}(T_1) - \frac{f_{O_2}}{f_{\text{fuel}}} \Delta h_{f,O_2}(T_1) - \Delta h_{cL}^{\circ}(T_1) \qquad (2.19)$$

With this information, an estimate for the temperature in the flame can be calculated.

Example 2.3 ***Higher and Lower Heating Values and Enthalpy of Formation***

A fuel oil contains 86.96% carbon and 13.04% hydrogen by weight. Its heating value is reported to be 44 kJ g^{-1}. Determine the higher and lower heating values and enthalpy of formation on a mole basis.

The fuel composition is

Element	wt %	Normalize with respect to C
C	86.96 ÷ 12 =	7.25 ÷ 7.25 = 1
H	13.04 ÷ 1 =	13.04 ÷ 7.25 = 1.8

The fuel composition is $CH_{1.8}$, and its formula weight is

$$M_f = 12 + (1.8)(1) = 13.8$$

Heating values are most commonly reported as the higher heating value; thus

$$\Delta \bar{h}_{cH}(T_1) = -\text{HHV} = -44 \text{ kJ g}^{-1}$$

The molar enthalpy of combustion is

$$\Delta h_{cH} = M_f \Delta \bar{h}_{cH} = (13.8)(-44000 \text{ J g}^{-1}) = -607{,}200 \text{ J mol}^{-1} \text{ K}^{-1}$$

Combustion of this fuel proceeds according to

$$CH_{1.8} + 1.45O_2 \longrightarrow CO_2 + 0.9H_2O$$

Thus, 0.9 mol of water is generated for each mole of fuel (carbon) burned. The latent heat of vaporization of water at 298 K is $\Delta h_v(298 \text{ K}) = 44{,}000 \text{ J mol}^{-1}$. Thus

$$\begin{aligned} \Delta h_{cL} &= \Delta h_{cH} + 0.90 \, \Delta h_v \\ &= -607{,}200 + 0.90 \times 44{,}000 \\ &= -567{,}600 \text{ J (mol C)}^{-1} \end{aligned}$$

The enthalpy of formation of this fuel may be determined using the lower heating value and the enthalpy of formation data from Table 2.5.

$$\begin{aligned}\Delta h_{f,CH_{1.8}}(T_1) &= \Delta h_{f,CO_2}(T_1) + 0.90\,\Delta h_{f,H_2O}(T_1) - 1.45\,\Delta h_{f,O_2}(T_1) - \Delta h_{cL}(T_1)\\ &= -394{,}088 + 0.90 \times (-242{,}174) - 1.45(0) - (-567{,}600)\\ &= -44{,}440 \text{ J (mol C)}^{-1}\end{aligned}$$

2.3.2 Adiabatic Flame Temperature

Combustion reactions generally occur very fast, on the order of 1 ms and little heat or work transfer takes place on the time scale of combustion. For this reason the maximum temperature achieved in the combustion process is often near that for adiabatic combustion. This so-called *adiabatic flame temperature* may readily be calculated by applying the first law of thermodynamics to an adiabatic combustor. Consider a steady-flow combustor, illustrated in Figure 2.5, burning a fuel with composition CH_m.

The combustion stoichiometry for fuel-lean combustion is

$$CH_m + \frac{\alpha_s}{\phi}(O_2 + 3.78N_2) \longrightarrow CO_2 + \frac{m}{2}H_2O + \alpha_s\left(\frac{1}{\phi} - 1\right)O_2 + \frac{3.78\alpha_s}{\phi}N_2 \tag{2.20}$$

where $\alpha_s = 1 + m/4$. The first law of thermodynamics becomes

$$\begin{aligned}f\Bigg[&\left[h(T) - h(T_0) + \Delta h_f^\circ(T_0)\right]_{CO_2} + \frac{m}{2}\left[h(T) - h(T_0) + \Delta h_f^\circ(T_0)\right]_{H_2O}\\ &+ \alpha_s\left(\frac{1}{\phi} - 1\right)\left[h(T) - h(T_0) + \Delta h_f^\circ(T_0)\right]_{O_2} + \frac{3.78}{\phi}\alpha_s\left[h(T)\right.\\ &\left. - h(T_0) + \Delta h_f^\circ(T_0)\right]_{N_2}\\ &- \left[h(T_f) - h(T_0) + \Delta h_f^\circ(T_0)\right]_f - \alpha_s\frac{1}{\phi}\left[h(T_a) - h(T_0) + \Delta h_f^\circ(T_0)\right]_{O_2}\\ &- \frac{3.78}{\phi}\alpha_s\left[h(T_a) - h(T_0) + \Delta h_f^\circ(T_0)\right]_{N_2}\Bigg] = Q - W_x = 0\end{aligned} \tag{2.21}$$

Sensible enthalpy and enthalpy of formation data for each of the species are used to solve for the adiabatic flame temperature, T. Using the linear approximation for the temperature dependence of the specific heats, $c_{pi} = a_i + b_i T$, we have

$$h_i(T) - h_i(T_0) = a_i(T - T_0) + \frac{b_i}{2}(T^2 - T_0^2) \tag{2.22}$$

Thus, with this approximate representation of the temperature dependence of the specific heat, the problem of determining the adiabatic flame temperature is reduced to solving a quadratic equation.

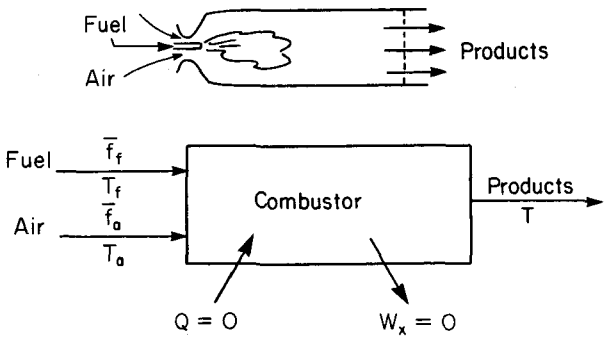

Figure 2.5 Steady flow combustor.

Example 2.4 ***Adiabatic Flame Temperature***

A heavy fuel oil with composition $CH_{1.8}$ and a higher heating value of 44 kJ g^{-1} is burned in stoichiometric air. The initial fuel and air temperatures, denoted by subscripts f and a, respectively, are $T_f = T_a = T_0 = 298$ K. The pressure is 101 kPa (1 atm). Calculate the temperature of the products of adiabatic combustion.

1. We are given the higher heating value that includes the latent heat of condensation of water vapor. The lower heating value is given by (2.18). Converting the higher heating value to the mole-based enthalpy of combustion, we have

$$\Delta h_{cL}(T_0) = -(44 \times 10^3 \text{ J g}^{-1})(12 + 1.8 \times 1) \text{ g mol}^{-1} + 0.9(44 \times 10^3) = -568 \times 10^3 \text{ J mol}^{-1}$$

2. Combustion stoichiometry yields from (2.20):

$$CH_{1.8} + 1.45(O_2 + 3.78N_2) \longrightarrow CO_2 + 0.9H_2O + 5.48N_2$$

3. First law of thermodynamics:

$$\begin{aligned} 1[h(T) - h(T_0) + \Delta h_f(T_0)]_{CO_2} + 0.9[h(T) - h(T_0) + \Delta h_f(T_0)]_{H_2O} \\ + 5.48[h(T) - h(T_0) + \Delta h_f(T_0)]_{N_2} - [h(T_1) - h(T_0) + \Delta h_f(T_0)]_{CH_{1.8}} \\ - 1.45[h(T_1) - h(T_0) + \Delta h_f(T_0)]_{O_2} - 5.48[h(T_1) - h(T_0) \\ + \Delta h_f(T_0)]_{N_2} = \frac{Q}{f_f} - \frac{W_x}{f_f} \end{aligned}$$

Grouping enthalpy of formation terms and noting that $T_1 = T_0$ yields

$$\begin{aligned} [h(T) - h(T_0)]_{CO_2} + 0.9[h(T) - h(T_0)]_{H_2O} + 5.48[h(T) - h(T_0)]_{N_2} \\ + \Delta h_{f,CO_2}(T_0) + 0.9\,\Delta h_{f,H_2O}(T_0) - \Delta h_{f,CH_{1.8}}(T_0) \\ - 1.45\,\Delta h_{f,O_2}(T_0) + 5.48[\Delta h_{f,N_2}(T_0) - \Delta h_{f,N_2}(T_0)] = 0 \end{aligned}$$

But

$$\Delta h_{cL}(T_0) = \Delta h_{f,CO_2}(T_0) + 0.9\,\Delta h_{f,H_2O}(T_0) - \Delta h_{f,CH_{1.8}}(T_0) - 1.45\,\Delta h_{f,O_2}(T_0)$$

So, since we are dealing with *complete combustion*, and because of the simplifications associated with the initial temperatures being T_0, we may write

$$[h(T) - h(T_0)]_{CO_2} + 0.9[h(T) - h(T_0)]_{H_2O} + 5.48[h(T) - h(T_0)]_{N_2} + \Delta h_{cL}(T_0) = 0$$

4. From Table 2.5, we find ($c_{p,i} = a_i + b_i T$)

Species	a_i (J mol^{-1} K^{-1})	b_i (J mol^{-1} K^{-2})
CO_2	44.319	0.00730
$H_2O_{(v)}$	32.477	0.00862
N_2	29.231	0.00307

$$h_i(T) - h_i(T_0) = \int_{T_0}^{T} c_{p,i}(T')\,dT' = a_i(T - T_0) + \frac{b_i}{2}(T^2 - T_0^2)$$

Substituting into the energy equation gives us

$$44.319(T - T_0) + \frac{0.00730}{2}(T^2 - T_0^2) + 0.9\left[32.477(T - T_0) + \frac{0.00862}{2}(T^2 - T_0^2)\right] + 5.48\left[29.231(T - T_0) + \frac{0.00307}{2}(T^2 - T_0^2)\right] + (-568{,}000) = 0$$

Grouping terms, we find

$$233.734(T - T_0) + 0.01594(T^2 - T_0^2) - 568{,}000 = 0$$

Solving this quadratic equation for T yields

$$T = 2356 \text{ K}$$

(*Note:* A solution based on linear interpolation on the more precise JANAF Tables data yields $T = 2338$ K, so the error associated with using $c_p = a + bT$ is, in this case, about 18 K or 0.8%.)

2.3.3 Chemical Equilibrium

We have, so far, assumed that the fuel reacts completely, forming only CO_2, H_2O, and other fully oxidized products. For fuel-lean combustion with product temperatures below about 1250 K, the stable species, CO_2, H_2O, O_2, and N_2, are the usual products and this is a good assumption (Glassman, 1977). Element balances are sufficient to determine the composition of the combustion products under these conditions. Most combustion systems, however, reach temperatures much higher than 1250 K. We have seen that

adiabatic flame temperatures can reach 2300 K for stoichiometric combustion. At such high temperatures, species that are stable at ambient temperatures can dissociate by reactions such as

$$CO_2 \rightleftharpoons CO + \tfrac{1}{2} O_2$$

$$H_2O \rightleftharpoons H_2 + \tfrac{1}{2} O_2$$

so carbon monoxide, hydrogen, and other reduced species may be present even though sufficient oxygen is available for complete combustion. In fact, these species are oxidized rapidly, but they are continually replenished by dissociation and other reactions that occur in the hot gases. The concentrations of these species are determined by the balance between those reactions that lead to their formation and those that consume them.

Chemical equilibrium provides a reasonable first approximation to the composition of the combustion products at high temperatures since the equilibrium state is that which would be achieved given a time sufficiently long for the chemical reactions to proceed. We will see that chemical equilibrium calculations also provide insight into pollutant formation.

The conditions for thermodynamic equilibrium are derived from the second law of thermodynamics. These conditions may be concisely stated in terms of the Gibbs free energy, $G = H - TS$ (Denbigh, 1971). For a closed system at a constant temperature and pressure, the Gibbs free energy is a minimum at thermodynamic equilibrium. Thus, for any change *away* from an equilibrium state at constant T and p, $dG > 0$. The Gibbs free energy is a function of the temperature, pressure, and composition [i.e., $G = G(T, p, n_1, n_2 \ldots)$]. Thus we may write

$$dG = \left(\frac{\partial G}{\partial T}\right)_{p,n_j} dT + \left(\frac{\partial G}{\partial p}\right)_{T,n_j} dp + \left(\frac{\partial G}{\partial n_1}\right)_{T,p,n_{j\neq 1}} dn_1 + \left(\frac{\partial G}{\partial n_2}\right)_{T,p,n_{j\neq 2}} dn_2 + \cdots \quad (2.23)$$

The partial derivative of the Gibbs free energy with respect to the number of moles of a species, i, is the chemical potential

$$\mu_i \equiv \left(\frac{\partial G}{\partial n_i}\right)_{T,p,n_{j\neq i}} \quad (2.24)$$

Recalling the definition of G, we may write

$$dG = dU + p\,dV - T\,dS + V\,dp - S\,dT + \sum_i \mu_i\,dn_i$$

Using the first law of thermodynamics, it can be shown that

$$dU + p\,dV - T\,dS = 0$$

Hence

$$dG = V\,dp - S\,dT + \sum_i \mu_i\,dn_i \tag{2.25}$$

The partial molar Gibbs free energy may be written

$$\mu_i = \frac{\partial}{\partial n_i}(H - TS)_{T,p,n_{j\neq i}} = h_i - Ts_i \tag{2.26}$$

where s_i *is the partial molar entropy of species* i. For the purposes of examining most combustion equilibria, we may focus on ideal gases and simple condensed phases since the pressures of combustion are generally near atmospheric. The enthalpy of an ideal gas is independent of pressure. The entropy is

$$s_i(T, p) = s_i^\circ(T_0) + \int_{T_0}^{T} \frac{c_{p,i}(T')}{T'}\,dT' + R \ln \frac{p_i}{p_0} \tag{2.27}$$

where $s_i^\circ(T_0)$ is the entropy at the reference state. Since the partial pressure is usually expressed in units of atmospheres, the partial pressure term of (2.27) is commonly expressed as $\ln p_i$. Since the heat capacity of an ideal gas is not a function of pressure, the pressure dependence of the partial molar Gibbs free energy for an ideal gas is simply that associated with the entropy change from the reference state, and we may write

$$\mu_i = \mu_i^\circ(T) + RT \ln p_i \tag{2.28}$$

where $\mu_i^\circ(T)$, the standard chemical potential of species i, is the chemical potential of i at the reference pressure, $p_0 = 1$ atm. Values of $s_i^\circ(T_0)$ are included with the thermodynamic data in Table 2.5.

For a pure condensed phase at modest pressures, the entropy depends only on temperature,

$$s(T) = s^\circ(T_0) + \int_{T_0}^{T} \frac{c_p(T')}{T'}\,dT'$$

Since the enthalpy is also independent of pressure, the partial molar Gibbs free energy is a function only of the temperature, that is,

$$\mu_i = \mu_i^\circ(T) \tag{2.29}$$

The condition for thermodynamic equilibrium may now be written as

$$(dG)_{T,p} = \sum_i \mu_i\,dn_i \geq 0 \tag{2.30}$$

for any change away from the equilibrium state. Consider a chemical reaction

$$\sum_j \nu_j A_j = 0 \tag{2.31}$$

We may express the progress of the reaction in terms of the number of moles of a product species generated divided by the stoichiometric coefficient, the extent of reaction [recall

(A.5)],

$$d\xi = \frac{dn_j}{\nu_j} \tag{2.32}$$

The condition of chemical equilibrium at constant T and p is then

$$\sum_j \nu_j \mu_j = 0 \tag{2.33}$$

This condition must be satisfied at equilibrium for any $d\xi$, regardless of sign. Using (2.28) we obtain

$$\sum_j \nu_j \mu_j^\circ + \sum_{j,\text{gas}} RT \ln p_j^{\nu_j} = 0 \tag{2.34}$$

at equilibrium. This expression now defines the equilibrium composition of the gas.

Separating the pressure-dependent terms from the temperature-dependent terms yields a relation between the partial pressures of the gaseous species and temperature, that is,

$$\prod_{j,\text{gas only}} p_j^{\nu_j} = \exp\left(-\sum_j \nu_j \frac{\mu_j^\circ}{RT}\right) \equiv K_p(T) \tag{2.35}$$

The function $K_p(T)$ is the equilibrium constant in terms of partial pressures. Note that the quantities of the pure condensed phases do not enter explicitly into this relation.

It is often convenient to work in terms of mole fractions or concentrations instead of partial pressures. The partial pressure is, according to Dalton's law,

$$p_i = y_i p \tag{2.36}$$

where y_i is the mole fraction of species i, calculated considering gas-phase species only. Substituting into the expression for K_p yields

$$\prod_{j,\text{gas only}} (y_j p)^{\nu_j} = K_p(T) \tag{2.37}$$

Similarly, using the ideal gas relation, $p_i = c_i RT$, the equilibrium constant in terms of concentrations is found to be

$$K_c(T) = K_p(T)\,(RT)^{-\Sigma_{i,\text{gas only}} \nu_i} = \prod_{j,\text{gas only}} c_j^{\nu_j} \tag{2.38}$$

The composition of a system at equilibrium is determined by solving a set of the equilibrium relations [(2.34), (2.35), (2.37), or (2.38)] subject to element conservation constraints.

When reactions involving condensed-phase species are considered, equilibria involving the condensed-phase species do not explicitly indicate the amounts of each of those species present. For example, the reaction

$$C_{(s)} + O_2 \rightleftarrows CO_2$$

yields the equilibrium relation

$$K_p(T) = \frac{p_{CO_2}}{p_{O_2}}$$

Only if the quantity of carbon in the system is sufficiently large relative to the amount of oxygen can the ratio p_{CO_2}/p_{O_2} equal $K_p(T)$, bringing this equilibrium into play. For smaller amounts of carbon, no solid carbon will be present at equilibrium.

Example 2.5 ***Carbon Oxidation***

Carbon is oxidized in stoichiometric air at $T = 3000$ K and atmospheric pressure. What are the mole fractions of carbon monoxide, carbon dioxide, and oxygen at chemical equilibrium? How much solid carbon remains?

From Table 2.5 we find

Species	$\Delta h_f^\circ(T_0)$ (J mol^{-1})	$s^\circ(T_0)$ (J mol^{-1})	$c_p = a + bT$ (J mol^{-1} K^{-1})	
			a	b
$C_{(s)}$	0	5.694	14.926	0.00437
CO	−110,700	197.810	29.613	0.00301
CO_2	−394,088	213.984	44.319	0.00730
N_2	0	191.777	29.231	0.00307
O_2	0	205.310	30.504	0.00349

The general expression for the chemical potential of species i is

$$\mu_i^\circ(T) = \int_{T_0}^{T} c_{p,i}\,dT' + \Delta h_{fi}^\circ(T_0) - T\left[s_i^\circ(T_0) + \int_{T_0}^{T} \frac{c_{p,i}}{T'}\,dT'\right]$$

$$= a_i\left(T - T_0 - T\ln\frac{T}{T_0}\right) - \frac{b_i}{2}(T - T_0)^2 + \Delta h_{fi}^\circ(T_0) - Ts_i^\circ(T_0)$$

At 3000 K and 1 atm:

Species	μ_i° (J mol^{-1})
$C_{(s)}$	−96,088
CO	−840,216
CO_2	−1,249,897
N_2	−710,007
O_2	−757,525

Neglecting any solid carbon in the products, the stoichiometry under consideration is

$$C + O_2 + 3.78N_2 \longrightarrow xCO + (1 - x)CO_2 + \frac{x}{2}O_2 + 3.78N_2$$

The species mole fractions are

$$y_{CO} = \frac{x}{4.78 + x/2}$$

$$y_{CO_2} = \frac{1 - x}{4.78 + x/2}$$

$$y_{O_2} = \frac{x/2}{4.78 + x/2}$$

$$y_{N_2} = \frac{3.78}{4.78 + x/2}$$

The problem of determining the equilibrium composition is now reduced to that of evaluating the parameter, x. We assume that CO and CO_2 are in equilibrium

$$CO_2 \overset{1}{\rightleftharpoons} CO + \tfrac{1}{2} O_2$$

The change in the chemical potential associated with a mole of CO formation by this reaction is

$$\begin{aligned}\Delta G_1 = \sum_j \nu_{j1}\mu_j^\circ &= \mu_{CO} + \tfrac{1}{2}\mu_{O_2} - \mu_{CO_2} \\ &= -840{,}216 + \tfrac{1}{2}(-757{,}525) - (-1{,}249{,}897) \\ &= +30{,}918 \text{ J mol}^{-1}\end{aligned}$$

where ν_{j1} denotes the stoichiometric coefficient for species j in reaction 1. Thus the equilibrium constant for this reaction is

$$\begin{aligned}K_{p1} &= \exp\left(-\frac{\sum_j \nu_{j1}\mu_j^\circ}{RT}\right) \\ &= \exp\left[-\frac{30{,}918 \text{ J mol}^{-1}}{(8.3144 \text{ J mol}^{-1} \text{ K})(3000 \text{ K})}\right] \\ &= 0.2895 \text{ atm}^{1/2}\end{aligned}$$

We may now solve for the equilibrium mole fractions. Since

$$K_{p1} = \frac{y_{CO} y_{O_2}^{1/2}}{y_{CO_2}} p^{1/2}$$

we may write

$$p^{-1/2} K_{p1} = \frac{x}{1 - x}\left(\frac{x/2}{4.78 + x/2}\right)^{1/2}$$

which leads to a cubic equation for x,

$$f(x) = \left(1 - \frac{K_{p1}^2}{p}\right)x^3 - 7.56\frac{K_{p1}^2}{p}x^2 + 18.12\frac{K_{p1}^2}{p}x - 9.56\frac{K_{p1}^2}{p} = 0$$

This equation may be solved iteratively using Newton's method. Beginning with a guess, x', an improved estimate is generated by

$$x = x' - \frac{f(x')}{df(x')/dx}$$

This new estimate is then used to obtain a better estimate until the desired degree of precision is achieved. Guessing initially that $x' = 0.9$, successive iterations yield

Estimate number	x
1	0.9
2	0.623
3	0.556
4	0.553
5	0.553

Thus the equilibrium composition is

$$y_{CO} = 0.109$$

$$y_{CO_2} = 0.0884$$

$$y_{O_2} = 0.0547$$

$$y_{N_2} = 0.748$$

We must now test to see whether there will be any residual carbon at equilibrium. Consider the reaction

$$CO_2 \overset{2}{\rightleftharpoons} C_{(s)} + O_2$$

for which

$$\Delta G_2 = 396{,}284 \text{ J mol}^{-1}$$

Thus

$$K_{p2} = \exp\left(\frac{-396{,}284}{8.3144 \times 3000}\right)$$

$$= 1.26 \times 10^{-7}$$

In terms of mole fractions at equilibrium,

$$\frac{y_{O_2}}{y_{CO_2}} = 0.619 > K_{p2} = 1.26 \times 10^{-7}$$

Thus there is too much oxygen in the system to allow any carbon to remain unreacted at chemical equilibrium.

The temperature dependence of the equilibrium constant can readily be expressed in terms of the enthalpy of reaction (Denbigh, 1971). Equation (2.35) may be written

$$\ln K_p = -\frac{1}{R} \sum_j \nu_j \frac{\mu_j^\circ}{T}$$

Differentiation yields

$$\frac{d \ln K_p}{dT} = -\frac{1}{R} \sum_j \nu_j \frac{d}{dT}\left(\frac{\mu_j^\circ}{T}\right) \tag{2.39}$$

To evaluate the derivative on the right-hand side, we observe from (2.25) that

$$\mu_i = \left(\frac{\partial G}{\partial n_i}\right)_{p,T,n_j}$$

$$S = -\left(\frac{\partial G}{\partial T}\right)_{p,n_i,n_j}$$

Since G is a state function, dG is an exact differential. Thus, from (2.25) we may obtain the reciprocity relations

$$\left(\frac{\partial \mu_i}{\partial T}\right)_{p,n_i,n_j} = -\left(\frac{\partial S}{\partial n_i}\right)_{p,T,n_j} = -s_i$$

Equation (2.26) may now be written

$$\mu_i = h_i + T\left(\frac{\partial \mu_i}{\partial T}\right)_{p,n_i,n_j}$$

which may be rearranged in the form we seek:

$$\left(\frac{\partial(\mu_i/T)}{\partial T}\right)_{p,n_i,n_j} = -\frac{h_i}{T^2}$$

Finally, recalling (2.28), this becomes

$$\left(\frac{\partial(\mu_i^\circ/T)}{\partial T}\right)_{p,n_i,n_j} = -\frac{h_i}{T^2} \tag{2.40}$$

Substituting (2.40) into (2.39) gives

$$\frac{d \ln K_p}{dT} = \frac{\sum_i \nu_i h_i}{RT^2}$$

The term $\Sigma_i \nu_i h_i$ is just the enthalpy of reaction $\Delta h_r(T)$. The resulting relation is called *van't Hoff's equation*,

$$\frac{d \ln K_p}{dT} = \frac{\Delta h_r}{RT^2} \tag{2.41}$$

Over small temperature ranges the enthalpy of reaction may be assumed to be approximately constant. Although either exact numerical evaluation of K_p from polynomial fits to the specific heat (e.g., Table 2.5) or the use of thermodynamic data tabulations is

preferred for calculations of compositions of mixtures at chemical equilibrium, the assumption of constant Δh_r and use of (2.41) will greatly simplify kinetic expressions we shall develop later using equilibrium constants.

The conditions for thermodynamic equilibrium have been derived for a system maintained at a prescribed temperature and pressure. The energy, enthalpy, entropy, and specific volume of a system may be calculated using the composition of the system, as determined from the equilibrium condition, and the thermodynamic properties of the constituents of the system. The equilibrium state of the system is, however, independent of the manner in which it was specified. Any two independent properties could be used in place of the pressure and temperature.

The temperature of a combustion system is rarely known a priori. The adiabatic flame temperature is often a good estimate of the peak temperature reached during combustion, provided that the reaction equilibria are taken into account. This requires solving a chemical equilibrium problem subject to constraints on the pressure and enthalpy (for a flow system) rather than temperature and pressure. Iterations on temperature to satisfy the first law of thermodynamics are now needed in addition to iterations on the composition variables. This procedure is best shown with an example.

Example 2.6 ***Adiabatic Combustion Equilibrium***

Example 2.4 considered stoichiometric combustion of a heavy fuel oil, $CH_{1.8}$, in stoichiometric air at atmospheric pressure. Initial fuel and air temperatures were 298 K. The adiabatic flame temperature calculated assuming complete combustion was 2356 K. How do reaction equilibria influence the temperature and composition of the reaction products?

Allowing for incomplete combustion, the combustion stoichiometry may be written

$$CH_{1.8} + 1.45(O_2 + 3.78N_2) \longrightarrow (1 - x)CO_2 + xCO + (0.9 - y)H_2O + yH_2 + \left(\frac{x}{2} + \frac{y}{2}\right)O_2 + 5.48N_2$$

The total number of moles of reaction products is

$$N_T = (1 - x) + x + (0.9 - y) + y + \left(\frac{x}{2} + \frac{y}{2}\right) + 5.48$$

$$= 7.38 + \frac{x}{2} + \frac{y}{2}$$

Two linearly independent equilibrium relations are needed to compute x and y. The reactions we choose to represent the equilibrium are arbitrary, as long as they are linearly independent. Possible reactions include

$$CO + H_2O \overset{1}{\rightleftharpoons} CO_2 + H_2 \qquad \text{(the so-called water-gas shift reaction)}$$

$$H_2O \overset{2}{\rightleftharpoons} H_2 + \tfrac{1}{2}O_2$$

$$CO_2 \overset{3}{\rightleftharpoons} CO + \tfrac{1}{2}O_2$$

We see by inspection that the first reaction can be obtained by subtracting reaction 3 from reaction 2, but any two of these reactions are linearly independent. The choice is dictated by computational expediency. We may choose, for example,

$$\mathrm{CO} + \mathrm{H_2O} \overset{1}{\rightleftharpoons} \mathrm{CO_2} + \mathrm{H_2}$$

$$\mathrm{H_2O} \overset{2}{\rightleftharpoons} \mathrm{H_2} + \tfrac{1}{2}\,\mathrm{O_2}$$

The corresponding equilibrium relations are

$$K_{p1} = \frac{1 - x}{x}\frac{y}{0.9 - y}$$

$$p^{-1/2}K_{p2} = \frac{y}{0.9 - y}\left(\frac{x/2 + y/2}{7.38 + x/2 + y/2}\right)^{1/2}$$

$$= \frac{y}{0.9 - y}\left(\frac{x + y}{14.76 + x + y}\right)^{1/2}$$

If we had replaced reaction 1 with 3, the first equilibrium relation would be replaced with

$$p^{-1/2}K_{p3} = \frac{x}{1 - x}\left(\frac{x + y}{14.76 + x + y}\right)^{1/2}$$

By selecting reaction 1 rather than 3 we have a somewhat simpler equilibrium expression to solve. In either case, the equilibrium composition corresponding to a specified temperature (and, therefore, specified K_ps) may now be calculated by simultaneous solution of the two nonlinear equilibrium relations. The same solution will be obtained regardless of the choice of equilibrium relations.

A number of methods are available for solving simultaneous nonlinear equations. Newton's method may be applied readily in this case. Suppose that we want the solution to two simultaneous equations:

$$f(x, y) = 0,$$
$$g(x, y) = 0$$

From an initial approximation (x_0, y_0) we attempt to determine corrections, Δx and Δy, such that

$$f(x_0 + \Delta x, y_0 + \Delta y) = 0 \qquad g(x_0 + \Delta x, y_0 + \Delta y) = 0$$

are simultaneously satisfied. If the functions are approximated by a Taylor series and only the linear terms are retained, the equations become

$$f_0 + f_{x0}\,\Delta x + f_{y0}\,\Delta y = 0$$
$$g_0 + g_{x0}\,\Delta x + g_{y0}\,\Delta y = 0$$

where the 0 subscripts indicate that the functions have been evaluated at (x_0, y_0) and the subscripts x and y denote $\partial/\partial x$ and $\partial/\partial y$, respectively. These linear equations are readily

solved for the correction terms, Δx and Δy. Improved estimates are then computed by

$$x = x_0 + \Delta x$$
$$y = y_0 + \Delta y$$

By iterating until Δx and Δy become sufficiently small, the solution of the equations can be found.

We may define the functions to be solved in the present problem as

$$f(x, y) = \frac{1 - x}{x}\frac{y}{0.9 - y} - K_{p1} = 0$$

$$g(x, y) = \frac{y}{0.9 - y}\left(\frac{x + y}{14.76 + x + y}\right)^{1/2} - p^{-1/2}K_{p2} = 0$$

The partial derivatives are

$$f_x = \frac{\partial f}{\partial x} = -\frac{y}{x^2(0.9 - y)}$$

$$f_y = \frac{0.9(1 - x)}{x(0.9 - y)^2}$$

$$g_x = \frac{y}{0.9 - y}\left(\frac{1}{2}\right)\left[\frac{14.76 + x + y}{x + y}\right]^{1/2}\left[\frac{14.76}{(14.76 + x + y)^2}\right]$$

$$g_y = \left[\frac{x + y}{14.76 + x + y}\right]^{1/2}\frac{0.9}{(0.9 - y)^2} + g_x$$

and the correction terms are

$$\Delta x = \frac{g_0 f_{y0} - f_0 g_{y0}}{f_{x0}g_{y0} - f_{y0}g_{x0}}$$

$$\Delta y = \frac{f_0 g_{x0} - g_0 f_{x0}}{f_{x0}g_{y0} - f_{y0}g_{x0}}$$

Thus, for specified equilibrium constants, we may readily iterate on x and y to find the corresponding equilibrium composition. Poor initial guesses x_0 and y_0 may lead to estimates of x and y outside the domain of solution,

$$0 \leq x \leq 1$$

$$0 \leq y \leq 0.9$$

If this occurs, one may still use the information regarding the *direction* of the solution by letting

$$x = x_0 + \beta\,\Delta x$$

$$y = y_0 + \beta\,\Delta y$$

where $\beta (0 < \beta \leq 1)$ is chosen to step toward the solution but not beyond the limits of feasible solutions.

Since the temperature of the equilibrium mixture is not known a priori, we must guess the temperature before the equilibrium constants can be evaluated and any calculations can be performed. We may note this temperature estimate as T'. Once the equilibrium composition is determined, we can see how good our guess was by applying the first law of thermodynamics,

$$F(T') = \sum_{i}^{\text{products}} \nu_i \left[h_i(T') - h_i(T_0) + \Delta h_{fi}^{\circ}(T_0)\right] - \sum_{i}^{\text{reactants}} \nu_i \left[h_i(T_i) - h_i(T_0) + \Delta h_{fi}^{\circ}(T_0)\right]$$

For adiabatic combustion, we should have $F(T) = 0$, but we are unlikely to find this on our first guess. If $F(T') > 0$, the initial temperature guess was too high. It is as if heat were transferred to the control volume. The temperature for adiabatic combustion must be lower than that estimate. If, on the other hand, $F(T') < 0$, the temperature is that of a system that has rejected heat to the environment. The temperature estimate must be increased in this case. We may use the first law, assuming constant composition, to give an improved estimate of the gas composition. The composition corresponding to this new temperature estimate can then be evaluated as was done for our initial guess. The whole process is then repeated until satisfactory convergence is achieved.

Returning to our example, the first law becomes

$$\begin{aligned}
&(1 - x)\left[h(T) - h(T_0) + \Delta h_f^{\circ}(T_0)\right]_{CO_2} + x\left[h(T) - h(T_0) + \Delta h_f^{\circ}(T_0)\right]_{CO} \\
&\quad + (0.9 - y)\left[h(T) - h(T_0) + \Delta h_f^{\circ}(T_0)\right]_{H_2O} + y\left[h(T) - h(T_0) + \Delta h_f^{\circ}(T_0)\right]_{H_2} \\
&\quad + \left(\frac{x}{2} + \frac{y}{2}\right)\left[h(T) - h(T_0) + \Delta h_f^{\circ}(T_0)\right]_{O_2} + 5.48\left[h(T) - h(T_0) + \Delta h_f^{\circ}(T_0)\right]_{N_2} \\
&\quad - \left[h(T_f) - h(T_0) + \Delta h_f^{\circ}(T_0)\right]_{\text{fuel, } CH_{1.8}} - 1.45\left[h(T_a) - h(T_0) + \Delta h_f^{\circ}(T_0)\right]_{O_2} \\
&\quad - 5.48\left[h(T_a) - h(T_0) + \Delta h_f^{\circ}(T_0)\right]_{N_2} = Q - W = 0
\end{aligned}$$

where T_f and T_a are the temperatures of the fuel and air, respectively. Grouping terms and noting that, for this problem, $T_f = T_a = T_0$, we have

$$\begin{aligned}
&\left[h(T) - h(T_0)\right]_{CO_2} + 0.9\left[h(T) - h(T_0)\right]_{H_2O} + 5.48\left[h(T) - h(T_0)\right]_{N_2} \\
&\quad + \Delta h_{f,CO_2}^{\circ}(T_0) + 0.9\,\Delta h_{f,H_2O}^{\circ}(T_0) - \Delta h_{f,CH_{1.8}}^{\circ}(T_0) - 1.45\,\Delta h_{f,O_2}^{\circ}(T_0) \\
&\quad - x\left[\left[h(T) - h(T_0)\right]_{CO_2} - \left[h(T) - h(T_0)\right]_{CO} - \tfrac{1}{2}\left[h(T) - h(T_0)\right]_{O_2}\right] \\
&\quad - x\left[\Delta h_{f,CO_2}^{\circ}(T_0) - \Delta h_{f,CO}^{\circ}(T_0) - \tfrac{1}{2}\,\Delta h_{f,O_2}^{\circ}(T_0)\right] \\
&\quad - y\left[\left[h(T) - h(T_0)\right]_{H_2O} - \left[h(T) - h(T_0)\right]_{H_2} - \tfrac{1}{2}\left[h(T) - h(T_0)\right]_{O_2}\right] \\
&\quad - y\left[\Delta h_{f,H_2O}^{\circ}(T_0) - \Delta h_{f,H_2}^{\circ}(T_0) - \tfrac{1}{2}\,\Delta h_{f,O_2}^{\circ}(T_0)\right] = 0
\end{aligned}$$

The first group of enthalpies of formation is seen to be the enthalpy of the complete combustion reaction at $T = T_0$. The enthalpy of formation terms that are multiplied by x equal the enthalpy of the dissociation reaction

$$CO_2 \rightleftarrows CO + \tfrac{1}{2} O_2$$

at temperature T. We have already seen that this reaction is simply the difference between reactions 2 and 1. Similarly, the last group of enthalpy of formation terms equals the enthalpy of reaction 2:

$$H_2O \rightleftarrows H_2 + \tfrac{1}{2} O_2$$

Thus we see that the heat release of the combustion process is reduced by the amount consumed by the dissociation reactions.

The thermodynamic data necessary for these calculations, from Table 2.5, are summarized below:

Species	$\Delta h_f^\circ(T_0)$ (J mol^{-1})	$s^\circ(T_0)$ (J mol^{-1} K^{-1})	$c_p = a + bT$ (J mol^{-1} K^{-1})	
			a	b
CO	−110,700	197.81	29.613	0.00301
CO_2	−394,088	213.98	44.319	0.00730
H_2	0	130.77	27.320	0.00335
H_2O	−242,174	188.99	32.477	0.00862
N_2	0	191.78	29.231	0.00307
O_2	0	205.31	30.504	0.00349

In terms of these thermodynamic data the chemical potentials become

$$\mu_i^\circ = a_i\left(T - T_0 - T\ln\frac{T}{T_0}\right) - \frac{b_i}{2}(T - T_0)^2 + \Delta h_{fi}^\circ(T) - T\,s_i^\circ(T)$$

In preparation for determinations of the equilibrium constants, it is convenient to compute the following sums:

Reaction 1

$$\Delta a_1 = a_{CO_2} + a_{H_2} - a_{CO} - a_{H_2O} = 9.549 \text{ J mol}^{-1} \text{ K}^{-1}$$

$$\Delta b_1 = b_{CO_2} + b_{H_2} - b_{CO} - b_{H_2O} = -0.00098 \text{ J mol}^{-1} \text{ K}^{-2}$$

$$\Delta h_1^\circ = \Delta h_{f,CO_2}^\circ + \Delta h_{f,H_2}^\circ - \Delta h_{f,CO}^\circ - \Delta h_{f,H_2O}^\circ = -41{,}214 \text{ J mol}^{-1}$$

$$\Delta s_1^\circ = s_{CO_2}^\circ + s_{H_2}^\circ - s_{CO}^\circ - s_{H_2O}^\circ = -42.05 \text{ J mol}^{-1} \text{ K}^{-1}$$

Reaction 2

$$\Delta a_2 = a_{H_2} + \tfrac{1}{2} a_{O_2} - a_{H_2O} = 10.095 \text{ J mol}^{-1} \text{ K}^{-1}$$

$$\Delta b_2 = b_{H_2} + \tfrac{1}{2} b_{O_2} - b_{H_2O} = -0.003525 \text{ J mol}^{-1} \text{ K}^{-2}$$

$$\Delta h_2^\circ = \Delta h_{f,H_2}^\circ + \tfrac{1}{2}\Delta h_{f,O_2}^\circ - \Delta h_{f,H_2O}^\circ = 242{,}174 \text{ J mol}^{-1}$$

$$\Delta s_2^\circ = s_{H_2}^\circ + \tfrac{1}{2} s_{O_2}^\circ - s_{H_2O}^\circ = 44.435 \text{ J mol}^{-1} \text{ K}^{-1}$$

Thus we have

$$K_{p1}(T) = \exp\left[\frac{9.549\,(T - T_0 - T\ln(T/T_0)) + (0.00098/2)\,(T - T_0)^2 - 41{,}214 + 42.05T}{8.3144T}\right]$$

$$K_{p2}(T) = \exp\left[\frac{10.095\,(T - T_0 - T\ln(T/T_0)) + (0.003525/2)\,(T - T_0)^2 + 242{,}174 - 44.435T}{8.3144T}\right]$$

Since the complete combustion calculation using these approximate thermodynamic data (Example 2.4) yielded a flame temperature estimate of 2356 K, we begin with a guess of 2300 K. At $T = 2300$ K,

$$K_{p1} = 0.1904$$

$$K_{p2} = 0.001900$$

Guessing initially that $x = y = 0.01$, our iterations yield the following successive estimates:

1	$x = 0.01$	$y = 0.01$
2	$x = 0.0407$	$y = 0.0325$
3	$x = 0.0585$	$y = 0.0222$
4	$x = 0.0818$	$y = 0.0198$
5	$x = 0.0967$	$y = 0.0189$
6	$x = 0.1002$	$y = 0.0187$
7	$x = 0.1003$	$y = 0.0187$

The energy equation becomes

$$234.213(T - T_0) + \frac{0.03188}{2}(T^2 - T_0^2) - 567{,}605$$
$$- x\left[-0.5456(T - T_0) + \frac{0.002545}{2}(T^2 - T_0^2) - 283{,}388\right]$$
$$- y\left[10.095(T - T_0) - \frac{0.003525}{2}(T^2 - T_0^2) - 242{,}174\right] = 0$$

which simplifies to

$$[0.01592 - 0.001273x + 0.001763y]T^2 + [234.213 + 0.5456x - 10.095y]T$$
$$+ [-638{,}853 + 283{,}338x + 244{,}870y] = 0$$

Substituting in the values for x and y, the temperature that satisfies the first law for this composition can be evaluated explicitly. We find

$$T = 2252 \text{ K}$$

The equilibrium constants at this temperature are

$$K_{p1} = 0.1960$$

$$K_{p2} = 0.001422 \text{ atm}^{1/2}$$

We may continue to iterate on x, y, and T until the results converge. We find

T	x	y
2300	0.1003	0.0187
2245	0.0802	0.0152
2266	0.0875	0.0165
2259	0.0875	0.0165
2261	0.0850	0.0160
2261	0.0857	0.0161
2261	0.0857	0.0161

Thus $T = 2261$ K. The mole fractions of the equilibrium reaction products for adiabatic combustion are

$$y_{CO_2} = 0.123$$

$$y_{CO} = 0.0115$$

$$y_{H_2O} = 0.119$$

$$y_{H_2} = 0.00217 = 2170 \text{ ppm}$$

$$y_{O_2} = 0.00685 = 6850 \text{ ppm}$$

$$y_{N_2} = 0.737$$

Comparing the present results with those for complete combustion, Example 2.4, we see that the dissociation reactions reduce the adiabatic flame temperature by about 95 K.

Example 2.7 ***Detailed Balancing***

The primary reaction leading to NO formation in flames is

$$N_2 + O \underset{k_-}{\overset{k_+}{\rightleftharpoons}} NO + N$$

The forward rate constant is

$$k_+ = 1.8 \times 10^8 \exp\left(-\frac{38{,}370}{T}\right) \text{ m}^3 \text{ mol}^{-1} \text{ s}^{-1}$$

Let us derive an expression for k_- using detailed balancing. From detailed balancing we may write

$$k_- = \frac{k_+}{K_c} = \frac{k_+}{K_p}$$

where we can use either K_c or K_p since the number of moles of reactants and products are equal. The thermodynamic data necessary to evaluate K_p are obtained from Table 2.5.

			$c_p = a + bT$	
Species	$\Delta h_f^\circ(T_0)$	$s^\circ(T_0)$	a	b
N_2	0	191.777	29.2313	0.00307
O	249,553	161.181	21.2424	−0.0002
NO	90,420	210.954	30.5843	0.00278
N	473,326	153.413	20.7440	0.00004

The standard chemical potentials may be written

$$\mu_i^\circ = a_i\left(T - T_0 - T\ln\frac{T}{T_0}\right) - \frac{b_i}{2}(T - T_0)^2 + \Delta h_{fi}^\circ(T_0) - Ts_i^\circ(T_0)$$

The equilibrium constant thus becomes

$$K_p = \exp\left[-\frac{0.8546(T - T_0 - T\ln(T/T_0)) - 7.84 \times 10^{-5}(T - T_0)^2 + 314{,}193 - 11.409T}{8.3144T}\right]$$

Direct use of this form of the equilibrium constant will give a complicated expression for the rate constant. Van't Hoffs' equation, (2.41),

$$\frac{d\ln K_p}{dT} = \frac{\Delta h_r}{RT^2}$$

provides a method for estimating the variation of K_p over a temperature range that is sufficiently narrow that the enthalpy of reaction, Δh_r, can be assumed to be constant. Integrating (2.41) from T_1 to T yields

$$\ln K_p(T) - \ln K_p(T_1) = -\frac{\Delta h_r(T_1)}{RT} + \frac{\Delta h_r(T_1)}{RT_1}$$

Rearranging, we find

$$K_p = K_p(T_1)\exp\left(\frac{\Delta h_r}{RT_1}\right)\exp\left(-\frac{\Delta h_r}{RT}\right) = B\exp\left(-\frac{\Delta h_r(T_1)}{RT}\right) \qquad (2.42)$$

where $B = K_p(T_1)\exp(\Delta h_r(T_1)/RT_1)$. Since NO formation occurs primarily at flame temperatures, we evaluate K_p at $T_1 = 2300$ K,

$$K_p(2300\text{ K}) = 3.311 \times 10^{-7}$$

The enthalpy of reaction is

$$\Delta h_r(2300\text{ K}) = 316{,}312\text{ J mol}^{-1}$$

Thus we find

$$K_p = 5.05\exp\left(-\frac{38{,}044}{T}\right)$$

The rate constant for the reverse reaction becomes

$$k_- = 3.6 \times 10^7 \exp\left(-\frac{330}{T}\right) \text{m}^3 \text{ mol}^{-1} \text{ s}^{-1}$$

The rate of the exothermic reverse reaction is found to be essentially independent of temperature.

We have, so far, limited our attention to the major products of combustion. Many of the pollutants with which we shall be concerned and the chemical species that influence their formation are present only in small concentrations. Calculations of the chemical equilibria governing trace species can be performed in the manner described above; however, care must be exercised to ensure that the equilibrium reactions used in the calculations are all linearly independent.

The calculation of the equilibrium concentrations can be simplified for species that are present only in such low concentrations that they do not significantly influence either the energy balance or the mole balances. The equilibrium distribution of the more abundant species can, in such cases, be calculated ignoring the minor species. The minor species can then be calculated using equilibrium reactions involving the major species. For example, the equilibrium concentration of nitric oxide, NO, in fuel-lean combustion products, generally can be calculated using the equilibrium between N_2 and O_2,

$$\tfrac{1}{2} N_2 + \tfrac{1}{2} O_2 \rightleftharpoons NO$$

$$y_{NO} = K_p (y_{N_2} y_{O_2})^{1/2}$$

If such equilibrium calculations indicate that the concentration of the species in question is large enough to influence the energy or element balances (i.e., larger than a few thousand parts per million), a more exact calculation taking the influence on element and energy balances into account is in order.

While the conditions for chemical equilibrium have been stated in terms of equilibrium constants and reactions, these reactions are only stoichiometric relationships between the species present in the system. The number of equilibrium relations required is equal to the number of species to be considered less the number of element balances available for the system. The reactions must be linearly independent but are otherwise arbitrary; that is, they have no relationship to the mechanism by which the reactions actually occur.

An alternative to the specification of a set of reactions for the equilibrium calculations is to minimize the Gibbs free energy directly, subject to constraints on the total number of moles of each of the elements in the system (White et al., 1958). Let b_i° be the number of moles of element i in the system and a_{ij} be the number of moles of element i in a mole of species j. If n_j is the number of moles of species j in the system, the elemental conservation constraint that must be satisfied takes the form

$$b_i^\circ - \sum_{j=1}^{n} a_{ij} n_j = 0, \qquad i = 1, 2, \ldots, l \tag{2.43}$$

where n is the total number of species in the system and l is the number of elements. The method of Lagrange multipliers can be used to solve this constrained minimization problem. We define Γ to be

$$\Gamma = G - \sum_{i=1}^{l} \lambda_i (b_i - b_i^\circ)$$

where

$$b_i = \sum_{j=1}^{n} a_{ij} n_j \tag{2.44}$$

and λ_i are Lagrange multipliers. The condition for equilibrium becomes

$$\delta\Gamma = 0 = \sum_{j=1}^{n} \left(\mu_j - \sum_{i=1}^{l} \lambda_i a_{ij} \right) \delta n_j - \sum_{i=1}^{l} (b_i - b_i^\circ)\, \delta\lambda_i$$

This must hold for all δn_j and $\delta\lambda_i$, so we must have

$$\mu_j - \sum_{i=1}^{l} \lambda_i a_{ij} = 0, \qquad j = 1, 2, \ldots, n \tag{2.45}$$

and the elemental constraints as $l + n$ equations in $l + n$ unknowns.

For ideal gases,

$$\mu_j = \mu_j^\circ + RT \ln \frac{n_j}{n_{\text{gas}}} + RT \ln \frac{p}{p_0}$$

where

$$n_{\text{gas}} = \sum_{j=1}^{\text{gas only}} n_j \tag{2.46}$$

is the total number of moles of gaseous species. For simple condensed phases,

$$\mu_j = \mu_j^\circ$$

Thus for gaseous species, the condition for equilibrium becomes

$$\frac{\mu_j^\circ}{RT} + \ln \frac{n_j}{n_g} + \ln \frac{p}{p_0} - \sum_{i=1}^{l} \pi_i a_{ij} = 0, \qquad j = 1, \ldots, n_g \tag{2.47}$$

where $\pi_i = \lambda_i / RT$, and for condensed-phase species,

$$\frac{\mu_j^\circ}{RT} - \sum_{i=1}^{l} \pi_i a_{ij}, \qquad j = n_{g+1}, \ldots, n \tag{2.48}$$

To determine the equilibrium composition, $n + l + 1$ simultaneous equations, (2.43), (2.46)–(2.48), must be solved. The number of moles of gaseous species j can

be found by rearranging (2.47):

$$n_j = n_{\text{gas}} \frac{p_0}{p} \exp\left(-\frac{\mu_j^\circ}{RT} - \sum_{i=1}^{l} \pi_i a_{ij} \right), \qquad j = 1, 2, \ldots, n_g$$

eliminating n_g of the equations, so only $n - n_g + l + 1$ equations must be solved. The exponential is similar to that obtained in deriving the equilibrium constant for a reaction leading to the formation of a mole of the gaseous species from the elements. The Lagrange multipliers, called *elemental potentials* because of this structure (Reynolds, 1986), thus are the key to determining the equilibrium composition by this route. The details of the procedures for determining the element potentials are beyond the scope of this book. Powerful, general-purpose equilibrium codes that use this method are available, however, and should be considered for complex equilibrium calculations [e.g., Gordon and McBride (1971) and Reynolds (1981)].

2.3.4 Combustion Equilibria

We have seen that at chemical equilibrium for stoichiometric combustion, substantial quantities of carbon monoxide and hydrogen remain unreacted, and that this incomplete combustion reduces the adiabatic flame temperature by nearly 100 K. Figure 2.6 shows how the equilibrium composition and temperature for adiabatic combustion of kerosene, $CH_{1.8}$, vary with equivalence ratio. The results determined using stoichiometry alone for fuel-lean combustion are shown with dashed lines. It is apparent that the major species concentrations and the adiabatic flame temperature for complete combustion are very good approximations for equivalence ratios less than about 0.8. As the equivalence ratio approaches unity, this simple model breaks down due to the increasing importance of the dissociation reactions. For fuel-rich combustion, the number of chemical species that are present in significant quantities exceeds the number of elements in the system, so we must rely on equilibrium to determine the adiabatic flame temperature and composition.

Chemical equilibrium provides our first insight into the conditions that favor the formation of pollutants. Carbon monoxide is a significant component of the combustion products at the adiabatic flame temperature for equivalence ratios greater than about 0.8. Nitric oxide formation from gaseous N_2 and O_2,

$$\tfrac{1}{2}\,N_2 + \tfrac{1}{2}\,O_2 \rightleftharpoons NO$$

is highly endothermic, $\Delta h_r(298\ \text{K}) = 90{,}420\ \text{J mol}^{-1}$. Because of the large heat of reaction, NO formation is favored only at the highest temperatures. Hence, as we will see in the next chapter, the equilibrium NO concentration peaks at equivalence ratios near unity and decreases rapidly with decreasing equivalence ratio due to the decrease in temperature. The equilibrium NO level decreases for fuel-rich combustion due to the combined effects of decreasing temperature and decreasing oxygen concentration.

The equilibrium composition of combustion gases is a strong function of temperature. The reason for this case can readily be seen by examining the equilibrium con-

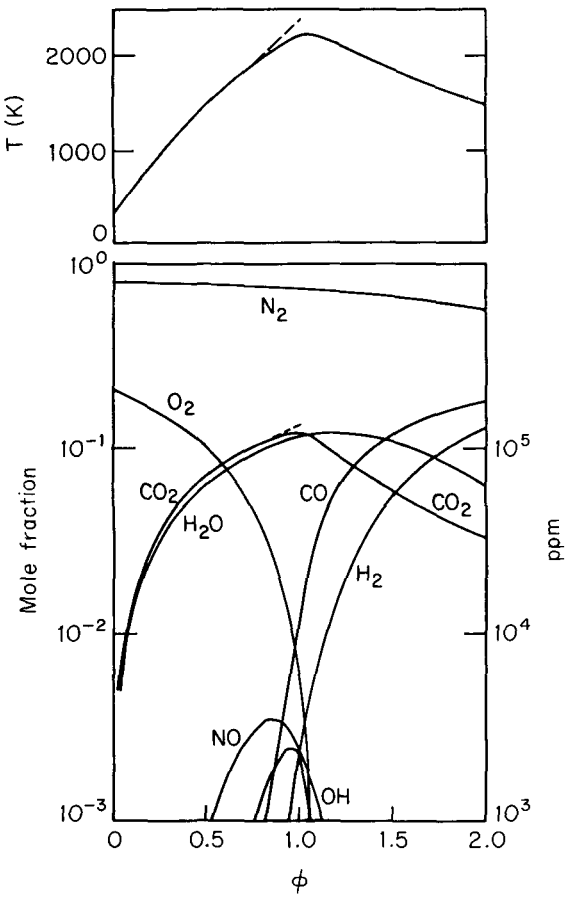

Figure 2.6 Equilibrium composition and temperature for adiabatic combustion of kerosene, $CH_{1.8}$, as a function of equivalence ratio.

stants for combustion reactions using the integrated form of van't Hoff's relation,

$$K_p = B \exp\left(-\frac{\Delta h_r(T_1)}{RT}\right)$$

where T_1 is a reference temperature at which the preexponential factor B, is evaluated. The dissociation reactions, for example,

$$CO_2 \overset{1}{\rightleftharpoons} CO + \tfrac{1}{2} O_2$$

$$H_2O \overset{2}{\rightleftharpoons} H_2 + \tfrac{1}{2} O_2$$

have large positive heats of reaction,

$$\Delta h_{r1} = 283{,}388 \text{ J mol}^{-1}$$

$$\Delta h_{r2} = 242{,}174 \text{ J mol}^{-1}$$

and are therefore strong functions of temperature. As the temperature increases, the extent to which the dissociation reactions proceed increases dramatically. At the adiabatic flame temperature, substantial quantities of carbon monoxide, hydrogen, and other partially oxidized products may be present even if there is sufficient oxygen for complete combustion available. As the temperature decreases, chemical equilibrium favors the formation of the stable products, CO_2, H_2O, N_2, and O_2, and destruction of the less stable species, CO, H_2, NO, O, H, OH, and so on, as illustrated in Figure 2.7. Below about 1300 K, only the most stable species are present in significant quantities in the combustion products *at equilibrium*. The fact that carbon monoxide, nitrogen oxides, and unburned hydrocarbons are emitted from fuel-lean combustion systems implies, therefore, that chemical equilibrium is not maintained as the combustion products cool.

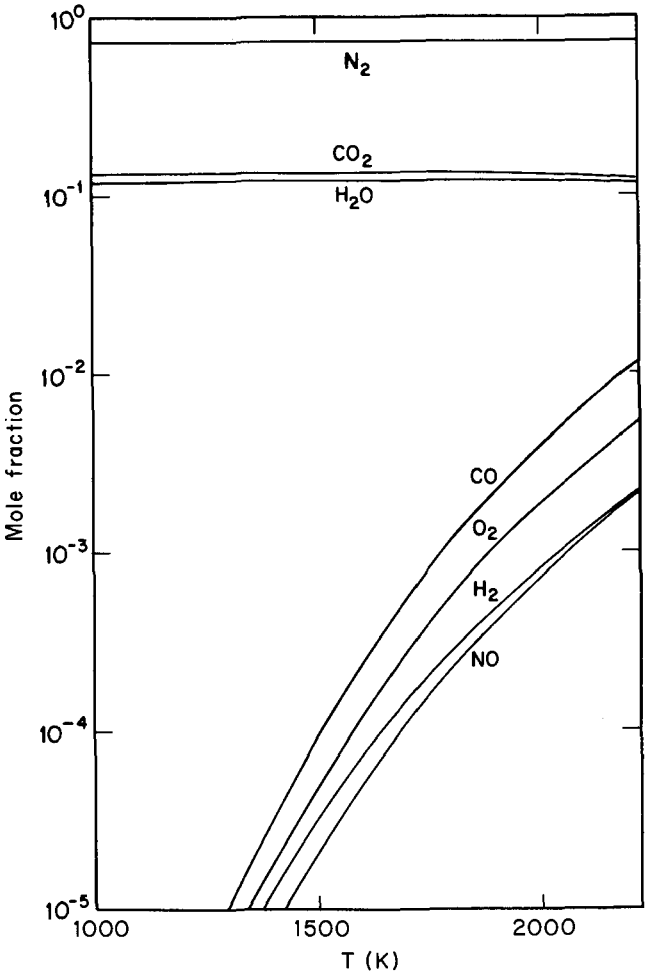

Figure 2.7 Variation of equilibrium composition with temperature for stoichiometric combustion of kerosene, $CH_{1.8}$.

2.4 COMBUSTION KINETICS

Chemical equilibrium describes the composition of the reaction products that would ultimately be reached if the system were maintained at constant temperature and pressure for a sufficiently long time. Chemical reactions proceed at finite rates, however, so equilibrium is not established instantaneously. We have seen that at equilibrium there would only be very small amounts of pollutants such as CO, NO, or unburned hydrocarbons in the gases emitted from combustors operated at equivalence ratios less than unity. Slow reactions allow the concentrations of these pollutants to be orders of magnitude greater than the equilibrium values when gases are finally emitted into the atmosphere. The sharp peak in the equilibrium NO concentration near $\phi = 1$ suggests that the amount of NO in the flame could be reduced significantly by reducing the equivalence ratio below about 0.5. Unfortunately, the combustion reactions also proceed at finite rates. Reducing the equivalence ratio lowers the temperature in the flame, thereby slowing the hydrocarbon oxidation reactions and the initial approach to equilibrium within the flame. The residence time in combustion systems is limited, so reducing the combustion rate eventually results in the escape of partially reacted hydrocarbons and carbon monoxide.

To understand the chemical factors that control pollutant emissions, therefore, it is necessary to examine the rate at which a chemical system approaches its final equilibrium state. The study of these rate processes is called *chemical kinetics*. The *reaction mechanism*, or the sequence of reactions involved in the overall process, and the rates of the individual reactions must be known to describe the rate at which chemical equilibrium is approached. In this section we examine the chemical kinetics of hydrocarbon fuel combustion, beginning with an overview of the detailed kinetics. Several approximate descriptions of combustion kinetics will then be examined. The kinetics that directly govern pollutant emissions will be treated in Chapter 3.

2.4.1 Detailed Combustion Kinetics

Combustion mechanisms involve large numbers of reactions even for simple hydrocarbon fuels. Consider propane combustion for which the overall stoichiometry for complete combustion is

$$C_3H_8 + 5O_2 \longrightarrow 3CO_2 + 4H_2O$$

The combustion reactions must break 15 chemical bonds (C—C, C—H, O—O) and form 14 new ones (C—O, H—O). As described in Chapter 1, hydrocarbon oxidation involves a large number of elementary bimolecular reaction steps. The many elementary reactions that comprise the combustion process generate intermediate species that undergo rapid reaction and, therefore, are not present in significant quantities in either the reactants or the products. A detailed description of combustion must include the intermediate species.

Detailed simulation of the chemical kinetics of combustion becomes quite formidable, even for simple, low-molecular-weight hydrocarbons such as CH_4, C_2H_2, C_2H_4, C_2H_6, C_3H_8, CH_3OH, and so on. Numerous studies of combustion mechanisms of such

simple fuels have been presented (Westbrook and Dryer, 1981a; Miller et al., 1982; Vandooren and Van Tiggelen, 1981; Westbrook, 1982; Venkat et al., 1982; Warnatz, 1984). Rate constants have been measured for many, but not all, of the 100 or so reactions in these mechanisms.

The description of the combustion kinetics for practical fuels is complicated by our incomplete knowledge of the fuel composition. Only rarely is the fuel composition sufficiently well known that detailed mechanisms could be applied directly, even if they were available for all the components of the fuel.

Our ultimate goal here is to develop an understanding of the processes that govern the formation and destruction of pollutants in practical combustion systems. Once combustion is initiated (as described below), the combustion reactions generally proceed rapidly. Such pollutant formation processes involve slow reaction steps or physical processes that restrain the approach to equilibrium, either during combustion or as the combustion products cool, and lead to unoxidized or partially oxidized fuel or intermediate species in the exhaust gases. Let us first examine the important features common to hydrocarbon combustion reaction mechanisms.

A mixture of a hydrocarbon (RH) fuel with air at normal ambient temperature will not react unless an ignition source is present. When the mixture is heated, the fuel eventually begins to react with oxygen. *Initiation* of the combustion reactions is generally thought to occur via the abstraction of a hydrogen atom from the hydrocarbon molecule by an oxygen molecule.

$$\mathrm{RH} + \mathrm{O_2} \xrightarrow{1} \mathrm{R}\cdot + \mathrm{HO_2}\cdot$$

An alternative initiation reaction for large hydrocarbon molecules is thermally induced dissociation to produce hydrocarbon radicals, that is,

$$\mathrm{RR'} + \mathrm{M} \xrightarrow{2} \mathrm{R}\cdot + \mathrm{R'}\cdot + \mathrm{M}$$

This reaction involves breaking a carbon–carbon or carbon–hydrogen bond. The energy required for bond breakage can be estimated using the bond strengths summarized in Table 2.6. Hydrogen abstraction reactions (reaction 1) involve breaking a carbon–hydrogen bond with a strength ranging from 385 to 453 kJ $\mathrm{mol^{-1}}$ and forming $\mathrm{HO_2}$, leading to a net energy of reaction of 190 to 250 kJ $\mathrm{mol^{-1}}$. Reaction 2 involves breaking a carbon–carbon bond. The single bond requires 369 kJ $\mathrm{mol^{-1}}$, with double and triple bonds requiring considerably more energy. Thus both reactions are endothermic, with reaction 2 having a significantly larger enthalpy of reaction since no new bonds are formed as the initial bond is broken.

The large enthalpy of reaction makes the reaction rate in the endothermic direction a strong function of temperature. Detailed balancing provided us with a relationship between the forward and reverse rate constants for elementary reactions, that is,

$$\frac{k_f(T)}{k_r(T)} = K_c(T)$$

TABLE 2.6 TYPICAL BOND STRENGTHS

Bond	kJ mol^{-1}
Diatomic Molecules	
H—H	437
H—O	429
H—N	360
C—N	729
C—O	1076
N—N	950
N—O	627
O—O	498
Polyatomic Molecules	
H—CH	453
H—CH_2	436
H—CH_3	436
H—C_2H_3	436
H—C_2H_5	411
H—C_3H_5	356
H—C_6H_5	432
H—CHO	385
H—NH_2	432
H—OH	499
HC≡CH	964
H_2C=CH_2	699
H_3C—CH_3	369
O=CO	536

The temperature dependence of the equilibrium constant can be expressed approximately using van't Hoff's relation (2.42),

$$K_p(T) \approx \left\{ K_p(T_1) \exp\left[\frac{\Delta h_r(T_1)}{RT_1} \right] \right\} \exp\left[-\frac{\Delta h_r(T)}{RT} \right]$$

$$\approx B(T_1) \exp\left[-\frac{\Delta h_r(T)}{RT} \right]$$

and the definition of $K_p(T)$, (2.38). Thus the rate constant in the forward direction is

$$k_f(T) = k_r(T)\, B(T_1) \exp\left[-\frac{\Delta h_r(T_1)}{RT} \right] [RT]^{-1}$$

Consider, for example, the dissociation of methane

$$CH_4 + M \underset{k_r}{\overset{k_f}{\rightleftharpoons}} CH_3\cdot + H\cdot + M$$

for which $k_r = 0.282T \exp[-9835/T]$ $m^6\ mol^{-2}\ s^{-1}$ (Westbrook, 1982). From the thermochemical property data of Table 2.5 and application of van't Hoff's relation, we find

$$K_p(T) = 4.11 \times 10^7 \exp\left[\frac{-34{,}700}{T}\right] \text{ atm}$$

from which we find

$$k_f(T) = k_r(T)\, K_p(T)\, [RT]^{-1}$$

$$= 1.41 \times 10^{11} \exp\left[\frac{-44{,}535}{T}\right] \text{ m}^3\ \text{mol}^{-1}\ \text{s}^{-1}$$

While the rate of the exothermic recombination reaction is, in this case, a strong function of temperature, the endothermic dissociation reaction is even more strongly dependent on temperature. In cases where the temperature dependence of rate coefficients results entirely from the exponential factor, that is, the rates are of the Arrheneus form, $k = A \exp(-E/RT)$, a plot of log k versus T^{-1}, known as an Arrheneus plot, clearly illustrates the influence of the large positive enthalpy of reaction on the temperature dependence of the rate of this reaction. The slope of the rate curve, shown in Figure 2.8, is equal to $-(\ln 10)^{-1}(E/R)$ and thus indicates the activation energy. The rates of exothermic or mildly endothermic reactions may be fast or slow for a variety of reasons as discussed in Chapter 1, but in general, highly endothermic reactions are slow except at very high temperatures.

Because of the relatively low rates of the highly endothermic initiation reactions, radicals are generated very slowly. After the radicals have accumulated for a period of time, their concentrations become high enough for the faster radical chemistry to become important. This delay between the onset of the initiation reactions and rapid combustion is called an induction period or ignition delay. After this delay, other reactions dominate the oxidation of the fuel and the initiation reactions are no longer important.

Hydrocarbon radicals react rapidly (due to low activation energies) with the abundant oxygen molecules to produce peroxy radicals

$$\text{R}\cdot + \text{O}_2 + \text{M} \xrightarrow{3} \text{RO}_2\cdot + \text{M}$$

or olefins (alkenes, R = R′) and the hydroperoxyl radical

$$\text{R}\cdot + \text{O}_2 \xrightarrow{4} \text{olefin} + \text{HO}_2\cdot$$

The olefin is then oxidized in a manner similar to the original hydrocarbon. Peroxy radicals undergo dissociation at high temperatures:

$$\text{RO}_2\cdot + \text{M} \xrightarrow{5} \text{R'CHO} + \text{R''}\cdot + \text{M}$$

These are called *chain carrying* reactions since the number of radicals produced equals the number consumed. The aldehydes (RCHO) may react with O_2:

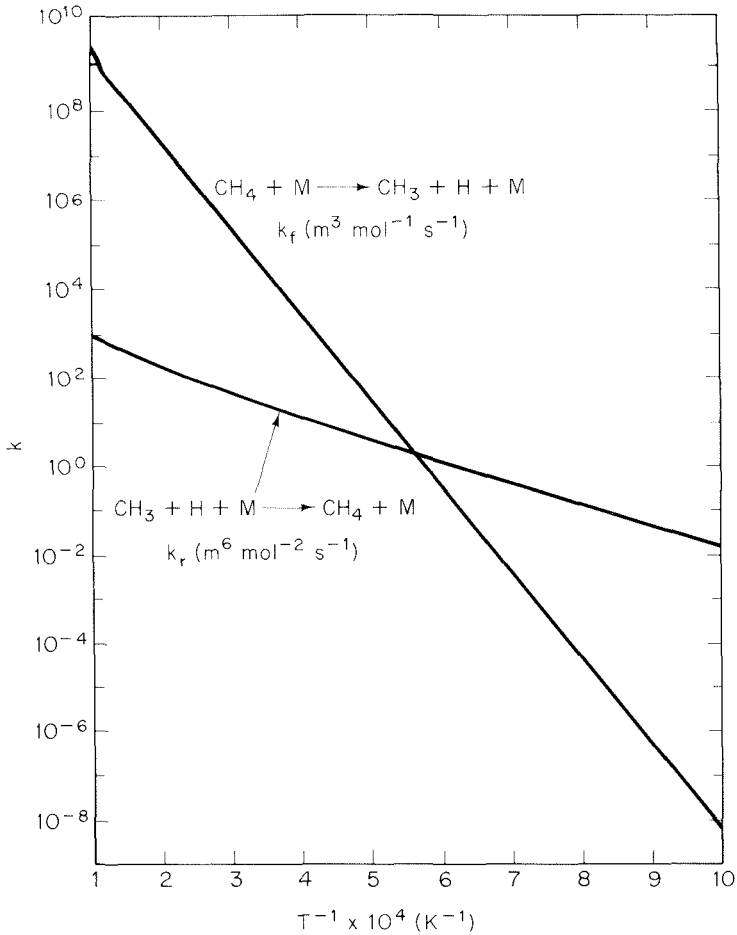

Figure 2.8 Reaction rate constants for forward and reverse reactions associated with methane decomposition.

$$\text{RCHO} + \text{O}_2 \xrightarrow{6} \text{R}\dot{\text{C}}\text{O} + \text{HO}_2\cdot$$

In the terminology of chain reactions, 6 is called a *branching* reaction since it increases the number of free radicals. The hydroperoxyl radicals rapidly react with the abundant fuel molecules to produce hydrogen peroxide:

$$\text{HO}_2\cdot + \text{RH} \xrightarrow{7} \text{HOOH} + \text{R}\cdot$$

Actually the single most important reaction in combustion is the chain-branching step:

$$\text{H}\cdot + \text{O}_2 \xrightarrow{8} \text{OH}\cdot + \text{O}\cdot$$

since it generates the OH and O needed for oxidation of the fuel molecules. The highly reactive hydroxyl radical reacts readily with the abundant fuel molecules:

$$OH\cdot + RH \xrightarrow{9} R\cdot + H_2O$$

At temperatures greater than about 1200 K, the hydroxyl radical is generally abundant enough to participate in a number of exchange reactions, generating much larger numbers of H·, O·, and OH· radicals than are present at lower temperatures:

$$OH\cdot + OH\cdot \overset{10}{\rightleftharpoons} H_2O + O\cdot$$

$$OH\cdot + O\cdot \overset{11}{\rightleftharpoons} H\cdot + O_2$$

$$OH\cdot + H\cdot \overset{12}{\rightleftharpoons} O\cdot + H_2$$

$$H_2 + OH\cdot \overset{13}{\rightleftharpoons} H_2O + H\cdot$$

$$H_2 + HO_2\cdot \overset{14}{\rightleftharpoons} H_2O + OH\cdot$$

$$HO_2\cdot + H\cdot \overset{15}{\rightleftharpoons} OH\cdot + OH\cdot$$

These reversible reactions are all mildly (8 to 72 kJ mol^{-1}) exothermic. The rate constants for these reactions have been determined experimentally and approach the rate corresponding to the frequency of collisions between the relevant radicals and molecules [i.e., the so-called gas kinetic limit represented by (A.11)]. The O· and H· radicals are, like hydroxyl, highly reactive. They rapidly react with the fuel molecules and hydrocarbon intermediates,

$$O\cdot + RH \overset{16}{\rightleftharpoons} R\cdot + OH\cdot$$

$$H\cdot + RH \overset{17}{\rightleftharpoons} R\cdot + H_2$$

The pool of radicals generated by these reactions drives the combustion reactions rapidly once the mixture is ignited.

The formation of carbon monoxide during this early phase of hydrocarbon oxidation occurs primarily by thermal decomposition of RCO radicals at high temperatures,

$$R\dot{C}O + M \overset{18}{\rightleftharpoons} R\cdot + CO + M$$

The dominant carbon monoxide oxidation process is the reaction with hydroxyl,

$$CO + OH\cdot \overset{19}{\rightleftharpoons} CO_2 + H\cdot$$

Three-body recombination reactions,

$$H\cdot + H\cdot + M \overset{20}{\rightleftharpoons} H_2 + M$$

$$H\cdot + OH\cdot + M \overset{21}{\rightleftharpoons} H_2O + M$$

$$O\cdot + O\cdot + M \overset{22}{\rightleftharpoons} O_2 + M$$

$$H\cdot + O_2 + M \overset{23}{\rightleftharpoons} HO_2\cdot + M$$

$$OH\cdot + OH\cdot + M \overset{24}{\rightleftharpoons} HOOH + M$$

reduce the total number of moles in the system. These reactions are exothermic but relatively slow since they require the intervention of a third molecule to stabilize the product. As combustion products cool, the slow recombination steps may allow radical concentrations to persist long after the equilibrium concentrations have dropped to extremely low levels.

Even though we have not attempted to list all the free-radical reactions involved in the combustion of hydrocarbons, we have already identified a large number of reactions. Detailed mechanisms for specific hydrocarbon molecules typically involve more than 100 reactions. It is noteworthy that the most important reactions in combustion, the chain branching reactions, do not involve the fuel molecules. This fact permits prediction of gross combustion features without full knowledge of the detailed reaction mechanism.

The mechanisms for different fuels involve common submechanisms (Westbrook and Dryer, 1981b). Combustion of carbon monoxide in the presence of hydrogen or water vapor involves the reactions of the hydrogen-oxygen mechanism. The combined CO–H_2–O_2 mechanism is, in turn, part of the mechanism for formaldehyde oxidation, which is a subset of the methane mechanism. In combustion of methane under fuel-lean conditions the carbon atom follows the sequence: $CH_4 \rightarrow CH_3 \rightarrow HCHO \rightarrow HCO \rightarrow CO \rightarrow CO_2$. Westbrook and Dryer (1981b) develop this hierarchical approach for fuels through C_2 and C_3 hydrocarbons, providing a framework for understanding the detailed combustion kinetics for a range of hydrocarbon fuels using as a starting point for each successive fuel the knowledge of the mechanisms of the simpler fuels. More complicated molecules, such as aromatic hydrocarbons (Venkat et al., 1982), will introduce additional reactions into this hierarchy, but the reactions already identified in studies of simpler molecules still contribute to the expanded overall mechanisms.

A detailed description of the dynamics of so many simultaneous reactions requires solution of a large number of simultaneous ordinary differential equations. The large enthalpies of combustion reaction and relatively slow heat transfer from a flame lead to large temperature changes during combustion. The first law of thermodynamics must be applied to evaluate the temperatures continuously throughout the combustion process. The large temperature changes result in very large changes in the many reaction rate constants. The integration of these rate equations is difficult since the equations contain several very different time scales, from the very short times of the free-radical reactions to the longer times of the initiation reactions. Such sets of equations are called *stiff*.

Since much of the chemistry with which we shall be concerned in our study of the

formation and destruction of pollutants takes place late in the combustion process, a complete description of the combustion process is not generally required for our purposes. Hydrocarbon oxidation in combustion is generally fast, leading to a rapid approach to equilibrium. This is fortunate since detailed combustion mechanisms are simply not known for many practical fuels such as coal or heavy fuel oils. Simplified models of the combustion process will, for these reasons, be used extensively in the discussion to follow.

2.4.2 Simplified Combustion Kinetics

One way to overcome the difficulties in modeling the combustion reactions is to represent the process by a small number of artificial reactions, each of which describes the results of a number of fundamental reaction steps. These so-called *global mechanisms* are stoichiometric relationships for which approximate kinetic expressions may be developed. Global reaction rate expressions may be derived from detailed kinetic mechanisms by making appropriate simplifying assumptions (e.g., steady-state or partial-equilibrium assumptions, which will be discussed later). Alternatively, correlations of observed species concentration profiles, flame velocity measurements, or other experimental data may be used to estimate global rate parameters.

Global mechanisms greatly reduce the complexity of kinetic calculations since a small number of steps are used to describe the behavior of a large number of reactions. Moreover, the simplified reactions generally involve the major stable species, greatly reducing the number of chemical species to be followed. This reduction may be either quite useful or an oversimplification, depending on the use to which the mechanism is to be put. If a combustion mechanism is to be used to describe the net rate of heat release during combustion, minor species are of little concern and a global mechanism can be quite effective. The minor species, on the other hand, strongly influence the formation of pollutants, and the simplified global mechanisms therefore may not contain sufficient chemical detail to describe the pollutant formation steps.

The simplest model of hydrocarbon combustion kinetics is the one-step, global model given at the beginning of Section 2.2,

$$C_nH_m + \left(n + \frac{m}{4}\right) O_2 \xrightarrow{k_{ov}} n\,CO_2 + \frac{m}{2} H_2O$$

where the subscript ov refers to "overall" model. The rate of this reaction can be expressed empirically by

$$R_{ov} = AT^n \exp\left(\frac{-E_a}{RT}\right) [C_nH_m]^a [O_2]^b \tag{2.49}$$

where the parameters A, n, E_a, a, and b are generally determined by matching R_{ov} to the observed oxidation rate inferred from flame speed or the rich and lean limits of stable laminar flames. The obvious advantage of the single-step model is its simplicity. It is very useful for calculating heat release rates and for examining flame stability. Unfor-

tunately, the single-step model does not include intermediate hydrocarbon species or carbon monoxide.

The hydrocarbons are rapidly consumed during combustion, forming CO, H_2, and H_2O. The oxidation of CO to CO_2 proceeds somewhat more slowly. The difference in reaction rates can be taken into account using two-step models that are only slightly more complicated than the single-step model but can separate the relatively slow oxidation of CO to CO_2 from the more rapid oxidation of the hydrocarbon to CO and H_2O (Hautman et al., 1981), that is,

$$C_nH_m + \left(\frac{n}{2} + \frac{m}{4}\right) O_2 \xrightarrow{k_A} nCO + \frac{m}{2} H_2O$$

$$CO + \tfrac{1}{2} O_2 \xrightarrow{k_B} CO_2$$

This description lumps together reactions 1–18 and 20–24 from the detailed mechanism of Section 2.4.1, with reaction 19 being treated separately. The rate for reaction A is generally expressed in the same empirically derived form as the hydrocarbon oxidation in the single-step model

$$R_A = A_A T^{n_A} \exp\left[\frac{-E_A}{RT}\right] [C_nH_m]^a [O_2]^b \tag{2.50}$$

Carbon monoxide oxidation is described empirically by

$$R_B = A_B T^{n_B} \exp\left[\frac{-E_B}{RT}\right] [H_2O]^c [O_2]^d [CO] \tag{2.51}$$

where the dependence on $[H_2O]$ may be determined empirically or estimated based on kinetic arguments as noted below. The inclusion of H_2O in the rate expression can be explained because most CO is consumed by reaction with OH that, to a first approximation, may be assumed to be in equilibrium with water.

Westbrook and Dryer (1981b) have used flammability limit data (the minimum and maximum equivalence ratios for sustained combustion) and flame speed data (which we will discuss shortly) for a variety of hydrocarbon fuels to determine the rate parameters for the various approximate combustion models. These parameters are summarized in Table 2.7. For each mechanism, the rate of the hydrocarbon consumption has been fitted to the form

$$r = A \exp\left(\frac{-E_a}{RT}\right) [\text{fuel}]^a [O_2]^b \tag{2.52}$$

For the two-step model, the oxidation of CO,

$$CO + \tfrac{1}{2} O_2 \longrightarrow CO_2$$

might, to a first approximation, be described using the global rate from Dryer and Glassman (1973):

$$r_f = 1.3 \times 10^{10} \exp\left(\frac{-20{,}130}{T}\right) [CO] [H_2O]^{0.5} [O_2]^{0.25} \text{ mol m}^{-3} \text{ s}^{-1} \tag{2.53}$$

TABLE 2.7 RATE PARAMETERS FOR QUASI-GLOBAL REACTION MECHANISMS GIVING BEST AGREEMENT BETWEEN EXPERIMENTAL AND COMPUTED FLAMMABILITY LIMITS[a]

	Single-step mechanism $C_nH_m + \left(n + \frac{m}{4}\right) O_2 \rightarrow nCO_2 + \frac{m}{2} H_2O$				Two-step mechanism $C_nH_m + \left(\frac{n}{2} + \frac{m}{4}\right) O_2 \rightarrow nCO + \frac{m}{2} H_2O$				Quasi-global mechanism $C_nH_m + \frac{n}{2} O_2 \rightarrow nCO + \frac{m}{2} H_2$			
Fuel	$A \times 10^{-6}$	$(E_a/R) \times 10^{-3}$	a	b	$A \times 10^{-6}$	$(E_a/R) \times 10^{-3}$	a	b	$A \times 10^{-6}$	$(E_a/R) \times 10^{-3}$	a	b
CH_4	130	24.4	−0.3	1.3	2800	24.4	−0.3	1.3	4000	24.4	−0.3	1.3
C_2H_6	34	15.0	0.1	1.65	41	15.0	0.1	1.65	63	15.0	0.3	1.3
C_3H_8	27	15.0	0.1	1.65	31	15.0	0.1	1.65	47	15.0	0.1	1.65
C_4H_{10}	23	15.0	0.15	1.6	27	15.0	0.15	1.6	41	15.0	0.15	1.6
C_5H_{12}	20	15.0	0.25	1.5	24	15.0	0.25	1.5	37	15.0	0.25	1.5
C_6H_{14}	18	15.0	0.25	1.5	22	15.0	0.25	1.5	34	15.0	0.25	1.5
C_7H_{16}	16	15.0	0.25	1.5	19	15.0	0.25	1.5	31	15.0	0.25	1.5
C_8H_{18}	14	15.0	0.25	1.5	18	15.0	0.25	1.5	29	15.0	0.25	1.5
C_9H_{20}	13	15.0	0.25	1.5	16	15.0	0.25	1.5	27	15.0	0.25	1.5
$C_{10}H_{22}$	12	15.0	0.25	1.5	14	15.0	0.25	1.5	25	15.0	0.25	1.5
CH_3OH	101	15.0	0.25	1.5	117	15.0	0.25	1.5	230	15.0	0.25	1.5
C_2H_5OH	47	15.0	0.15	1.6	56	15.0	0.15	1.6	113	15.0	0.15	1.6
C_6H_6	6	15.0	−0.1	1.85	7	15.0	−0.1	1.85	13	15.0	−0.1	1.85
C_7H_8	5	15.0	−0.1	1.85	6	15.0	−0.1	1.85	10	15.0	−0.1	1.85
C_2H_4	63	15.0	0.1	1.65	75	15.0	0.1	1.65	136	15.0	0.1	1.65
C_3H_6	13	15.0	−0.1	1.85	15	15.0	−0.1	1.85	25	15.0	−0.1	1.85
C_2H_2	205	15.0	0.5	1.25	246	15.0	0.5	1.25	379	15.0	0.5	1.25

[a]Units: *m*, s, *mol*, K.

Source: Westbrook and Dryer, 1981b.

The rate of the reverse of the CO oxidation reaction was estimated by Westbrook and Dryer (1981b) to be

$$r_r = 1.6 \times 10^7 \exp\left(\frac{-20{,}130}{T}\right) [CO_2][H_2O]^{0.5}[O_2]^{-0.25} \text{ mol m}^{-3} \text{ s}^{-1} \quad (2.54)$$

One must be cautious in using such rate expressions. Since (2.53) and (2.54) were obtained from flame observations, they may not be appropriate to postflame burnout of CO. This issue will be addressed in Chapter 3 when we discuss the CO emission problem.

Lumping all the reactions that lead to CO formation into a single step means that the dynamics of these reactions can only be described approximately. The endothermic initiation reactions proceed slowly for some time before the radical population becomes large enough for rapid consumption of fuel and O_2. Little CO is produced during this ignition delay, so efforts to model CO formation frequently overlook the initiation process. Assuming direct production of H_2O means the transients in the production and equilibration of H, OH, O, HO_2, and so on, are not described. Thus the two-step model does not accurately describe the processes occurring early in combustion. It is, however, a marked improvement over the single-step model in that it allows CO oxidation to proceed more slowly than fuel consumption. Although the two-step model does not adequately describe processes occurring early in combustion, the omission of the radical chemistry is not serious if one is primarily interested in processes that take place after the main combustion reactions are complete (e.g., the highly endothermic oxidation of N_2 to form NO).

Additional reactions can be incorporated to develop quasi-global reaction mechanisms with improved agreement between calculations and experimental observations while avoiding the complications and uncertainties in describing detailed hydrocarbon oxidation kinetics. Edelman and Fortune (1969) pushed this process toward its logical limit, describing the oxidation of the fuel to form CO and H_2 by a single reaction and then using the detailed reaction mechanisms for CO and H_2 oxidation. Because all the elementary reactions and species in the CO–H_2–O_2 system are included, this approach can provide an accurate description of the approach to equilibrium and of postflame processes such as nitric oxide formation from N_2 and CO burnout as the combustion products are cooled.

The quasi-global model requires oxidation rates for both CO and H_2. Although lumped reaction models can be used, the major advantage of the quasi-global model is that it can be used in conjunction with a detailed description of the final stages of combustion. Westbrook and Dryer (1981b) compared the flame structure predictions of the quasi-global model with those of a detailed mechanism for methanol-air flames. The reactions and corresponding rate coefficients for the CO–H_2–O_2 system that were needed for the quasi-global model are summarized in Table 2.8. Predictions of temperature profiles, fuel concentrations, and general flame structure are in close agreement for the two models. The predicted concentrations of CO and radical species (O, H, and OH) showed qualitatively different behavior for the two models because reactions of the radicals with unburned fuel are not taken into account in the quasi-global model.

TABLE 2.8 C–H–O KINETIC MECHANISM

Reaction	k_f (units: m^3, mol, K, s)	Reference
	CO oxidation	
$CO + OH \rightleftarrows CO_2 + H$	$4.4\ T^{1.5} \exp(+373/T)$	Warnatz (1984)
$CO + O_2 \rightleftarrows CO_2 + O$	$2.5 \times 10^6 \exp(-24{,}060/T)$	Warnatz (1984)
$CO + O + M \rightleftarrows CO_2 + M$	$5.3 \times 10^1 \exp(+2285/T)$	Warnatz (1984)
$CO + HO_2 \rightleftarrows CO_2 + OH$	$1.5 \times 10^8 \exp(-11{,}900/T)$	Westbrook and Dryer (1981a)
	Exchange reactions	
$H + O_2 \rightleftarrows O + OH$	$1.2 \times 10^{11}\ T^{-0.91} \exp(-8310/T)$	Warnatz (1984)
$H_2 + O \rightleftarrows H + OH$	$1.5 \times 10^1\ T^2 \exp(-3800/T)$	Warnatz (1984)
$O + H_2O \rightleftarrows OH + OH$	$1.5 \times 10^4\ T^{1.14} \exp(-8680/T)$	Warnatz (1984)
$OH + H_2 \rightleftarrows H + H_2O$	$1.0 \times 10^2\ T^{1.6} \exp(-1660/T)$	Warnatz (1984)
$O + HO_2 \rightleftarrows O_2 + OH$	2.0×10^7	Warnatz (1984)
$H + HO_2 \rightleftarrows OH + OH$	$1.5 \times 10^8 \exp(-500/T)$	Warnatz (1984)
$H + HO_2 \rightleftarrows H_2 + O_2$	$2.5 \times 10^7 \exp(-350/T)$	Warnatz (1984)
$OH + HO_2 \rightleftarrows H_2O + O_2$	2.0×10^7	Warnatz (1984)
$HO_2 + HO_2 \rightleftarrows H_2O_2 + O_2$	2.0×10^7	Warnatz (1984)
	Recombination reactions	
$H + O_2 + M \rightleftarrows HO_2 + M$	$1.5 \times 10^3 \exp(-500/T)$	Westbrook and Dryer (1984)
$OH + OH + M \rightleftarrows H_2O_2 + M$	$9.1 \times 10^2 \exp(+2550/T)$	Westbrook and Dryer (1984)
$O + H + M \rightleftarrows OH + M$	1.0×10^4	Westbrook and Dryer (1984)
$O + O + M \rightleftarrows O_2 + M$	$1.0 \times 10^5\ T^{-1}$	Warnatz (1984)
$H + H + M \rightleftarrows H_2 + M$	$6.4 \times 10^5\ T^{-1}$	Warnatz (1984)
$H + OH + M \rightleftarrows H_2O + M$	$1.41 \times 10^{11}\ T^{-2}$	Warnatz (1984)

Quasi-global rate models may be suitable for the systems from which they were derived, but caution must be exercised in their use. Assumptions made in their derivation or the conditions of the particular experiment used in the estimation of the rate parameters strongly influence the predicted rates. For example, different preexponential factors must be used for flow systems and stirred reactors (Edelman and Fortune, 1969) and for flames (Westbrook and Dryer, 1981b). Nevertheless, quasi-global models often represent a practical compromise between comprehensive kinetic mechanisms based entirely on elementary reaction steps and simple one-step models of the combustion process.

While the chemical kinetics of combustion describe much of what happens when a fuel burns, chemical kinetics alone cannot describe combustion in practical systems. Calculations of the rate of combustion reactions, using either detailed combustion mechanisms or global models, reveal that the reactions proceed extremely slowly unless the temperature exceeds a critical value. To understand combustion, therefore, we need to examine the physical processes that heat the reactants to this temperature so that reaction can take place.

2.5 FLAME PROPAGATION AND STRUCTURE

We now turn our attention from combustion thermochemistry to the physical processes that govern the way fuels burn. One of the striking features of most combustion is the existence of a flame, a luminous region in the gas that is associated with the major heat release. Some flames, such as that of a candle, are relatively steady, whereas others fluctuate wildly due to turbulent motions of the gas. The flame is a reaction front created by diffusion of energy or free radicals from the hot burned gases into the cooler unreacted gas or by the mixing of fuel and air.

A flame that is stabilized at a fixed location is actually propagating into a flow of fuel and/or air. In this case the propagation velocity must match the gas velocity for the flame itself to remain fixed in space. This is illustrated schematically in Figure 2.9(a) for the bunsen burner flame. Here a mixture of fuel and air is introduced through a pipe at a velocity, v. The flame appears as a conical region of luminosity above the pipe outlet. The height of the conical flame depends on the gas velocity; that is, low velocities produce short flames while higher velocities produce longer flames. The shape of the flame is determined by the way the reaction propagates from hot burned gases into cooler unburned gases. We shall see that the reaction front moves into the unburned gases at a velocity that is determined by the combined effects of molecular diffusion and chemical kinetics. This propagation velocity is the laminar flame speed, S_L. If the gas velocity, v, is greater than S_L, the flame assumes a shape such that the component of the gas velocity normal to the flame exactly balances the flame speed, as illustrated in Figure 2.9(a).

The gas velocity at the wall is zero, allowing the flame to propagate close to the burner outlet. Heat transfer to the pipe prevents the flow from propagating into the pipe in normal operation, so the flame is stabilized at the pipe outlet by the combined effects of diffusion and heat transfer.

When, as in the bunsen burner flame, a gaseous fuel and air are uniformly mixed prior to combustion, a *premixed flame* results. Such a combustible mixture can easily explode, so premixed combustion is used in relatively few systems of practical importance; for example, laboratory bunsen and Meeker burners mix fuel and air prior to combustion, the carburetor on an automobile engine atomizes liquid gasoline into the combustion air in order to achieve premixed combustion, and some premixing of fuel and air takes place in gas cooking stoves.

Within the automobile engine immediately prior to combustion, there is no flow. Combustion is initiated by a spark and then propagates through the mixture as illustrated in Figure 2.9(b). In spite of the different appearances of these two flames, the physics and chemistry that govern the structure of the propagating flame are the same as those of stabilized flames, although geometry and fluid motions can vary greatly from situation to situation.

More commonly, fuel and air enter the combustion zone separately and must mix before reaction is possible. The chemistry of the so-called *diffusion flame* that results cannot be described by a single equivalence ratio since, as illustrated in Figure 2.9(c), gases with the entire range of compositions, from pure air to pure fuel, are present in

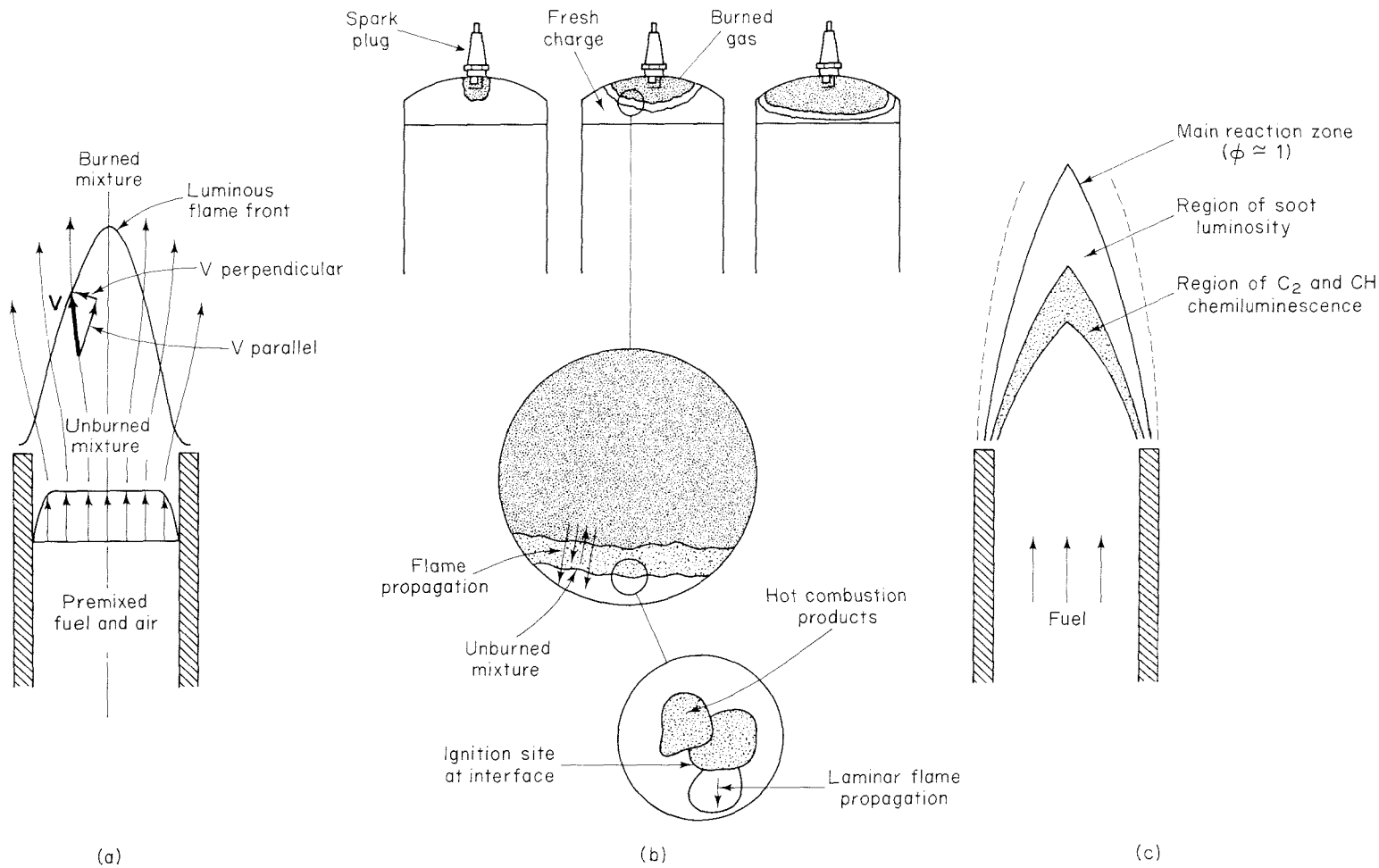

Figure 2.9 Flame propagation and structure: (a) bunsen burner flame; (b) spark ignition engine; (c) diffusion flame.

the combustion zone. An overall equivalence ratio may be useful in describing the net flow of fuel and air into the combustor, but that value does not correspond to the local composition (on a molecular scale) that governs combustion chemistry. Within the diffusion flame illustrated in Figure 2.9(c), there is a central core that contains pure gaseous fuel. This core is surrounded by a zone in which air diffuses inward and fuel diffuses outward. The visible flame front sits approximately at the location of stoichiometric composition in this zone. The different luminous zones correspond to regions in which chemiluminescent (or light-emitting) chemical reactions take place and in which soot (small carbonaceous particles) emits thermal radiation.

The shape of this diffusion flame is, as in the stabilized premixed flame, determined by the competition between flow and diffusion. The flame length increases as the fuel velocity increases. At sufficiently high fuel velocities, the flame ceases to be uniform in shape due to the onset of turbulence. The turbulent velocity fluctuations increase the rate at which fuel and air come into contact and, therefore, cause the flame to shorten as the velocity is increased further. Ultimately, as illustrated in Figure 2.10, the flame length approaches an asymptotic value.

Each of these flame types, the premixed flame and the diffusion flame, can be further subdivided into *laminar* and *turbulent* flames. Heat and mass transfer in laminar flames occur by molecular conduction and diffusion. In many systems, the existence of either laminar or turbulent flow is determined by the value of the Reynolds number

$$\mathrm{Re} \equiv \frac{\rho v L}{\mu}$$

a dimensionless ratio of inertial to viscous forces, where ρ is the gas density, v and L are characteristic velocity and length scales for the flow, and μ is the viscosity of the fluid. For example, the Reynolds number must be less than about 2200 to assure laminar

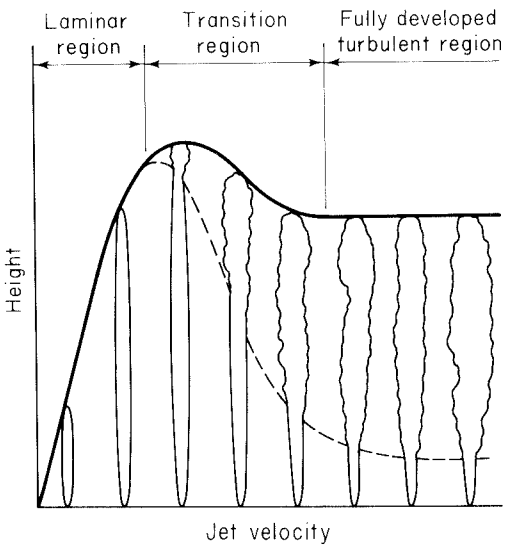

Figure 2.10 Diffusion flame length variation with fuel jet velocity.

flow in a pipe. Turbulence can, however, be promoted at Reynolds numbers below this value by flow obstructions.

Most flames of practical significance are turbulent. Even in turbulent flames, molecular diffusion plays an important role, albeit on a scale much smaller than that of the flow system. For this reason, we shall examine the structure of laminar flames before addressing turbulent flames.

Our primary objective is to understand those aspects of flame structure that directly influence the production of pollutants. The rate of flame spread and consumption of fuel determines whether combustion will be complete and how long the combustion products will reside at high temperature. Flame stability is also important since a flame that nearly extinguishes and reignites due to instabilities may allow combustion products or reaction intermediates to escape.

2.5.1 Laminar Premixed Flames

The simplest type of flame is the laminar premixed flame. From the study of these flames, we can explore important aspects of flame propagation. The propagation velocity, or *laminar flame speed*, is particularly important to our discussion since it determines how rapidly a fuel–air mixture is burned.

A conceptually simple laminar, premixed flame can be produced by flowing a fuel–air mixture through a porous plug, as illustrated in Figure 2.11. A luminous flame appears as a thin planar front that remains at a fixed distance from the porous plug. The fuel–air mixture passes through the plug with a velocity, v. For the flame to remain stationary, it must propagate at an equal and opposite velocity toward the fuel–air flow. The laminar flame speed, S_L, is the speed at which the flame propagates into the cold fuel–air mixture (i.e., $S_L = v$). The flame speed is determined by the rates of the combustion reactions and by diffusion of energy and species into the cold unreacted mixture. Heat transfer raises the gas temperature to the point that the combustion reactions can proceed at an appreciable rate. Free-radical diffusion supplies the radicals necessary for rapid combustion without the ignition delay that would result from the slow initiation reactions if only energy were transferred. Once reaction begins, combustion is very rapid, typically requiring on the order of 1 ms for completion. As a result, the flame is generally thin. The flat flame shown in Fig. 2.11 can exist only if the gas is supplied at a velocity below a limiting value that is determined by the rates of diffusion of energy and radicals ahead of the flame and of reaction within the flame. We shall use a simple model to examine how this balance between diffusion ahead of the flame and reaction within the flame determines the speed at which a flame will spread into a mixture of fuel and air.

The propagation of laminar flames has been the subject of numerous investigations since Mallard and LeChâtelier proposed in 1885 that conduction heating of the fuel–air mixture to an "ignition temperature" controls the propagation (Glassman, 1977). The ignition temperature is unfortunately not a well-defined quantity. Nonetheless, this model illustrates many of the important features of flame propagation without the complications of the more elaborate theories.

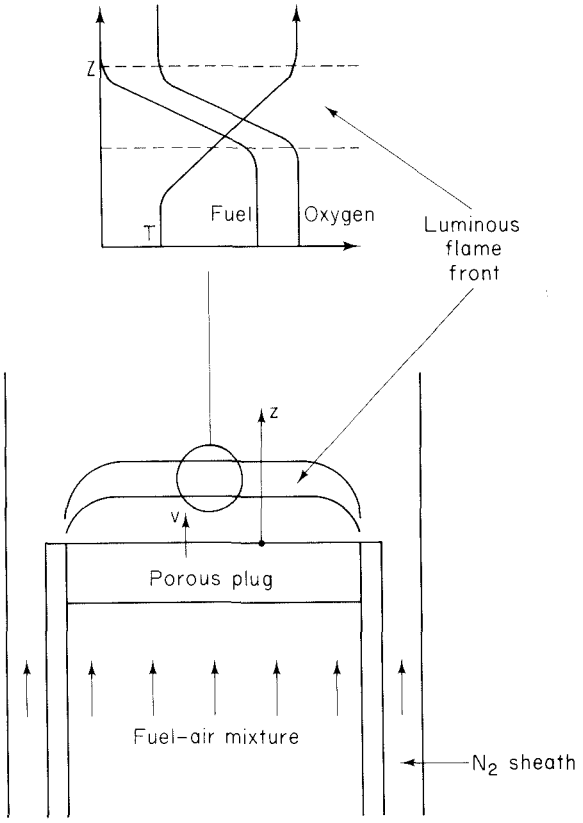

Figure 2.11 Porous plug burner with a flat flame.

Mallard and LeChâtelier stated that the heat conducted ahead* of the flame must, for steady propagation, be equal to that required to heat the unburned gases from their initial temperature, T_0, to the ignition temperature, T_i. The flame is then divided into two zones, as illustrated in Figure 2.12. The enthalpy rise of the fuel–air mixture in the preheat zone is $fc_p(T_i - T_0)$, where f is the mass flux through the flame front. This enthalpy must be supplied by conduction from the reaction zone. Thus we have

$$fc_p(T_i - T_0) = k\frac{dT}{dz} \tag{2.55}$$

where k is the thermal conductivity of the gas. The mass flux is directly related to the speed, S_L, at which the laminar flame propagates into the cold fuel–air mixture,

$$f = \rho_0 S_L \tag{2.56}$$

Approximating the temperature profile with a constant slope, $dT/dz = (T_f - T_i)/\delta$, where δ is the flame thickness and T_f is the adiabatic flame temperature, the laminar

*The terminology "ahead of the flame" customarily refers to the cold fuel/air mixture into which the flame is propagating.

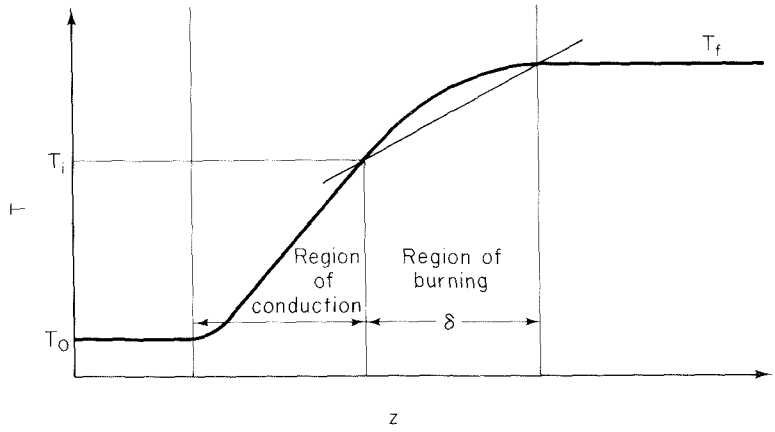

Figure 2.12 Two zones of a premixed flame.

flame speed becomes

$$S_L = \frac{k}{\rho_0 c_p} \frac{T_f - T_i}{T_i - T_0} \frac{1}{\delta} \tag{2.57}$$

The flame thickness is related to the flame speed and the characteristic time for the combustion reactions. Defining the characteristic reaction time as

$$\tau_c = \frac{[\text{fuel}]_0}{r_f} \tag{2.58}$$

where r_f is the overall fuel oxidation rate, the flame thickness becomes

$$\delta = S_L \tau_c = \frac{S_L [\text{fuel}]_0}{r_f} \tag{2.59}$$

Substituting into (2.57) and rearranging yields

$$S_L = \left[\frac{k}{\rho_0 c_p} \frac{T_f - T_i}{T_i - T_0} \frac{r_f}{[\text{fuel}]_0} \right]^{1/2} \tag{2.60}$$

Global oxidation rates such as (2.49) can be used to explore factors that influence the flame speed. It is apparent from (2.49) and (2.60) and the ideal gas law that

$$S_L \approx p^{(a+b-2)/2}$$

Since the overall reaction order $(a + b)$ for most hydrocarbon fuels is approximately two (see Table 2.7), the flame speed is seen to be only weakly dependent on pressure. The reaction rate is a highly nonlinear function of temperature due to the exponential term. Although the reaction may begin at lower temperature, most of the reaction takes place after the gases have been heated very nearly to the final temperature (i.e., near the adiabatic flame temperature). The activation energies for the combustion of most hydro-

carbon fuels are similar, as are the adiabatic flame temperatures and the thermal conductivities of the fuel–air mixtures. Thus one would expect flame velocities of different hydrocarbon fuels to be similar. The flame temperature is highest near stoichiometric combustion and drops significantly at lower or higher equivalence ratios.

Example 2.8 ***Laminar Flame Speed***

Use the single-step global rate expression for methane combustion to estimate the laminar flame speed for stoichiometric combustion in air with $T_0 = 298$ K and at $p = 1$ atm.

To estimate the laminar flame speed, we need to know the flame temperature, T_f, and the ignition temperature, T_i. T_f may be approximated by the adiabatic flame temperature. The combustion stoichiometry is

$$CH_4 + 2(O_2 + 3.78N_2) \longrightarrow CO_2 + 2H_2O + 7.56N_2$$

and the energy equation for adiabatic combustion becomes

$$[h(T) - h(T_0)]_{CO_2} + 2[h(T) - h(T_0)]_{H_2O} + 7.56[h(T) - h(T_0)]_{N_2}$$
$$+ \Delta h^\circ_{f,CO_2}(T_0) + 2\,\Delta h^\circ_{f,H_2O}(T_0) - \Delta h^\circ_{f,CH_4}(T_0) - 2\,\Delta h^\circ_{f,O_2}(T_0) = 0$$

Using the approximate thermodynamic data of Table 2.5, we recall that

$$[h(T) - h(T_0)]_i = \int_{T_0}^{T} c_{pi}\,dT' = \int_{T_0}^{T} (a_i + b_i T')\,dT' = a_i(T - T_0) + \frac{b_i}{2}(T^2 - T_0^2)$$

The necessary data are:

Species	Δh_f° (T_0) (J mol^{-1})	a	b
CH_4	−74,980	44.2539	0.02273
O_2	0	30.5041	0.00349
CO_2	−394,088	44.3191	0.00730
H_2O	−242,174	32.4766	0.00862
N_2	0	29.2313	0.00307

Substituting in the coefficient values, the energy equation become

$$330.26(T - T_0) + 0.02387(T^2 - T_0^2) - 803{,}456 = 0$$

or

$$0.02387T^2 - 330.26T - 904{,}045 = 0$$

which yields

$$T = 2341 \text{ K}$$

We now have an estimate for $T_f = 2341$ K. The global rate expression for methane combustion is (from Table 2.7)

$$r_{CH_4} = 1.3 \times 10^8 \exp\left(-\frac{24{,}400}{T}\right)[CH_4]^{-0.3}[O_2]^{1.3} \text{ mol m}^{-3}\text{ s}^{-1}$$

Since the reaction rate is a strong function of temperature, the characteristic time for the reaction should be evaluated near the peak temperature. At the adibatic flame temperature,

$$\tau_c = \frac{[CH_4]_0}{1.3 \times 10^8 \exp(-24{,}400/T)[CH_4]^{-0.3}[O_2]^{1.3}}$$

In the reactants, the species mole fractions are

$$y_{CH_4} = \frac{1}{10.56} = 0.0947$$

$$y_{O_2} = \frac{2}{10.56} = 0.189$$

Using the ideal gas law to calculate the concentrations, we find

$$\tau_c = 1.05 \times 10^{-4} \text{ s}$$

The heat transfer occurs at lower temperature. Evaluating the gas mixture properties at, say, 835 K (the geometric mean of the extreme values), we find for the mixture

$$\rho_0 = 0.403 \text{ kg m}^{-3}$$

$$\bar{c}_p = 1119 \text{ J kg}^{-1} \text{ K}^{-1}$$

As an approximation, we use the thermal conductivity for air,

$$k = 0.0595 \text{ J m}^{-1} \text{ K}^{-1} \text{ s}^{-1}$$

The ignition temperature should be near the flame temperature due to the exponential dependence of the reaction rate (Glassman, 1977). Substituting into (2.60) assuming that $T_i = 2100$ K yields

$$S_L = \left(\frac{0.0595 \text{ J m}^{-1} \text{ K}^{-1} \text{ s}^{-1}}{0.403 \text{ kg m}^{-3} \times 1119 \text{ J kg}^{-1} \text{ K}^{-1}} \times \frac{2341 - 2100}{2100 - 298} \times \frac{1}{1.05 \times 10^{-4} \text{ s}} \right)^{1/2}$$

$$= 0.41 \text{ m s}^{-1}$$

We may also examine the flame thickness using (2.59):

$$\delta = S_L \tau_c \approx 0.41 \text{ m s}^{-1} \times 1.05 \times 10^{-4} \text{ s}$$

$$\approx 4 \times 10^{-5} \text{ m}$$

$$\approx 0.04 \text{ mm}$$

Because the flame is so thin, studies of the structure of premixed flames are frequently conducted at reduced pressures to expand the flame.

2.5.2 Turbulent Premixed Flames

The automobile is the major practical system in which fuel and air are thoroughly mixed prior to burning. In the automobile engine, combustion takes place in a confined volume. Combustion is initiated in a small fraction of this volume by a spark. A flame spreads from the ignition site throughout the volume. The fluid motion in the cylinder is chaotic

due to the turbulence generated by the high-velocity flows through the intake valves and by motions induced as the piston compresses the gas.

The velocities of the random turbulent motions may far exceed the laminar flame velocity, leading to wild distortions of the flame front as it propagates. Figure 2.13 is a simplified schematic of the way that turbulent velocity fluctuations may influence the propagation of a premixed flame. Here we consider a flame front that is initially flat. If this flame were to propagate at the laminar flame speed, it would move a distance $S_L\,\delta t$ in a time δt. This motion is limited to propagation from the burned gas into the unburned gas. On the other hand, velocity fluctuations with a root-mean-square value of u' would distort the front between the burned and unburned gases about the initial flame-front location. Without bringing molecular diffusion into play, no molecular scale mixing of burned and unburned gases would take place, and the quantity of burned gas would not increase. The rate of diffusive propagation of the flame from the burned gases into the unburned gases is governed by a balance between molecular diffusion and the kinetics of the combustion reactions (i.e., the same factors that were considered in the original analysis of laminar flame propagation). Thus the propagation of the flame from the distorted front into the unburned gases is characterized by the laminar flame speed, and the position of the flame front after a small time is the combination of these two effects.

The microscales for the composition and velocity fluctuations in a turbulent flow, λ_c and the Taylor microscale, λ, respectively, discussed in Appendix D of Chapter 1,

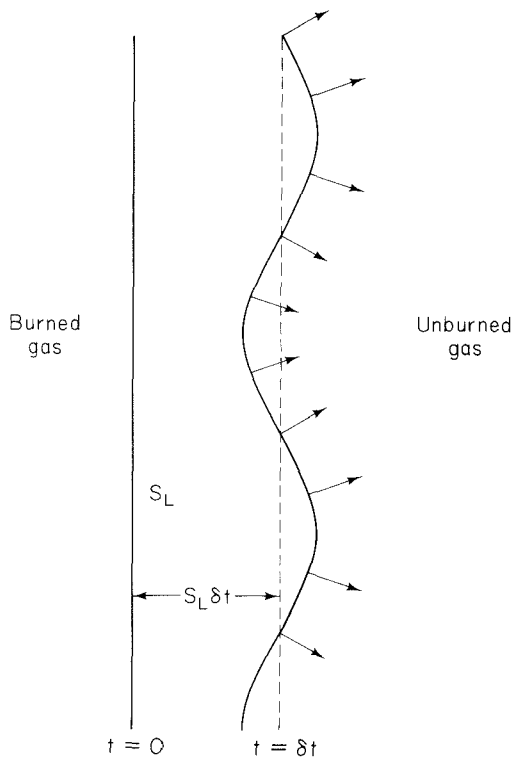

Figure 2.13 Enhancement of flame speed by turbulent motion.

are the scales that are characteristic of the fluctuations in the position of the flame front and, therefore, of the distance over which the flame must propagate diffusively. A time scale that characterizes the burning of the gas in these regions of entrained unburned gas is

$$\tau_b = \frac{\lambda_c}{S_L} \tag{2.61}$$

This time scale differs from that for dissipation of concentration fluctuations in nonreacting flows, (D.30),

$$\tau_d = \frac{\lambda^2}{6\nu}$$

since the rapid combustion reactions lead to large gradients in the flame front, enhancing the rate of diffusion of energy and radicals.

Observations of the small-scale structure of turbulent flow (Tennekes, 1968) provide important insights into the mechanism of turbulent flame propagation and the basis for a quantitative model of combustion rates and flame spread (Tabaczynski et al., 1977). Within the turbulent fluid motion, turbulent dissipation occurs in small so-called vortex tubes with length scales on the order of the Kolmogorov microscale, η (D.1). Chomiak (1970, 1972) postulated that the vortex tubes play an essential role in the flame propagation. When the combustion front reaches the vortex tube, the high shear rapidly propagates the combustion across the tube. The burned gases expand, increasing the pressure in the burned region of the vortex tube relative to the unburned region, providing the driving force for the motion of the hot burned gases toward the cold gases and leading to rapid propagation of the flame along the vortex tube with a velocity that is proportional to u', the turbulent intensity.

In contrast to the vigorous shear in the vortex tubes, the fluid between the tubes is envisioned to be relatively quiescent. The flame propagates in these regions through the action of molecular diffusion of heat and mass (i.e., at the laminar flame speed, S_L). The distance over which the flame must spread by diffusion is the spacing between the vortex tubes. This distance is assumed to be characterized by the composition microscale, λ_c.

This model for turbulent premixed flame propagation is illustrated in Figure 2.14. Ignition sites propagate at a velocity that is the sum of the local turbulent velocity fluctuation and the laminar flame speed, $u' + S_L$. The rate at which mass is engulfed within the flame front can be expressed as

$$\frac{dm_e}{dt} = \rho_u A_e (u' + S_L) \tag{2.62}$$

where m_e is the mass engulfed into the flame front, ρ_u is the density of the unburned gas, and A_e is the flame front area.

Once unburned fluid is engulfed, a laminar flame is assumed to propagate through it from the burned regions. Since the mean separation of the dissipative regions is of order λ_c, the characteristic time for the ignited mixture to burn is of order $\tau_b = \lambda_c / S_L$.

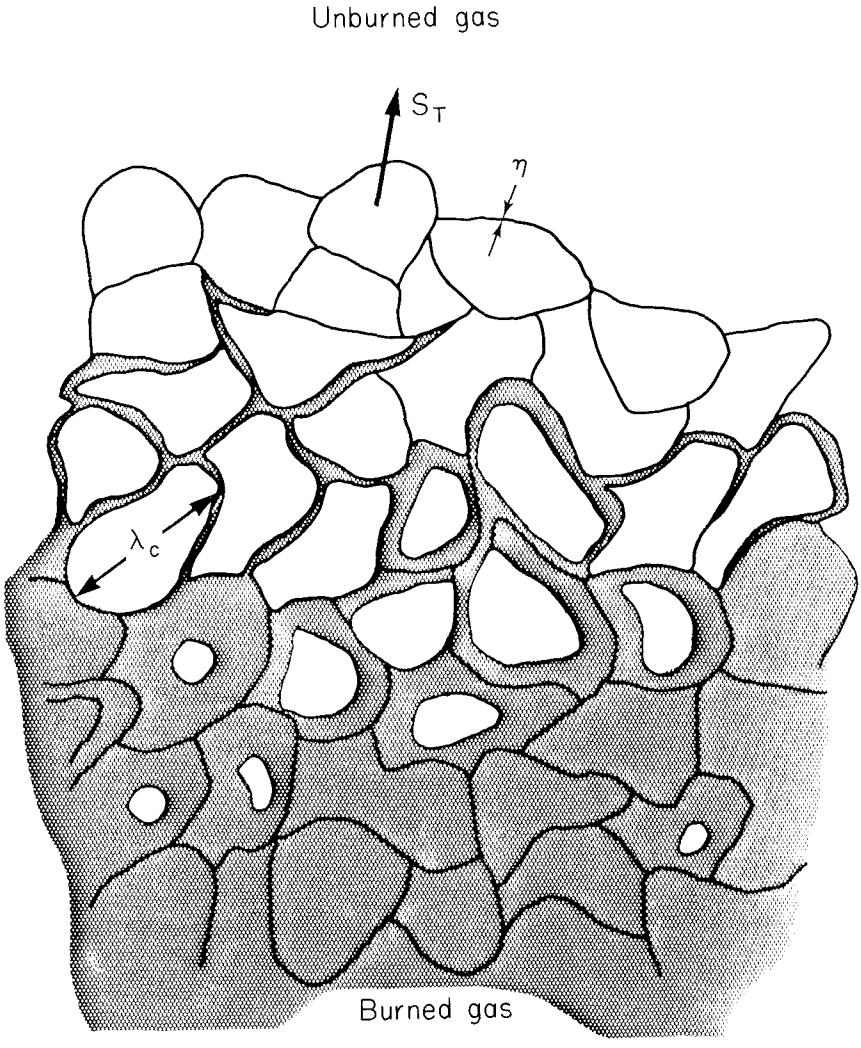

Figure 2.14 Turbulent premixed flame.

The mass of unburned mixture behind the flame is $(m_e - m_b)$. The rate at which the entrained mixture is burned may be approximated by

$$\frac{dm_b}{dt} = \frac{m_e - m_b}{\tau_b} \tag{2.63}$$

In the limit of instantaneous burning, $\tau_b \to 0$, of the engulfed gas (i.e., $m_b = m_e$), this degenerates to Damkohler's (1940) model for the turbulent flame in which $S_T = S_L + u'$ and all the gas behind the flame front is assumed to be burned. The rate of burning is generally slower than the rate of engulfment, however, because of the time required

for burning on the microscale. Moreover, the turbulent combustion rate depends on equivalence ratio and temperature because the rate of diffusional (laminar) flow propagation on the microscale is a function of these parameters.

In contrast to a laminar flame, the turbulent flame front is thick and can contain a large amount of unburned mixture. The flame thickness is approximately

$$l_F \approx u'\tau_b \approx \frac{u'\lambda_c}{S_L} \tag{2.64}$$

Substituting (D.15) and (D.28) for λ_c yields

$$l_F \approx \left(\frac{60}{A}\right)^{1/2} \left(\frac{u'L}{\nu}\right)^{1/2} \frac{D}{S_L} \tag{2.65}$$

The flame thickness increases slowly with u' and more rapidly with decreasing S_L.

If the total distance the flame must propagate is w (which may be substantially greater than the length scale that governs the turbulence), the time required for flame spread is

$$\tau_s \approx \frac{w}{u' + S_L} \tag{2.66}$$

Unless the time for microscale burning, τ_b, is much smaller than τ_s, that is,

$$\frac{\tau_b}{\tau_s} = \frac{\lambda_c}{w}\left(1 + \frac{u'}{S_L}\right) << 1$$

and is also much less than the available residence time in the combustion chamber, τ_R,

$$\frac{\tau_b}{\tau_R} = \frac{\lambda_c}{S_L \tau_R} << 1$$

the possibility exists that some of the mixture will leave the chamber unreacted. Since the laminar flame speed drops sharply on both the fuel-rich and fuel-lean sides of stoichiometric, combustion inefficiencies resulting from the finite time required for combustion limit the useful equivalence ratio range for premixed combustion to a narrow band about stoichiometric. Automobiles are thus generally restricted to operating in the range $0.8 < \phi < 1.2$.

Example 2.9 ***Flame Propagation in a Pipe Flow***

Estimate the flame propagation velocity and flame thickness for stoichiometric combustion of premixed methane in air flowing in a 0.1-m-diameter pipe with a cold gas velocity of 10 m s^{-1}. The initial pressure and temperature are 1 atm and 298 K, respectively.

The Reynolds number of the cold flowing gas is

$$\text{Re} = \frac{Ud}{\nu} = \frac{10 \text{ m s}^{-1} \times 0.1 \text{ m}}{1.5 \times 10^{-5} \text{ m}^2 \text{ s}^{-1}} = 66{,}700$$

which is greater than that required for turbulent flow (Re = 2200), so the flow may be assumed to be turbulent. To estimate the turbulent flame speed, we need to know the tur-

bulent dissipation rate. The dissipation rate can be estimated by considering the work done due to the pressure drop in the pipe flow since the work done by the fluid is dissipated through the action of turbulence. From thermodynamics, we estimate the work per unit mass due to a pressure drop, Δp, to be

$$w = -\frac{1}{\rho}\Delta p$$

The pressure drop in a turbulent pipe flow can be calculated using the Fanning friction factor, f_F:

$$\Delta p = -f_F \frac{L}{d}\frac{\rho U^2}{2}$$

where L is the length of the segment of pipe being considered. The mass flow rate through the pipe is $\rho U(\pi/4)\, d^2$, so the total power dissipated in the length, L, is

$$\begin{aligned} P &= -\frac{1}{\rho}\Delta p \frac{\pi}{4} d^2 \rho U \\ &= -\frac{1}{\rho}\left(-f_F \frac{L}{d}\frac{\rho U^2}{2}\right)\frac{\pi}{4} d^2 \rho U \\ &= f_F \frac{\pi}{8}\rho\, dLU^3 \end{aligned}$$

The turbulent dissipation rate is the rate of energy dissipation per unit mass, which we find by dividing by the total mass contained in the length L,

$$\epsilon = \frac{P}{m} = \frac{f_F(\pi/8)\rho\, dLU^3}{(\pi/4)\rho\, d^2 L} = f_F \frac{U^3}{2d}$$

From Bird et al. (1960), we find

$$f_F = \frac{0.0791}{\mathrm{Re}^{1/4}} \qquad 2100 < \mathrm{Re} < 10^5$$

so for the present problem, $f_F = 0.00492$ and

$$\epsilon = (0.00492)\frac{(10\ \mathrm{m\ s^{-1}})^3}{2 \times 0.1\ \mathrm{m}} = 24.6\ \mathrm{m^2\ s^{-3}}$$

ϵ is related to the characteristic velocity fluctuation by (D.14):

$$\epsilon \approx \frac{Au'^3}{d}$$

where A is a constant of order unity. Assuming that $A = 1$, we estimate

$$u' \approx (\epsilon d)^{1/3} = (24.6\ \mathrm{m^2\ s^{-3}} \times 0.1\ \mathrm{m})^{1/3}$$

or

$$u' \approx 1.35\ \mathrm{m\ s^{-1}}$$

From (D.15) we find the Taylor microscale:

$$\lambda = d\left(\frac{15}{A\ \mathrm{Re}}\right)^{1/2} = 0.1\left(\frac{15}{66{,}700}\right)^{1/2} = 0.00150\ \mathrm{m}$$

This is significantly larger than the smallest scale of the turbulent motion, the Kolmogorov microscale (D.1)

$$\eta = \left(\frac{\nu^3}{\epsilon}\right)^{1/4} = \left[\frac{(1.5 \times 10^{-5}\ \mathrm{m^2\ s^{-1}})^3}{24.6\ \mathrm{m^2\ s^{-3}}}\right]^{1/4}$$

$$= 0.00011\ \mathrm{m}$$

According to our model, the flame spreads at a velocity of

$$S_T = u' + S_L$$

The measured laminar flame speed for stoichiometric combustion of methane in air is $S_L = 0.38\ \mathrm{m\ s^{-1}}$, so

$$S_T \approx 1.35 + 0.38 \approx 1.73\ \mathrm{m\ s^{-1}}$$

$$l_F \approx \frac{u'\lambda_c}{S_L}$$

Assuming that $\lambda_c \approx \lambda$, we find

$$l_F \approx \frac{1.35 \times 0.00150}{0.38}$$

$$\approx 0.00533\ \mathrm{m} = 5.33\ \mathrm{mm}$$

which is considerably larger than the laminar flame thickness calculated in Example 2.8.

2.5.3 Laminar Diffusion Flames

When fuel and air enter a combustion system separately, they must mix on a molecular level before reaction can take place. The extent of reaction is strongly influenced by the extent to which that mixing has occurred prior to combustion. This mixing may be achieved solely by molecular diffusion, as in a candle flame, or may be enhanced by turbulence. We shall again begin our discussion with the laminar flame because of the simplicity it affords.

A laminar diffusion flame was illustrated in Figure 2.9(c). Fuel and air enter in separate streams, diffuse together, and react in a narrow region. While a single value of the equivalence ratio could be used to characterize a premixed flame, the equivalence ratio in the diffusion flame varies locally from zero for pure air to infinity for pure fuel. Combustion in a confined flow may be characterized by an overall equivalence ratio based on the flow rates of fuel and air, but that value may differ dramatically from the value in the flame region. A hydrocarbon diffusion flame may have two distinct zones: (1) the primary reaction zone, which is generally blue, and (2) a region of yellow luminosity. Most of the combustion reactions take place in the primary reaction zone where the characteristic blue emission results from the production of electronically ex-

cited molecules that spontaneously emit light, so-called chemiluminescence. Small particles composed primarily of carbon, known as *soot*, are formed in extremely fuel-rich (C/O ratio of order 1), hot regions of the flame and emit the brighter yellow radiation. The soot particles generally burn as they pass through the primary reaction zone, but may escape unburned if the flame is disturbed.

If the combustion reactions were infinitely fast, the combustion would take place entirely on a surface where the local equivalence ratio is equal to 1. This "thin flame sheet" approximation is the basis of an early model developed by Burke and Schumann (1928) and has been used in much more recent work [e.g., Mitchell and Sarofim (1975)]. Assuming that fuel and oxygen cannot coexist at any point greatly simplifies the calculations by replacing the chemical kinetics with stoichiometry or, at worst, chemical equilibrium calculations. The simplified calculations yield remarkably good results for adiabatic laminar diffusion flames larger than several millimeters in size since the reaction times at the adiabatic flame temperature near stoichiometric combustion are short compared to typical diffusion times. Only when heat is transferred from the flame at a high rate, as when the flame impinges on a cold surface, or when the scale of the flame is very small, as in the combustion of a small droplet, does the reaction time approach the diffusion time.

2.5.4 Turbulent Diffusion Flames

The small-scale structures of the turbulent flow fields in premixed and diffusion flames are similar. Many of the features of the flow in diffusion flames are made apparent by the distribution of composition in the flame. Large-scale eddies, shown in Figure 2.15 persist for long times in turbulent flows (Brown and Roshko, 1974). The development of a turbulent flow is controlled by such structures. Entrainment of one fluid stream into another takes place when fluid is engulfed between large coherent vortices.

Fuel and air are introduced separately into turbulent diffusion flames. Since the reactants must be mixed on a molecular scale to burn, this entrainment and the subsequent mixing control the combustion rate. As in the laminar diffusion flame, the gas composition in the flame is distributed continuously from pure fuel to pure air. The

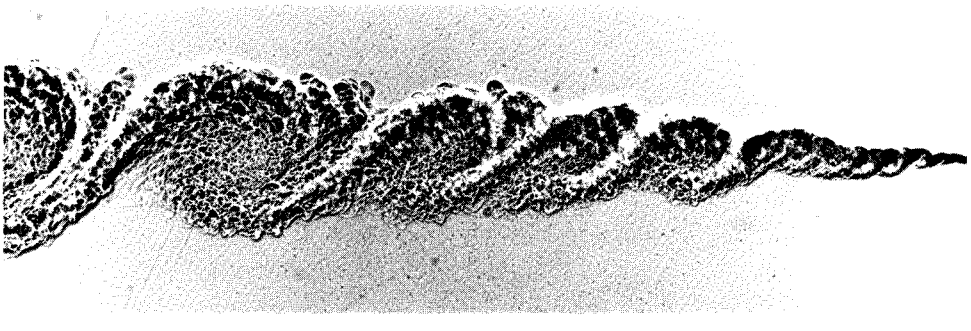

Figure 2.15 Coherent structures in turbulent shear flow (Brown and Roshko, 1974). Reprinted by permission of Cambridge University Press.

structure of a turbulent diffusion flame that results when a fuel jet is released into air was illustrated in Figure 2.9(c). For some distance, the central core of the jet contains unreacted fuel. Combustion takes place at the interface between the fuel and air flows. The flame front is distorted by the turbulent motion but is, as in the laminar diffusion flame, relatively thin. Whether combustion will be complete depends on both the combustion kinetics and the mixing processes in the flame.

Simple jet flames are used in relatively few combustion systems because they are easily extinguished. A continuous ignition source must be supplied to achieve stable combustion. This is commonly accomplished by inducing flow recirculation, either with a bluff body or with a swirling flow, as illustrated in Figure 2.16. The low-pressure region in the near wake of the bluff body or in the center of the swirling flow causes a reverse flow bringing hot combustion products into the vicinity of the incoming fuel and air. Generally, only a small fraction of the combustion takes place within the recirculation zone. The remaining fuel burns as it mixes with air and hot products downstream of the recirculation zone. The flame in this downstream region may be a clearly defined jet that entrains gases from its surroundings, as in large industrial boilers, or may fill the entire combustor.

The extent of mixing in the flame can be characterized in terms of a *segregation* factor, originally proposed by Hawthorne et al. (1951). Arguing that in a high-temperature hydrogen-oxygen flame, hydrogen and oxygen would not be present together at any time, the time-average hydrogen and oxygen concentrations were used as a measure of the fraction of the fluid in the sample that is locally fuel-rich or fuel-lean.

Pompei and Heywood (1972) used similar arguments to infer the distribution of composition in a turbulent flow combustor burning a hydrocarbon fuel. Their combustor consisted of a refractory tube into which kerosene fuel was injected using an air-blast atomizer in which a small, high-velocity airflow disperses the fuel, as illustrated in Figure 2.17. Swirl, induced using stationary vanes, was used to stabilize the flame. The turbulence level in the combustor was controlled by the input of mechanical power introduced by the flow of high-pressure air used to atomize the fuel. Mixing in this ap-

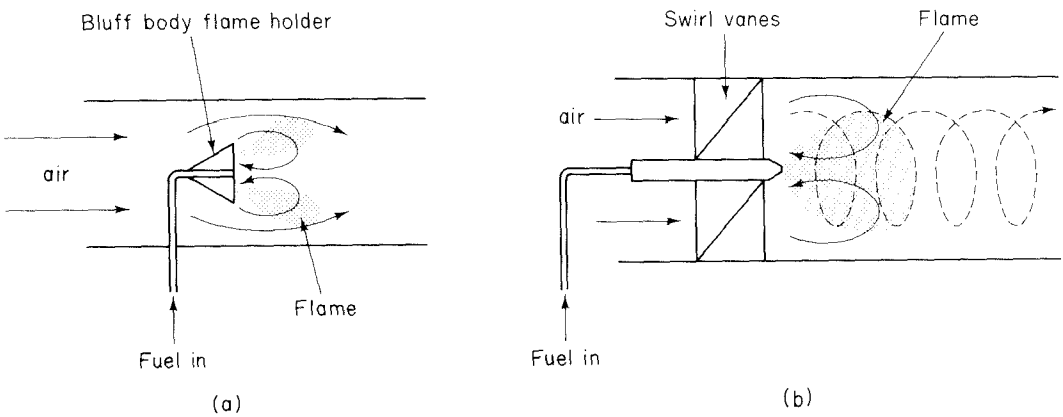

Figure 2.16 Flow recirculation: (a) bluff body; (b) swirl vanes.

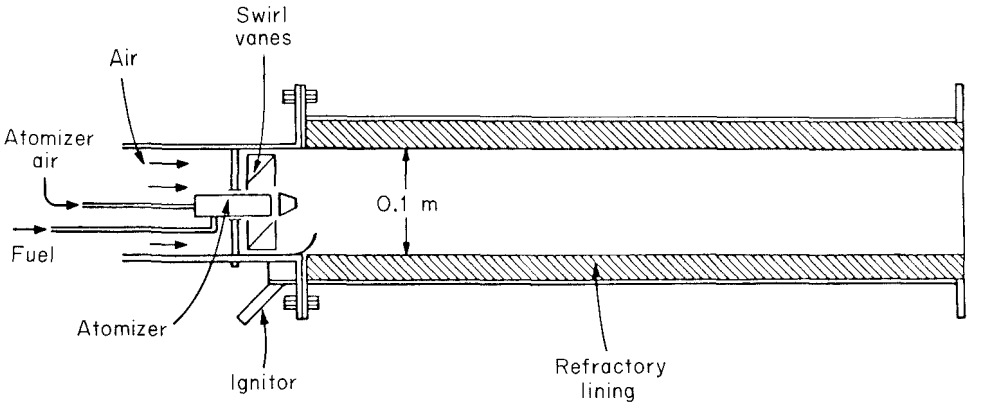

Figure 2.17 Turbulent flow combustor used by Pompei and Heywood (1972).

paratus is readily characterized since the mean composition at any axial location is uniform over the entire combustor cross section. For this reason and because of the volume of pollutant formation data obtained with this system, we shall make extensive use of this system to illustrate the influence of turbulence on combustion and emissions.

Figure 2.18 shows the measured mean oxygen concentration for stoichiometric combustion as a function of position along the length of the combustor. Several profiles are shown, each corresponding to a different pressure for the atomizing air, which, as noted above, controls the initial turbulence level in the combustor. At a low atomizing pressure and correspondingly low turbulence level, the oxygen mole fraction decreases

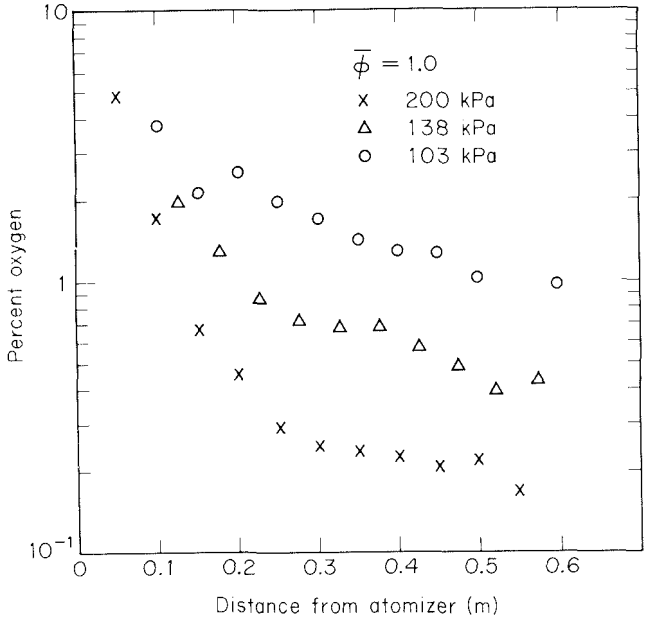

Figure 2.18 Measured mean oxygen concentration for stoichiometric combustion as a function of length along the combustor (Pompei and Heywood, 1972). Reprinted by permission of The Combustion Institute.

to about 3% within the first two diameters and then decreases more slowly to an ultimate value of 1%. Even this final value is far above that corresponding to chemical equilibrium at the adiabatic flame temperature. When the atomizing pressure is increased, raising the turbulence intensity, the oxygen mole fraction drops more rapidly in the first two diameters of the combustor. The rate of decrease then slows dramatically, indicating a reduction in the turbulence level after the atomizer-induced turbulence is dissipated.

If we assume that combustion is instantaneous (i.e., oxygen cannot coexist with fuel or carbon monoxide except for the minor amounts present at equilibrium), the mean oxygen concentration during stoichiometric combustion provides us with a direct measure of the inhomogeneity or segregation in the combustor. A probability density function for the local equivalence ratio may be defined such that the fraction of the fluid at an axial position, z, in the combustor with equivalence ratio between ϕ and $\phi + d\phi$ is $p(\phi, z)\, d\phi$. If the number of moles of O_2 per unit mass is $w_{O_2}(\phi) = [O_2]_\phi/\rho$, the mean amount of oxygen in the combustor at z is

$$\overline{w_{O_2}(z)} = \int_0^\infty w_{O_2}(\phi)\, p(\phi, z)\, d\phi \tag{2.67}$$

We have used moles per unit mass since mass is conserved in combustion but moles are not. The mean mole fraction of oxygen is

$$\overline{y_{O_2}(z)} = \bar{M} \int_0^\infty w_{O_2}(\phi)\, p(\phi, z)\, d\phi \tag{2.68}$$

where $\bar{M}$ is the mean molecular weight. Since the oxygen level decreases with increasing equivalence ratio and is insignificant (for present purposes) in the fuel-rich portions of the flame (as illustrated in Figure 2.19) the mean oxygen level for stoichiometric com-

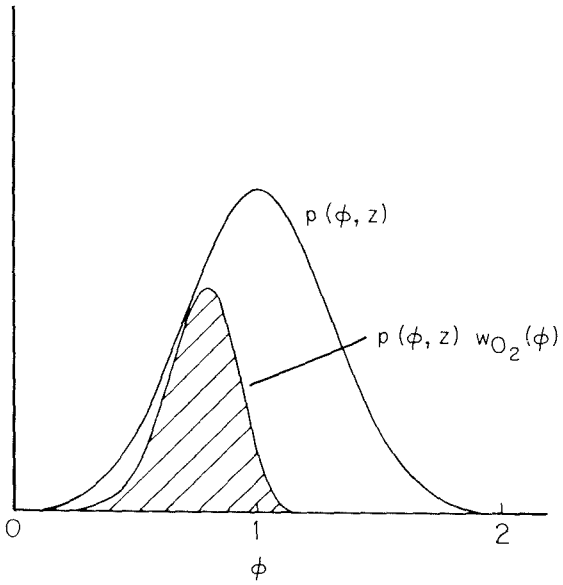

Figure 2.19 Probability density function for equivalence ratio and oxygen distribution.

bustion gives a direct indicator of the breadth of the probability density function, $p(\phi, z)$.

The form of the probability density function, $p(\phi, z)$, is not known a priori. In order to examine the effects of composition fluctuations on emissions, Pompei and Heywood (1972) assumed that the distribution of local equivalence ratios would be Gaussian, that is,

$$p(\phi, z) = \frac{1}{\sqrt{2\pi}\sigma} \exp\left[-\frac{(\phi - \bar{\phi})^2}{2\sigma^2}\right] \tag{2.69}$$

where $\sigma(z)$ is the standard deviation of the distribution and $\bar{\phi}$ is the mean equivalence ratio. Since the mean equivalence ratio is controlled by the rates at which fuel and air are fed to the combustor, it is known. Only one parameter is required to fit the distribution to the data, namely σ. This fit is readily accomplished by calculating and plotting the mean oxygen concentration as a function of σ. The value of σ at any position in the combustor is then determined by matching the observed oxygen level with that calculated using the assumed distribution function, shown in Figure 2.20 as mean concentration as a function of the segregration parameter S.

To describe the extent of mixing in nonstoichiometric combustion, Pompei and

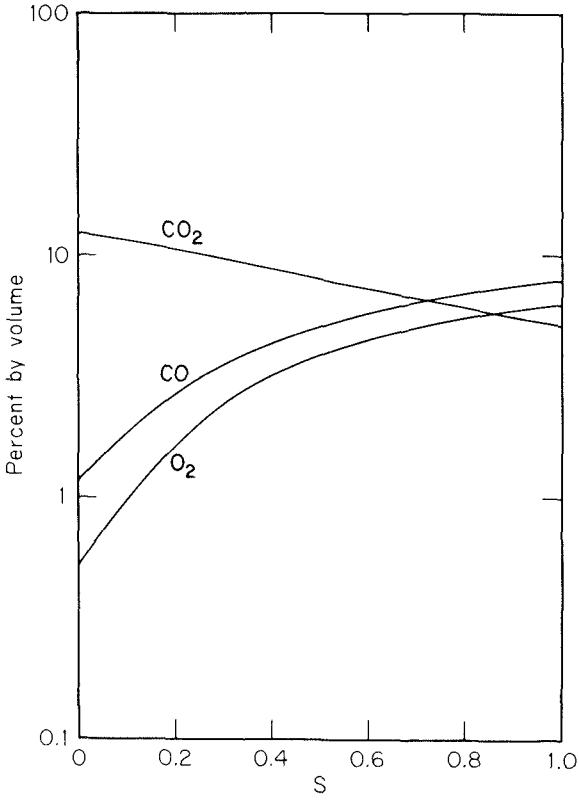

Figure 2.20 Mean composition of products of stoichiometric combustion as a function of the segregation parameter S.

Heywood (1972) assumed that turbulent mixing in their combustor is not affected significantly by changes in the equivalence ratio as long as the flow rate is maintained constant. Under these conditions, the coefficient of variation of the composition probability density function, or segregation.

$$S \equiv \frac{\sigma}{\bar{\phi}} \tag{2.70}$$

determined from the stoichiometric combustion experiments can be applied to other mean equivalence ratios.

The fact that oxygen remains in the products of stoichiometric combustion means that carbon monoxide and other products of incomplete combustion must also be present. Figure 2.21 shows the measured CO levels at the outlet of the combustor as a function of atomizing pressure for several equivalence ratios (Pompei and Heywood, 1972). Assuming that chemical equilibrium is established locally, the mean CO concentration may be calculated using the values of S inferred from the oxygen data, that is,

$$\overline{w_{CO}} = \int_0^\infty \frac{[CO]_e}{\rho} p(\phi, S)\, d\phi \tag{2.71}$$

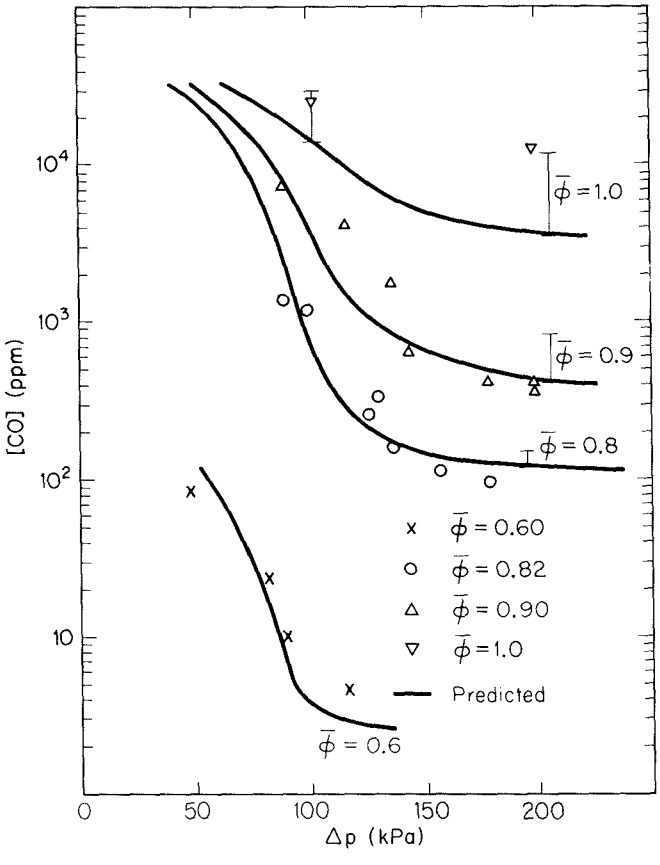

Figure 2.21 Measured CO levels at the outlet of the combustor of Pompei and Heywood (1972) as a function of atomizing pressure at four equivalence ratios. Reprinted by permission of The Combustion Institute.

The results from these calculations are also shown in Figure 2.21. Heat losses to the combustor wall have been taken into account in computing the local equilibrium composition (Pompei and Heywood, 1972). At high atomizing pressures, the combustor approaches the well-mixed condition. The higher CO levels at low atomizing pressures clearly result from incomplete mixing. It is interesting to note that CO emissions from a single piece of combustion equipment can vary by more than two orders of magnitude at fixed equivalence ratio and total fuel and air flow rates due to relatively minor changes in the combustor operating parameters.

2.6 TURBULENT MIXING

We have seen that good mixing is required to achieve high combustion efficiency and corresponding low emission of partially oxidized products like CO. It would seem that, as in the laboratory studies, all combustors should be operated with the turbulence levels necessary to achieve good mixing. In this section we examine the extent to which this can be achieved in practical combustors.

Following Appendix D of Chapter 1 it can be shown that the rate of change in the concentration of a nonreactive tracer due to turbulent mixing can be described by

$$\frac{d\langle c^2 \rangle}{dt} = -\frac{\langle c^2 \rangle}{\tau_d(t)} \tag{2.72}$$

where the characteristic time for turbulent mixing is a function of the correlation scale for the composition fluctuations, λ_c (D.26):

$$\tau_d = \frac{\lambda_c^2(t)}{12D} \tag{2.73}$$

The concentration microscale may vary with time due to variations in the turbulent dissipation rate, ϵ. The variance of the composition of a nonreactive tracer becomes

$$\langle c^2(t) \rangle = \langle c^2(0) \rangle \exp\left[-\int_0^t \frac{dt'}{\tau_d(t')} \right] \tag{2.74}$$

A convenient tracer for characterization of mixing in a turbulent flame is total carbon per unit mass, that is, the sum of contributions of fuel, hydrocarbon intermediates, CO, and CO_2. This is directly related to the equivalence ratio, so $\langle c^2 \rangle$ is related to the variance, σ^2, in the equivalence ratio distribution. Thus τ_d is the characteristic time describing the approach of the equivalence ratio distribution to uniformity.

The mixing time can be related to turbulence quantities through application of (D.15) and (D.30):

$$\tau_d = \frac{\lambda_c^2}{12D} \approx \frac{\lambda^2}{6\nu} = A'\left(\frac{\epsilon}{L^2}\right)^{-1/3} \tag{2.75}$$

where A' is an undetermined constant that is presumably of order unity. Here we see a major problem in achieving efficient mixing: the time scale decreases only as the one-third power of increasing turbulent energy.

To maintain a steady turbulence level in a burner, turbulent kinetic energy must be supplied to the system at a rate equal to the dissipation rate. The rate at which kinetic energy, E_k, is supplied to the system is the sum of the contributions of all the flows entering the system:

$$E_k = \sum_i (\rho_i u_i A_i) \frac{u_i^2}{2} \tag{2.76}$$

The air blast atomizer used by Pompei and Heywood (1972) uses a sonic velocity air jet to atomize a liquid fuel and to generate turbulence. For a choked (sonic) flow through the atomizer orifice, the air mass flow rate is directly proportional to the absolute pressure on the upstream side of the orifice. The total flow rate through the combustor was about 0.016 kg s^{-1}, with a maximum atomizer airflow rate of 0.0012 kg s^{-1}. The power input by the atomizer jet was

$$E_k \approx 0.0012 \text{ kg s}^{-1} \tfrac{1}{2} (330 \text{ m s}^{-1})^2 \approx 65 \text{ W}$$

Flame structure observations suggest that this energy was dissipated in the first two diameters of the 0.1-m-diameter combustor, which contained a mass of approximately

$$m \approx \frac{\pi}{4} (0.1 \text{ m})^2 (0.2 \text{ m})(0.18 \text{ kg m}^{-3})$$

$$\approx 0.00028 \text{ kg}$$

assuming a mean temperature of 2000 K. Thus the minimum mixing time is of order

$$\tau_d \approx \left(\frac{0.00028 \text{ kg } (0.1 \text{ m})^2}{65 \text{ W}} \right)^{1/3} \approx 0.0035 \text{ s}$$

The minimum atomizer airflow rate was about 0.00047 kg s^{-1}, leading to a power input of 25 W and a mixing time of about 0.0048 s. These times may be compared with the residence time in the mixing zone,

$$\tau_R = \frac{(\pi/4)(0.1 \text{ m})^2 (0.2 \text{ m})(0.18 \text{ kg m}^{-3})}{0.016 \text{ kg s}^{-1}} \approx 0.018 \text{ s}$$

Thus we see that the mixing time is comparable to the residence time. When the time scales are similar, small changes in the mixing time significantly affect the combustion efficiency.

What would happen if no effort were made to enhance the turbulence in the combustor? If we assume that the turbulence would correspond to that in a pipe, $u' \approx 0.1U$, the dissipation rate is

$$\epsilon \approx \frac{0.001U^3}{L}$$

and the mixing time becomes

$$\tau_d \approx \left[\frac{L^3}{0.001U^3}\right]^{1/3} \approx \frac{0.1\ \text{m}}{0.001^{1/3}(11\ \text{m s}^{-1})} \approx 0.09\ \text{s}$$

Without the air-assist atomization the turbulence would not be sufficient to mix fuel and air, even within the 0.05-s residence time in the combustor. The slow mixing downstream of the atomizer influenced zone is indicative of this low dissipation rate.

Equation (2.75) provides a simple scaling criterion for geometrically similar burners (Corrsin, 1957). Consider the power required to maintain a constant mixing time when the size of burner is increased by a factor, κ. The integral scale of turbulence is proportional to the flow-system dimensions; hence

$$L' = \kappa L \quad \text{and} \quad m' = \kappa^3 m$$

$\tau' = \tau$ is achieved when

$$E_k' = \kappa^5 E_k$$

Thus we see that the power required to achieve constant mixing time increases as the fifth power of the burner size. The power per unit mass increases as the square of the scale factor. The rate at which kinetic energy can be supplied to a burner is limited, so mixing rates for large burners tend to be lower than for small burners.

For very large combustors, such as utility boilers, a number of relatively small burners, typically 1 m in diameter, are generally used instead of one larger burner to achieve good mixing. Air velocities through these burners are generally limited to about 30 m s^{-1}, leading to mixing times in the range 0.03 to 0.3 s, depending on the efficiency of conversion of the input kinetic energy (about 10 kW) to turbulence. These times are long compared with the laboratory experiments described above, but are short enough to assure good mixing within typical residence times of several seconds in large boilers. The initial combustion will, however, take place under poorly mixed conditions, a fact that strongly influences the formation of NO and other pollutants.

A typical utility boiler has 10 to 20 burners of this size. If they were combined into one large burner using the same air velocity, the mixing time would increase to 0.2 to 2 s, large enough that good mixing is unlikely.

2.7 COMBUSTION OF LIQUID FUELS

Liquid fuels are generally sprayed into a combustor as relatively fine droplets. Volatile fuels, such as kerosene, vaporize completely prior to combustion. Heavy fuel oils may partially vaporize, leaving behind a carbonaceous solid or liquid residue that then undergoes surface oxidation. The nature of the combustion process and pollutant emissions depends strongly on the behavior of the condensed-phase fuel during combustion.

The combustion of a fuel spray is governed by the size and volatility of the fuel droplets. Fuel droplets take a finite amount of time to vaporize, so not all of the fuel is immediately available for reaction. In order to vaporize, the droplet temperature must

first be raised from the temperature at which it is introduced, T_i, to its vaporization temperature, T_s. The latent heat of vaporization, $\bar{L}$, must then be supplied. The energy required to vaporize a unit mass of fuel is

$$\bar{q} = \bar{c}_{pf}(T_s - T_i) + \bar{L} \tag{2.77}$$

where $\bar{c}_{pf}$ is the specific heat of the liquid. For a small particle of radius a moving at a low velocity relative to the gas ($\mathrm{Re} = 2\rho ua/\mu < 1$), the convective heat transfer rate to the particle is

$$Q = 4\pi a^2 k\left(\frac{dT}{dr}\right)_s \tag{2.78}$$

where k is the thermal conductivity of the gas. Although it may be important in some flames, radiative heat transfer will be neglected in the present analysis. Once the droplet temperature has been raised to T_s, only the energy corresponding to the latent heat of vaporization, $\bar{L}$, must be supplied. An energy balance at the particle surface of the vaporizing droplet then yields

$$\bar{L}\bar{R}_v = 4\pi a^2 k\left(\frac{dT}{dr}\right)_s \tag{2.79}$$

where $\bar{R}_v$ is the rate of mass loss from the droplet by vaporization.

The vapor is transported away from the surface by convection and diffusion [see (B.3)]. Since only vapor leaves the surface, we may write

$$\bar{R}_v = 4\pi a^2 \rho u_s x_{vs} - 4\pi a^2 \rho D\left(\frac{dx_v}{dr}\right)_s \tag{2.80}$$

where x_{vs} is the vapor mass fraction at the droplet surface. Noting that $4\pi a^2 \rho u_s = \bar{R}_v$, this becomes

$$\bar{R}_v(1 - x_{vs}) = -4\pi a^2 \rho D\left(\frac{dx_v}{dr}\right)_s \tag{2.81}$$

The mass, energy, and species conservation equations are (B.1), (B.25), and (B.5). The time required to establish the temperature and composition profiles around the evaporating droplet is generally short compared to that for the droplet to evaporate, so we may assume that the radial profiles of temperature and composition achieve a quasi-steady state. For the case of pure evaporation, the chemical reaction source term can also be eliminated. The conservation equations thus reduce to*

$$\frac{1}{r^2}\frac{d}{dr}(\rho u r^2) = 0 \tag{2.82}$$

$$\rho u \bar{c}_p \frac{dT}{dr} = \frac{1}{r^2}\frac{d}{dr}\left(r^2 k \frac{dT}{dr}\right) \tag{2.83}$$

*The transport properties k and ρD are generally functions of temperature.

$$\rho u \frac{dx_v}{dr} = \frac{1}{r^2} \frac{d}{dr}\left(r^2 \rho D \frac{dx_v}{dr}\right) = 0 \tag{2.84}$$

From (2.82), we see that the velocity at any radial position can be related to that at the droplet surface, i.e.,

$$4\pi\rho u r^2 = 4\pi\rho u_s a^2 = \bar{R}_v \tag{2.85}$$

Substituting into the energy and species conservation equations yields

$$\bar{R}_v \bar{c}_p \frac{dT}{dr} = 4\pi \frac{d}{dr}\left(r^2 k \frac{dT}{dr}\right) \tag{2.86}$$

$$\bar{R}_v \frac{dx_v}{dr} = 4\pi \frac{d}{dr}\left(r^2 \rho D \frac{dx_v}{dt}\right) \tag{2.87}$$

Integrating, we find

$$\bar{R}_v \bar{c}_p (T + C_1) = 4\pi r^2 k \frac{dT}{dr}$$

$$\bar{R}_v (x_v + C_2) = 4\pi r^2 \rho D \frac{dx_v}{dr}$$

Applying the boundary conditions at the particle surface ($r = a$) yields

$$C_1 = \frac{4\pi a^2 k (dT/dr)_s}{\bar{R}_v \bar{c}_p} - T_s$$

$$= \frac{\bar{L}}{\bar{c}_p} - T_s$$

and

$$C_2 = \frac{4\pi a^2 \rho D (dx_v/dr)_s}{\bar{R}_v} - x_{vs}$$

$$= -(1 - x_{vs}) - x_{vs}$$

$$= -1$$

Thus we have

$$\bar{R}_v \bar{c}_p \left(T - T_s + \frac{\bar{L}}{\bar{c}_p}\right) = 4\pi r^2 k \frac{dT}{dr}$$

$$\bar{R}_v (x_v - 1) = 4\pi r^2 \rho D \frac{dx_v}{dr}$$

Integrating again, assuming k and ρD are independent of T, and evaluating the constants in terms of the values as $r \to \infty$, we find

$$-\frac{\bar{R}_v \bar{c}_p}{4\pi r k} = \ln \frac{T - T_s + \bar{L}/\bar{c}_p}{T_\infty - T_s + \bar{L}/\bar{c}_p}$$

$$-\frac{\bar{R}_v}{4\pi r \rho D} = \ln \frac{x_v - 1}{x_{v\infty} - 1}$$

from which we obtain two expressions for the vaporization rate in terms of the values at the droplet surface:

$$\bar{R}_v = 4\pi a (k/\bar{c}_p) \ln \left[1 + \frac{\bar{c}_p (T_\infty - T_s)}{\bar{L}} \right] \tag{2.88}$$

$$\bar{R}_v = 4\pi a \rho D \ln \left(1 + \frac{x_{v\infty} - x_{vs}}{x_{vs} - 1} \right) \tag{2.89}$$

To evaluate T_s and x_{vs}, we can equate these two rates:

$$\frac{k}{\bar{c}_p} \ln \left[1 + \frac{\bar{c}_p (T_\infty - T_s)}{\bar{L}} \right] = \rho D \ln \left(1 + \frac{x_{v\infty} - x_{vs}}{x_{vs} - 1} \right) \tag{2.90}$$

Using thermodynamic data to relate the equilibrium vapor mass fraction at the droplet surface to temperature, one iterates on T until (2.90) is satisfied. The temperature dependence of the vapor pressure can be described with the Clapeyron equation, that is,

$$p_v(T) = \left[p_v(T_1) \exp (L/RT_1) \right] \exp (-L/RT) \tag{2.91}$$

The equilibrium vapor mass fraction is obtained from

$$x_{vs} = \frac{\rho_{vs}}{\rho} = \frac{c_{vs}}{c} \frac{M_v}{M} = \frac{p_{vs}}{p} \frac{M_v}{M} \tag{2.92}$$

Since the particle radius does not appear in (2.90), the surface temperature and vapor mass fraction at the surface are seen to be independent of droplet size.

Once the surface temperature is known, we may calculate the time required to vaporize the droplet. Define the transfer number

$$B_T = \frac{\bar{c}_p (T_\infty - T_s)}{\bar{L}} \tag{2.93}$$

The time rate of change of the droplet mass is

$$\frac{dm}{dt} = -4\pi a \frac{k}{\bar{c}_p} \ln (1 + B_T) \tag{2.94}$$

Since the droplet mass is $m = (4\pi/3) \rho_d a^3$, (2.94) may be integrated to find the droplet radius as a function of time:

$$a^2 - a_0^2 = 2(k/\bar{c}_p) \ln (1 + B_T) t \tag{2.95}$$

where a_0 is the initial radius. The time required for the droplet to vaporize completely is found by setting $a = 0$,

$$\tau_e = \frac{a_0^2 \bar{c}_p}{2k \ln (1 + B_T)} \tag{2.96}$$

This droplet lifetime is an important parameter in spray combustion. If τ_e approaches the residence time in the combustor, τ_R, liquid fuel may be exhausted from the combustor, or vapors that are released late may not have time to mix with fuel-lean gases and burn completely. Thus a long droplet lifetime may lead to low combustion efficiencies and emissions of unreacted fuel vapor or products of incomplete combustion. Since the droplet lifetime varies as the square of its initial radius, it is imperative that the maximum droplet size be carefully limited.

As a droplet vaporizes in hot, fuel-lean gases, the fuel vapors may burn in a thin diffusion flame surrounding the droplet as illustrated in Figure 2.22. The approach outlined above can be applied to determine the rate of droplet burning by considering the rate of diffusion of oxygen (or other oxidant) toward the droplet and the energy release by the combustion reactions. In this analysis it is common to make the thin flame approximation, assuming that fuel vapor diffusing from the droplet is instantaneously consumed by the counter diffusing oxygen at the flame front. The heat release due to combustion substantially increases the gas temperature at this surface. This increases the rate of heat transfer to the droplet surface and, therefore, accelerates the evaporation. The rates of transport of energy, fuel vapor, and oxygen must be balanced at the flame front.

The steady-state conservation equations may be written

$$\bar{R}_v \bar{c}_p \frac{dT}{dr} = \frac{d}{dr}\left(4\pi r^2 k \frac{dT}{dr}\right) + 4\pi r^2 q \tag{2.97}$$

$$\bar{R}_v \frac{dx_v}{dr} = \frac{d}{dr}\left(4\pi r^2 \rho D_v \frac{dx_v}{dr}\right) + 4\pi r^2 r_v \tag{2.98}$$

$$\bar{R}_v \frac{dx_o}{dr} = \frac{d}{dr}\left(4\pi r^2 \rho D_o \frac{dx_o}{dr}\right) + 4\pi r^2 r_o \tag{2.99}$$

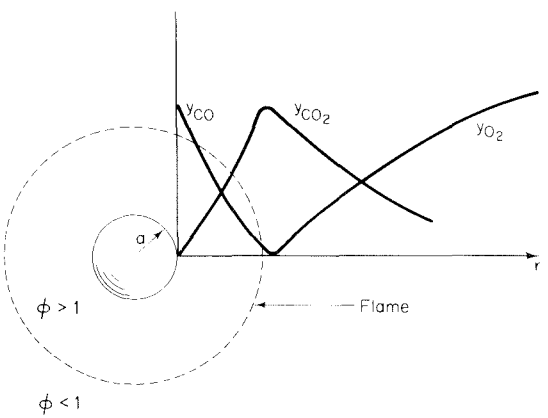

Figure 2.22 Vaporization of a fuel droplet and associated diffusion flame.

where $-r_v$ and $-r_o$ denote the rates of consumption of fuel vapor and oxidant by gas-phase reaction, respectively, and q is the heat release due to the combustion reactions. The boundary conditions at $r = a$ are

$$4\pi a^2 k\left(\frac{dT}{dr}\right)_s = \bar{R}_v \bar{L}$$

$$4\pi a^2 \rho D_v\left(\frac{dx_v}{dr}\right)_s = -\bar{R}_v(1 - x_{vs}) \tag{2.100}$$

$$4\pi a^2 \rho D_o\left(\frac{dx_o}{dr}\right)_s = 0, \qquad x_{os} = 0$$

From combustion stoichiometry we may write

$$r_v = \nu r_o \tag{2.101}$$

where ν is the mass-based stoichiometric coefficient for complete combustion. The heat release, q, due to the combustion reactions is

$$q = -\Delta\bar{h}_{cL}\, r_v = -\nu\, \Delta\bar{h}_{cL}\, r_o \tag{2.102}$$

If $D_o = D_v = k/\rho\bar{c}_p$ (equal molecular and thermal diffusivities), (2.97)–(2.99) can be combined to eliminate the reaction rate terms, i.e.,

$$\bar{R}_v \frac{d}{dr}(x_v - \nu x_o) = \frac{d}{dr}\left(4\pi r^2 \rho D \frac{d}{dr}(x_v - \nu x_o)\right) \tag{2.103}$$

$$\bar{R}_v \frac{d}{dr}(\bar{c}_p T + \Delta\bar{h}_{cL}\, x_v) = \frac{d}{dr}\left(4\pi r^2 \rho D \frac{d}{dr}(\bar{c}_p T + \Delta\bar{h}_{cL}\, x_v)\right) \tag{2.104}$$

$$\bar{R}_v \frac{d}{dr}(\bar{c}_p T + \nu\, \Delta\bar{h}_{cL}\, x_o) = \frac{d}{dr}\left(4\pi r^2 \rho D \frac{d}{dr}(\bar{c}_p T + \nu\, \Delta\bar{h}_{cL}\, x_o)\right) \tag{2.105}$$

Integrating twice and imposing the boundary conditions yield

$$\frac{\bar{R}_v}{4\pi r \rho D} = \ln\left(\frac{1 + \nu x_{o,\infty}}{1 - x_v + \nu x_o}\right) \tag{2.106}$$

$$\frac{\bar{R}_v}{4\pi r \rho D} = \ln\left[\frac{\bar{c}_p(T_\infty - T_s) - \Delta\bar{h}_{cL} + \bar{L}}{\bar{c}_p(T - T_s) - \Delta\bar{h}_{cL}(1 - x_v) + \bar{L}}\right] \tag{2.107}$$

$$\frac{\bar{R}_v}{4\pi r \rho D} = \ln\left[\frac{\bar{c}_p(T_\infty - T_s) + \nu\, \Delta\bar{h}_{cL}\, x_{o,\infty} + \bar{L}}{\bar{c}_p(T - T_s) + \nu\, \Delta\bar{h}_{cL}\, x_o + \bar{L}}\right] \tag{2.108}$$

Finally, the evaporation rate may be evaluated by equating (2.106)–(2.108) at the droplet surface and using an equilibrium relation for the vapor mass fraction at the droplet sur-

face. In terms of the surface conditions, the vaporization rate becomes

$$\bar{R}_v = 4\pi a\rho D \ln\left[1 + \frac{x_{vs} + \nu x_{o,\infty}}{1 - x_{vs}}\right] \tag{2.109}$$

$$\bar{R}_v = 4\pi a\rho D \ln\left[1 + \frac{\bar{c}_p(T_\infty - T_s) - \Delta\bar{h}_{cL}\, x_{vs}}{\bar{L} - \Delta\bar{h}_{cL}(1 - x_{vs})}\right] \tag{2.110}$$

$$\bar{R}_v = 4\pi a\rho D \ln\left[1 + \frac{\bar{c}_p(T_\infty - T_s) + \nu\,\Delta\bar{h}_{cL}\, x_{o,\infty}}{\bar{L}}\right] \tag{2.111}$$

Since we have assumed equal diffusivities and unit Lewis number ($\mathrm{Le} = k/\rho\bar{c}_p D$), the surface conditions in steady-state evaporation are obtained from

$$\frac{x_{vs} + x_{o,\infty}}{1 - x_{vs}} = \frac{\bar{c}_p(T_\infty - T_s) - \Delta\bar{h}_{cL}\, x_{vs}}{\bar{L} - \Delta\bar{h}_{cL}(1 - x_{vs})} = \frac{\bar{c}_p(T_\infty - T_s) + \nu\,\Delta\bar{h}_{cL}\, x_{o,\infty}}{\bar{L}} \tag{2.112}$$

Equation (2.111) quickly yields a reasonable estimate of the burn time since the sensible enthalpy term is generally small,

$$\bar{c}_p(T_\infty - T_s) \ll \left|\Delta\bar{h}_{cL}\, x_{vs}\right|$$

The vaporization rate can thus be approximated by

$$\bar{R}_v \approx 4\pi a\rho D \ln\left[1 + \frac{\nu\,\Delta\bar{h}_{cL}\, x_{o,\infty}}{\bar{L}}\right] \tag{2.113}$$

Once the burning rate is known, the position of the flame front can readily be calculated from (2.106) by setting $x_v = x_o = 0$. We find

$$r_{\text{flame}} = \frac{\bar{R}_v}{4\pi\rho D \ln(1 + \nu x_{o,\infty})} \tag{2.114}$$

For small oxygen concentrations the flame radius rapidly becomes large. In dense fuel sprays, the oxygen is quickly consumed. The predicted flame radius may then exceed the mean droplet separation, δ, as illustrated in Figure 2.23. Although some reaction may take place in the fuel-rich regions between particles in such a dense spray, the flame front will ultimately surround the cloud of droplets (Labowsky and Rosner, 1978). The cloud of droplets then acts as a distributed source of fuel vapor.

The way a fuel is atomized can profoundly influence the combustion process through (1) the droplet lifetime, which varies as the square of the droplet radius; (2) the uniformity of the spatial distribution of droplets; and (3) the generation of turbulence due to the kinetic energy delivered to the flow by the spray. The drop size is determined by a balance between the fluid mechanical forces, which tend to pull the liquid apart, and the surface tension, σ, which tends to hold it together. The classical model for drop

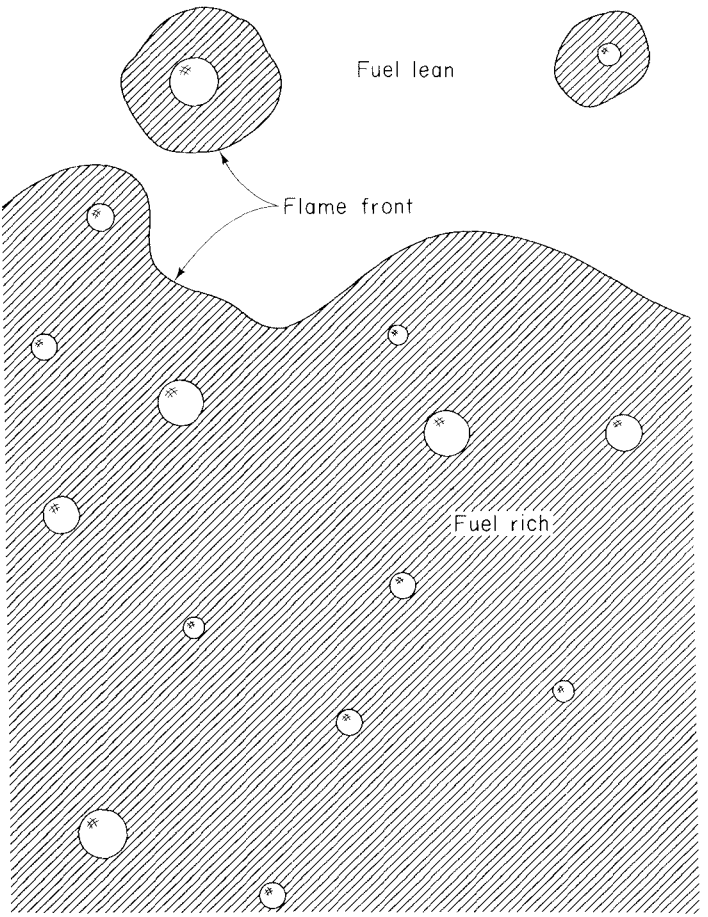

Figure 2.23 Droplet combustion in a dense spray.

stability was developed by Prandtl (1949). An estimate of the maximum stable diameter of droplets is obtained by equating the dynamic pressure of the airflow past the drop and the surface tension force,

$$d_{\max} \approx C\sigma/\rho v^2 \tag{2.115}$$

where v is the relative velocity between the liquid and the gas, ρ is the gas density, and the proportionality constant, C, is equal to 15.4. A high relative velocity will produce the smallest droplets.

The motion of the liquid relative to the gas can be created by forcing the liquid through an orifice with high pressure (pressure atomization) or by using a high-velocity gas flow (air-assist atomization). These two types of atomizers are illustrated in Figure 2.24. The more common pressure atomizer is somewhat limited in the maximum velocity due to pressure constraints and the fouling of very small orifices by contaminant

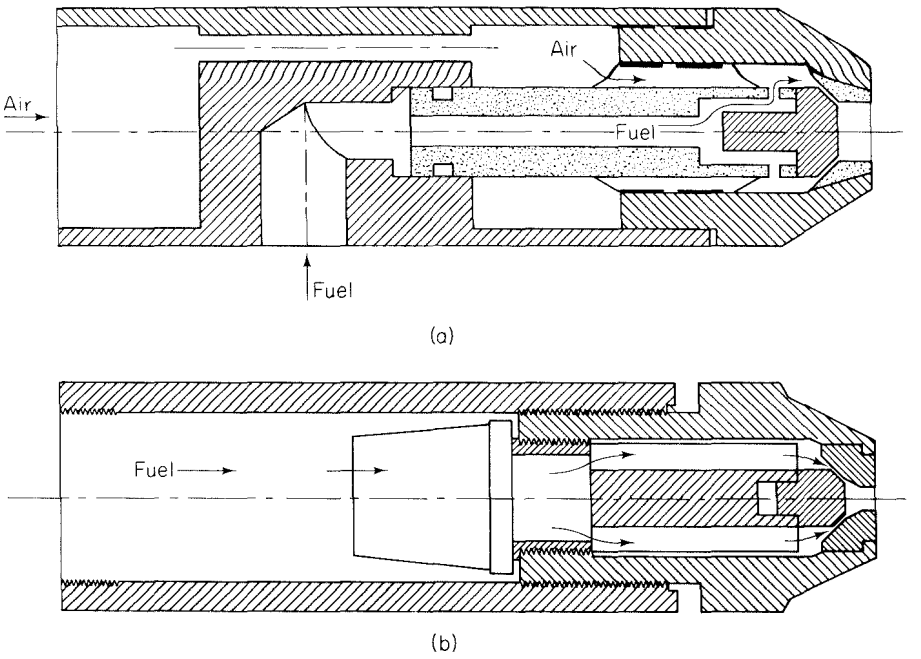

Figure 2.24 Liquid fuel atomizers: (a) air-assist atomizer; (b) pressure atomizer. Komiyama et al. (1977). Reprinted by permission of The Combustion Institute.

particles in the fuel. The fluid velocity through the orifice of a pressure atomizer is

$$v = (2\ \Delta p\ C_D/\rho_f)^{1/2} \tag{2.116}$$

where Δp is the pressure drop across the orifice and C_D is the discharge coefficient (typically, $0.6 < C_D < 1$). High atomizer pressures, say 50 atm (5×10^6 Pa), can result in velocities as high as 100 m s^{-1}. Typical surface tensions for hydrocarbon liquids are 0.2 to 0.8 N m^{-1}. As the liquid stream breaks up, it quickly decelerates, so the maximum droplet size can be much larger than the approximately 40 μm that this velocity would suggest. In diesel engines, where the fuel must be injected very quickly, much higher atomization pressures are generally used, and smaller droplets may be generated.

In the air-assist atomizer, a high-velocity gas flow is used to atomize the liquid and disperse the droplets. The airflow velocity can be as high as the local speed of sound, about 330 m s^{-1} in ambient-temperature air. Drop formation takes place within the atomizer, where the velocity is high, so small drops can be generated [i.e., (2.115) suggests an upper bound on the droplet size of about 4 μm].

The air-assist atomizer also introduces a large amount of kinetic energy that is ultimately dissipated through turbulence. The pressure atomizer does not have this impact due to the lower velocity and the lower mass flow entering through the atomizer. Thus, when the pressure atomizer is used, the turbulence levels in the flame region are

governed by the main combustion airflow rather than by the atomizer. Low turbulence levels suggest that mixing will be incomplete and combustion will be inefficient. Experiments conducted by Komiyama et al. (1977) using a pressure atomizer on the combustor of Pompei and Heywood (1972) show that droplet combustion has a rather striking influence on the combustion efficiency. Figure 2.25 shows that the oxygen consumption for combustion of the same kerosene fuel used by Pompei and Heywood (solid points) is much more rapid than would result from gas mixing alone (dashed line). Moreover, studies of a variety of single component fuels (open points) reveal that the combustion efficiency decreases with increasing fuel volatility (i.e., with decreasing evaporation time). As a droplet evaporates, vapors diffuse into the surrounding fluid. If the drop evaporates slowly, particularly while it moves through the gas with an appreciable velocity, the vapors are distributed along a fine path where molecular diffusion is effective. On the other hand, a droplet that evaporates quickly leaves a more concentrated vapor cloud that must then mix through the action of turbulence. The difference in combustion behavior of high- and low-volatility fuels may be accentuated by differences in surface tension.

Thus we see that droplets act as point sources of fuel vapor that can accelerate the mixing of fuel and air by introducing vapor on a very small length scale. Injection at

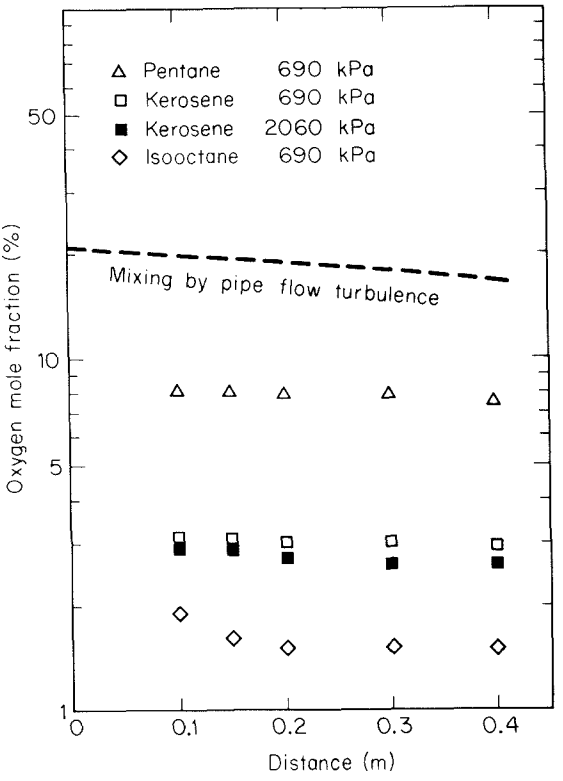

Figure 2.25 Oxygen concentrations for combustion of four fuels as a function of distance along the combustor length. Komiyama et al. (1977). Reprinted by permission of The Combustion Institute.

high velocities can distribute the fuel throughout the combustion gases. As droplets enter the combustor at high velocity, their Reynolds numbers may be large enough that convective transport enhances drop evaporation. The correlation proposed by Ranz and Marshall (1952) can be used to take forced convection into account, that is,

$$\bar{R}_v = \bar{R}_{v0}(1 + 0.36\ \mathrm{Re}^{1/2}\ \mathrm{Sc}^{1/3}) \tag{2.117}$$

where $\bar{R}_{v0}$ is the vaporization rate for purely diffusive vaporization, $\mathrm{Re} = \rho v d/\mu$ is the droplet Reynolds number, and $\mathrm{Sc} = \mu/\rho D$ is the Schmidt number of the gas.

We have examined the evaporation and combustion of a single-component fuel. Practical fuels are complex mixtures of hydrocarbons. As droplets are heated, the more volatile components evaporate more rapidly than the less volatile components, so the fuel volatility gradually decreases. Diffusional resistance within the droplet can become a significant hindrance to vaporization (Hanson et al., 1982; Law and Law, 1981). Components that vaporize slowly may be heated to high temperatures, possibly leading to the formation of solid carbonaceous particles of coke. These solid particles can be very difficult to burn and are often emitted with the exhaust gases.

2.8 COMBUSTION OF SOLID FUELS

Solid fuels are burned in a variety of systems, some of which are similar to those fired by liquid fuels. In large industrial furnaces, particularly boilers for electric power generation, coal is pulverized to a fine powder (typically, 50 μm mass mean diameter and 95% smaller by mass than about 200 μm) which is sprayed into the combustion chamber and burned in suspension as illustrated in Figure 2.26. The combustion in the pulverized coal system has many similarities to the combustion of heavy fuel oils. Smaller systems generally utilize fixed- or fluidized-bed combustors that burn larger particles. The latter technologies are also applied to the combustion of wood, refuse, and other solid fuels. Air is fed into a fluidized bed at a sufficiently high velocity to levitate the particles, producing a dense suspension that appears fluidlike. Heat transfer in the bed must be high enough and heat release rates low enough to keep the bed relatively cool and prevent the ash particles from fusing together to form large ash agglomerates known as clinkers. Noncombustible solids are often used to dilute the fuel and keep the temperature low; most commonly, limestone is used in order to retain the sulfur in the bed at the same time. In contrast to the rapid mixing in a fluidized bed, only a fraction of the air comes in contact with the fuel in a fixed bed, or stoker, combustion system, with the remainder being introduced above the bed of burning fuel. Large amounts of excess air are required to achieve reasonable combustion efficiency, and even with the large airflows, hydrocarbon and carbon monoxide emissions can be quite high, due to poor mixing above the bed. The increased air requirements lower the thermal efficiency of stoker units, so pulverized coal or fluidized-bed combustion is favored for large systems. Most large systems currently in use burn pulverized coal. We shall, for this reason, focus on these systems.

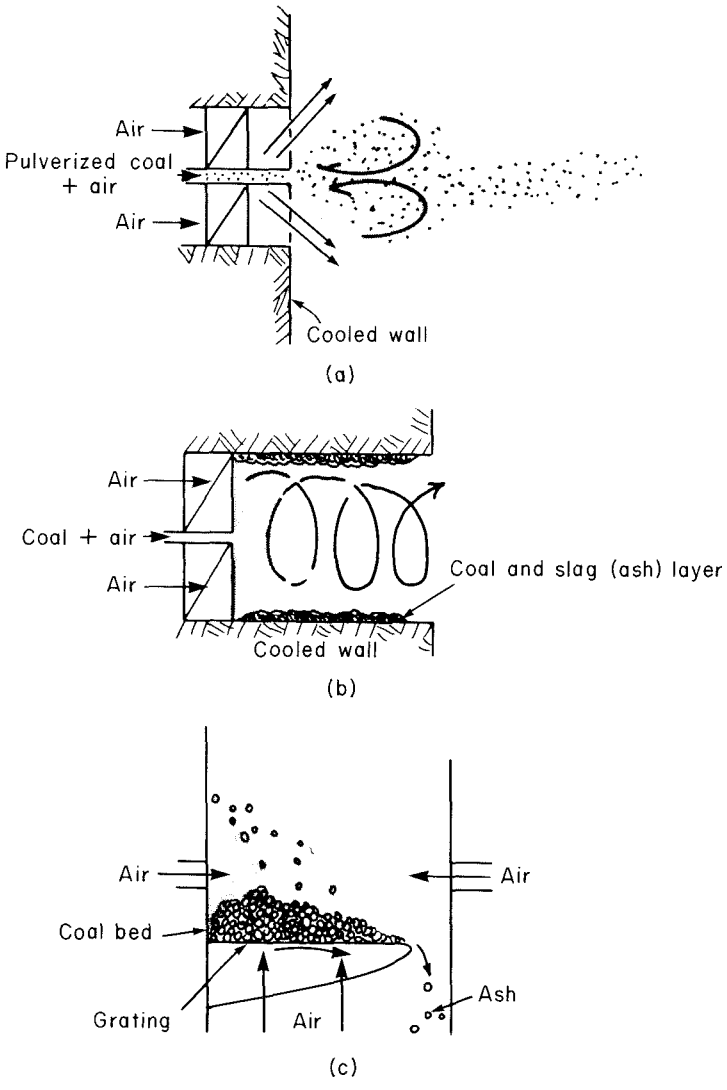

Figure 2.26 Coal combustion systems: (a) pulverized coal burner; (b) cyclone burner; (c) spreader stoker; (d) fluidized-bed combustor.

2.8.1 Devolatilization

When coal particles are sprayed into a combustion chamber, they undergo a number of transformations. Water is first driven off as the particle is heated. As the fuel is heated further, it devolatilizes, a process that involves the release of hydrocarbons in the coal and the cracking of the molecular structure of the coal. This complex chemical process has received considerable attention (Gavalas, 1982), but we shall examine here only one

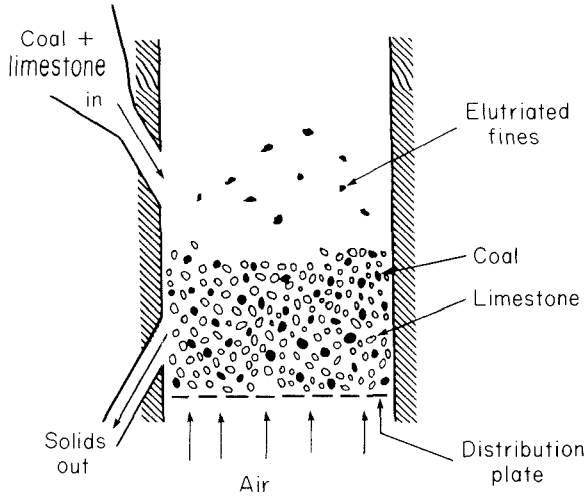

(d)

Figure 2.26 (*Continued*)

of the simpler models. The devolatilization has been modeled as competing chemical reactions (Kobayashi et al., 1977), that is,

$$\text{coal} \begin{cases} \xrightarrow{k_1} (1 - \alpha_1) R_1 + \alpha_1 V_1 \\ \xrightarrow{k_2} (1 - \alpha_2) R_2 + \alpha_2 V_2 \end{cases}$$

Each of the two reactions produces volatile matter (V_i) and residual char (R_i), which does not undergo additional pyrolysis. The fraction of the mass of coal undergoing reaction i that is released as volatile matter is α_i. Reaction 1 is assumed to be a low-temperature reaction that produces an asymptotic volatile yield α_1. Reaction 2 is assumed to have a higher activation energy and therefore contributes significantly only at high temperature. Rapid heating brings reaction 2 into play, while substantial coal remains unreacted, leading to higher volatile yields than at low temperature.

The parameters in this simplified model must be empirically determined. α_1 is generally chosen to equal the volatile yield measured in the proximate analysis, a low-temperature pyrolysis test. The remaining parameters of this model, as estimated by Stickler et al. (1979), are summarized in Table 2.9. With this simple model, the release of volatile matter and the quantity of char residue can be estimated. The fractional conversion of the char is described by the rate equation

$$\frac{dx_{\text{coal}}}{dt} = -k_1 x_{\text{coal}} - k_2 x_{\text{coal}} \tag{2.118}$$

where x_{coal} is the mass fraction of the coal that has not undergone reaction.

TABLE 2.9 TWO-REACTION COAL PYROLYSIS MODEL OF STICKLER ET AL. (1979)[a]

Frequency factors	A_1	$3.7 \times 10^5\ s^{-1}$
	A_2	$1.46 \times 10^{13}\ s^{-1}$
Activation energies	E_1/R	8857 K
	E_2/R	30,200 K
Mass coefficients	α_1	Proximate analysis volatile matter
	α_2	0.8

[a] $k_i = A_i \exp(-E_i/RT)$.

The volatiles are formed within the coal particle, and escape to the surrounding atmosphere involves flow through the coal matrix. This is frequently a violent process, characterized by vigorous jetting as flow channels open in the char to allow the release of the high pressures built up by volatile production in the core of the particle. These complications preclude the application of the drop combustion models derived in the preceding section to the combustion of coal volatiles. Nonetheless, the volatiles play a very important role in coal combustion, particularly in ignition and stabilization of coal flames. Knowledge of volatile release is also essential to specifying the initial condition for the next phase of coal combustion, the surface oxidation of char residue.

Example 2.10 ***Coal Devolatilization***

A dry coal particle intially 50 μm in diameter is suddenly heated to 2000 K in air. The proximate analysis of the coal is

Volatile matter	43.69%
Fixed carbon	46.38%
Ash	9.94%

The carbon and ash densities are 1.3 and 2.3 g cm^{-3}, respectively. Using the Kobayashi model and assuming that the particle temperature remains constant throughout devolatilization, estimate the mass of char remaining after devolatilization and the density of the particle.

Consider first devolatilization. Equation (2.118) expresses a relation for the fraction of unreacted coal as a function of time. Integrating (2.118) and noting that $x_{coal} = 1$ at $t = 0$, we find

$$x_{coal} = e^{-t/\tau_D}$$

where the characteristic time for devolatilization is

$$\tau_D = (k_1 + k_2)^{-1}$$

The fraction of the coal that is converted to char by reaction i is $1 - \alpha_i$, so

$$\frac{dx_{char}}{dt} = (1 - \alpha_1)\, k_1 x_{coal} + (1 - \alpha_2)\, k_2 x_{coal}$$

$$= \left[(1 - \alpha_1)\, k_1 + (1 - \alpha_2)\, k_2\right] e^{-t/\tau_D}$$

Integrating and letting $x_{char} = 0$ at $t = 0$ yields

$$x_{char} = \frac{(1 - \alpha_1)k_1 + (1 - \alpha_2)k_2}{k_1 + k_2}(1 - e^{-t/\tau_D})$$

The limit as $t \rightarrow \infty$ is

$$x_{char}(t \longrightarrow \infty) = \frac{(1 - \alpha_1)k_1 + (1 - \alpha_2)k_2}{k_1 + k_2}$$

From Table 2.9,

$$k_i = A_i e^{-E_i/RT}$$

$$\alpha_1 = \frac{0.4369}{1 - 0.0994} = 0.485 \qquad \alpha_2 = 0.8$$

$$A_1 = 3.7 \times 10^5 \text{ s}^{-1} \qquad A_2 = 1.46 \times 10^{13} \text{ s}^{-1}$$

$$E_1/R = 8857 \text{ K} \qquad E_2/R = 30{,}200 \text{ K}$$

Evaluating at 2000 K, we find that

$$k_1 = 4400 \text{ s}^{-1} \qquad k_2 = 4.06 \times 10^6 \text{ s}^{-1}$$

Thus

$$\tau_D = 2.46 \times 10^{-7} \text{ s} = 0.246 \ \mu\text{s}$$

and

$$x_{char} = \frac{(1 - 0.485)\,4.4 \times 10^3 + (1 - 0.8) \times 4.06 \times 10^6}{4.4 \times 10^3 + 4.06 \times 10^6} = 0.200$$

Only 20% of the original carbonaceous material remains in the char.

2.8.2 Char Oxidation

The combustion of coal char or other entrained carbonaceous particles (such as coke produced in combustion of heavy fuel oils) is governed by the diffusion of oxidizer (O_2, OH, O, CO_2, H_2O, etc.) to the carbon surface and by surface reaction kinetics. Coal char is highly porous and presents a surface area for oxidation that is much larger than the external surface. Mulcahy and Smith (1969) identified several modes of char combustion: regime 1, in which the rate is controlled strictly by surface reactions, allowing the reaction to take place uniformly throughout the char volume; regime 2, in which pore diffusion and surface reactions both influence the rate; and regime 3, in which external diffusion controls the oxidation rate. Pulverized coal combustion generally falls in regime 2.

We begin our discussion of char oxidation with an examination of the role of the external diffusional resistance in the char oxidation kinetics. For this purpose we may use detailed models of the intrinsic surface reaction kinetics in combination with a model of the porous structure of the char and the diffusional resistance within these pores. Alternatively, we may use a global rate expression that describes the total rate of reaction

in terms of the apparent external surface area. We shall use the latter approach at present and examine the processes taking place inside the char particle later.

The rate of char oxidation is the sum of several reactions that convert carbon to CO, primarily

$$C_{(s)} + \tfrac{1}{2} O_2 \xrightarrow{k_1} CO$$

$$C_{(s)} + CO_2 \xrightarrow{k_2} 2CO$$

The apparent rates of these reactions may be expressed in the form

$$\bar{r}_i = A_i e^{E_i/RT} p_i^n \qquad (\text{kg C m}^{-2}\,\text{s}^{-1}) \tag{2.119}$$

where p_i is the partial pressure of the oxidizer. Numerous measurements of the rate parameters for various chars have been reported. Table 2.10 presents selected rate coefficients.

TABLE 2.10 CHAR OXIDATION RATE PARAMETERS[a]

Parent coal	A	E/R (K)	n
Petroleum coke	70	9,910	0.5
Pittsburgh seam (swelling bituminous coal, USA)	41,870	17,100	0.17
Illinois No. 6 (swelling bituminous coal, USA)	63,370	17,200	0.17
Brodsworth (swelling bituminous coal, UK)	1,113	121,300	1.0
East Hetton (swelling bituminous coal, UK)	6,358	17,100	1.0
Anthracite and semianthracite (UK and Western Europe)	204	9,560	1.0
Millmerran (nonswelling subbituminous coal, Australia)	156	8,810	0.5
Ferrymoor (nonswelling subbituminous coal, UK)	703	10,820	1.0
Whitwick (nonswelling bituminous coal, UK)	504	8,910	1.0
Yallourn brown coal (Australia)	93	8,150	0.5

[a] $\bar{r} = Ae^{-E/RT} p_{O_2}^n$ kg m^{-2} s^{-1}, p in atm.
Source: Data from Smith (1982).

The char oxidation rate is the net result of the rate of oxidizer diffusion to the char surface and the rate of surface reaction. Since the activation energies of the oxidation reactions are large, the particle temperature is very important in determining the rate of oxidation. Because of the high temperatures reached and the large emissivity of carbon, radiation can be a major mechanism for heat transfer from the burning char particle. If the temperature of the surrounding surfaces is T_w, the radiative flux to the particle is

$$q_r = \sigma\epsilon(T_w^4 - T_s^4) \qquad \text{W m}^{-2} \tag{2.120}$$

where $\sigma = 5.67 \times 10^{-8}$ W m^{-2} K^{-4} is the Stefan-Boltzmann constant, and ϵ is the particle emissivity. Conduction heat transfer

$$q_c = -k\left(\frac{\partial T}{\partial r}\right)_s \tag{2.121}$$

is also very important for small particles. Large particles encountered in fluidized-bed combustors and small particles injected at high velocities may have large enough Reynolds numbers ($\text{Re} = \rho v d/\mu$) that convection must be taken into account, and the rate of heat transfer is expressed in terms of a heat transfer coefficient, h,

$$q_c = h(T_\infty - T_s) \tag{2.122}$$

where h is generally obtained from correlations of the Nusselt number ($\text{Nu} = hd/k$), for example (Bird et al., 1960),

$$\text{Nu} = 2 + 0.60\ \text{Re}^{1/2}\ \text{Pr}^{1/3} \tag{2.123}$$

where the Prandtl number is defined by $\text{Pr} = c_p\mu/k$. Species transport to and from the particle surface also influences the energy balance. The net enthalpy flux to the particle due to species transport is given by

$$q_s = \sum_j \bar{f}_j \bar{h}_j^\circ(T_s) \tag{2.124}$$

where $\bar{h}_j^\circ = [(\bar{h}(T_s) - \bar{h}(T_0) + \Delta\bar{h}_f^\circ(T_0)]_j$ is the total enthalpy of species j at the temperature of the particle surface and $\bar{f}_j$ is the species mass flux toward the particle surface.

The net species transport from the particle surface is directly related to the rate of reaction:

$$\bar{R} = 4\pi a^2(\bar{r}_1 + \bar{r}_2) = 4\pi a^2\bar{f}_{\text{CO},s}/\nu_{\text{CO}} = -4\pi a^2\bar{f}_{\text{O}_2,s}/\nu_{\text{O}_2} - 4\pi a^2\bar{f}_{\text{CO}_2,s}/\nu_{\text{CO}_2} \tag{2.125}$$

where ν_j denotes the mass-based stoichiometric coefficients for reactions 1 and 2, respectively:

$$\nu_{\text{CO}} = \frac{12 + 16}{12} = 2.33$$

$$\nu_{O_2} = \frac{32}{2 \times 12} = 1.33$$

$$\nu_{CO_2} = \frac{44}{12} = 3.67$$

Combining (2.120), (2.121), and (2.124), the time rate of change of the particle energy becomes

$$\frac{dU}{dt} = 4\pi a^2 \{-\nu_{CO,1}\bar{r}_1\bar{h}^\circ_{CO}(T_s) + \nu_{O_2}\bar{r}_1\bar{h}^\circ_{O_2}(T_s) - \nu_{CO,2}\bar{r}_2\bar{h}^\circ_{CO}(T_s) + \nu_{CO_2}\bar{r}_2\bar{h}^\circ_{CO_2}(T_s)\} \tag{2.126}$$

The rate of change of the particle energy is

$$\frac{dU}{dt} = \frac{d}{dt}(m\bar{u}^\circ) = \bar{u}^\circ \frac{dm}{dt} + m\frac{d\bar{u}^\circ}{dt}$$

Assuming quasi-steady combustion ($d\bar{u}^\circ/dt \approx 0$) and noting that, for solid carbon, $\bar{h}^\circ_C \approx \bar{u}^\circ_C$, we find

$$\frac{dU}{dt} \approx \bar{h}^\circ_C(\bar{r}_1 + \bar{r}_2)$$

Combining these terms, the quasi-steady energy balance on the surface of the burning particle becomes

$$\sigma\epsilon(T_v^4 - T_s^4) - k\left(\frac{dT}{dr}\right)_s + \bar{r}_1 \Delta\bar{h}_{r1}(T_s) + \bar{r}_2 \Delta\bar{h}_{r2}(T_s) = 0 \tag{2.127}$$

Uniform particle temperature has been assumed in this analysis.

To evaluate the reaction rates, $\bar{r}_1$ and $\bar{r}_2$, we need to know both the temperature and the concentrations of the oxidizing species at the particle surface. The species fluxes at the particle surface are obtained from the condition

$$\bar{f}_{js} = x_{js}\sum_k \bar{f}_{ks} - \rho D\left(\frac{dx_j}{dz}\right)_s \tag{2.128}$$

The net mass flux away from the particle surface equals the rate of carbon consumption

$$\sum_k f_{ks} = \bar{r}_1 + \bar{r}_2 \tag{2.129}$$

The fluxes of the oxidizing species are

$$\bar{f}_{js} = -\bar{r}_j\nu_j \tag{2.130}$$

where ν_j is the mass of oxidizer j consumed per unit mass of carbon consumed by reaction j. The surface boundary conditions for the oxidizing species become

$$\nu_j\bar{r}_j + (\bar{r}_1 + \bar{r}_2) = 4\pi\rho D_j\left(\frac{dx_j}{dz}\right)_s \tag{2.131}$$

Assuming that the particle is spherical and that CO is only oxidized far from the particle surface, the combustion rate determination follows the approach of the liquid fuel evaporation problem. We begin with the energy and species conservation equations:

$$(\bar{R}_1 + \bar{R}_2)\,\bar{c}_p \frac{dT}{dr} = \frac{d}{dr}\left(4\pi r^2 k \frac{dT}{dr}\right) \tag{2.132}$$

$$(\bar{R}_1 + \bar{R}_2)\frac{dx_j}{dr} = \frac{d}{dr}\left(4\pi r^2 \rho D_j \frac{dx_j}{dr}\right) \qquad j = 1, \ldots, 3 \tag{2.133}$$

where the total rate of reaction j is $\bar{R}_j = 4\pi a^2 \bar{r}_j$. The solutions are

$$\frac{\bar{R}_1 + \bar{R}_2}{4\pi a(k/\bar{c}_p)} = \ln\left[1 + \frac{\bar{c}_p(T_s - T_\infty)(\bar{R}_1 + \bar{R}_2)}{-\bar{R}_1\,\Delta\bar{h}_{R1}(T_s) - \bar{R}_2\,\Delta\bar{h}_{R2}(T_s) + 4\pi a^2\sigma\epsilon(T_w^4 - T_s^4)}\right] \tag{2.134}$$

$$\frac{\bar{R}_1 + \bar{R}_2}{4\pi a\rho D_j} = \ln\left[1 + \frac{(x_{j\infty} - x_{js})(\bar{R}_1 + \bar{R}_2)}{(\bar{R}_1 + \bar{R}_2)x_{js} + \bar{R}_j \nu_j}\right] \tag{2.135}$$

Equating these rates and requiring that the reaction rate expressions, (2.119), be satisfied, yields, after iterative solutions, the values of the temperature and mass fractions of the oxidizers at the particle surface. The terms on the right-hand side of (2.134) and (2.135) are analogous to the transfer number for the evaporation of a liquid fuel, B_T (2.93). If the thermal and molecular diffusivities are equal [i.e., Lewis number = Le $= k/(\rho\bar{c}_p D) = 1$], the transfer numbers derived from (2.134) and (2.135) are equal:

$$B_T = \frac{\bar{c}_p(T_s - T_\infty)(\bar{R}_1 + \bar{R}_2)}{-\bar{R}_1\,\Delta\bar{h}_{R1}(T_s) - \bar{R}_2\,\Delta\bar{h}_{R2}(T_s) + 4\pi a^2\sigma\epsilon(T_w^4 - T_s^4)}$$

$$= \frac{(x_{j\infty} - x_{js})(\bar{R}_1 + \bar{R}_2)}{(\bar{R}_1 + \bar{R}_2)x_{js} + \bar{R}_j\nu_j} \tag{2.136}$$

The special case of very rapid surface reaction corresponds to diffusion-limited combustion (i.e., Mulcahy and Smith's regime 3 combustion) and allows significant simplification. Assume that only the oxygen reaction 1 is important. If oxygen is consumed as fast as it reaches the particle surface, $x_{O_2,s} = 0$. Thus (2.135) becomes

$$\bar{R}_1 = 4\pi a\rho D \ln\left(1 + \frac{x_{O_2,\infty}}{\nu_{O_2}}\right) \tag{2.137}$$

This is an upper bound on the char combustion rate. Diffusion-limited combustion is a reasonable assumption for combustion of large particles at high temperatures. As either particle size or temperature decreases, reaction kinetics become increasingly important in controlling char oxidative kinetics. Combustion of small particles of pulverized coal is generally in regime 2 (i.e., both diffusional and kinetic resistances become important).

The prediction of the combustion rate requires knowledge of the reaction rate as a function of external surface area and oxidizer concentration. So far, we have relied on global rate expressions, which, as shown by the data in Table 2.10, vary widely from one char to another. Much of this variability can be attributed to differences in the porous structure of the char and the resistance to diffusion to the large surface area contained in that structure. The pore structure varies from one coal to another. Since the quantity of char residue depends on the heating rate, it stands to reason that the char structure will also vary with the devolatilization history. A priori prediction of the char structure is not possible at this time, but the role of the porous structure can be understood.

A number of models of combustion of porous particles have been developed (Simons, 1982; Gavalas, 1981; Smith, 1982). We limit our attention to one of the simpler diffusional resistance models.

The pore structure presents a large surface area for surface oxidation within the volume of the char particle. The pores are small enough that they present a substantial resistance to diffusion. The pore structure can be crudely characterized in terms of the total surface area per unit mass, S, most commonly measured by the BET gas adsorption method (Hill, 1977), and the total pore volume fraction in the char, ϵ_p. If we assume the pores to be uniformly sized and cylindrical, the pore volume fraction and surface area per unit mass of char are

$$\epsilon_p = \pi \bar{\xi}^2 L_{\text{tot}}$$

$$S = \frac{2\pi \bar{\xi} L_{\text{tot}}}{\rho_a}$$

where L_{tot} is the total length of pores per unit volume of char, $\bar{\xi}$ is the mean pore radius, and ρ_a is the apparent density of the char. Combining these expressions to eliminate L_{tot} and solving for $\bar{\xi}$, we find

$$\bar{\xi} = \frac{2\epsilon_p}{\rho_a S} \tag{2.138}$$

Consider, for example, a char with a BET surface area of 100 $m^2\ g^{-1}$ and a porosity of $\epsilon_p = 0.4$. The mean pore radius is 0.012 μm (assuming a char density of 1.5 g cm^{-3}).

If the pore radius is large compared to the mean free path λ of the gas molecules, then the mechanism of diffusion through the pore is the usual continuum transport. (We will discuss the mean free path of gas molecules in Section 5.2.) If the pore radius is small compared to λ, then diffusion of the molecules through the pore occurs by collisions with the walls of the pore. For air at ambient temperature and pressure, $\lambda \approx 0.065$ μm. At combustion temperatures, the mean free path increases to 0.2 to 0.5 μm. The ratio of the mean free path to the pore radius, known as the Knudsen number,

$$\text{Kn} = \frac{\lambda}{\bar{\xi}} \tag{2.139}$$

indicates whether it is reasonable to apply continuum transport models. The continuum models are valid for Kn $\ll$ 1 (see also Chapter 5). At very large Knudsen numbers,

the kinetic theory of gases gives the following result for diffusivity of molecules in cylindrical pores,

$$D_k = \frac{2}{3}\bar{\xi}\sqrt{\frac{8RT}{\pi M}} \tag{2.140}$$

At intermediate values of Kn, the pore diffusivity is approximately (best for equimolar counter diffusion, $N_A = -N_B$)

$$D_p \approx \frac{1}{1/D_k + 1/D_{AB}} \tag{2.141}$$

The effective diffusivity within the porous particle is reduced by the fraction of voids in the particle, ϵ_p, and by the tortuous path through which the gas must diffuse in the particle, characterized by a tortuosity factor, τ, that is typically about 2, that is,

$$D_e \approx \frac{\epsilon_p D_p}{\tau} \tag{2.142}$$

The diffusion of oxidant within the pores of the char and the reactions on the pore surfaces can now be calculated. Consider the reaction of oxygen with the char,

$$2C_{(s)} + O_2 \longrightarrow 2CO$$

for which we shall assume first-order intrinsic reaction kinetics,

$$\bar{r}_i = k_1(T)p_{O_2} \qquad \text{kg C m}^{-2}\,\text{s}^{-1} \tag{2.143}$$

The net local rate of carbon oxidation per unit of char volume is $\bar{r}_i S\rho_a$ (kg m^{-3} s^{-1}), where ρ_a is the apparent density of the char (density of carbon, including pores). The quasi-steady transport and reaction of oxygen within the porous char can be expressed as

$$4\pi r^2 \rho u \frac{dx_{O_2}}{dr} = \frac{d}{dr}\left(4\pi r^2 \rho D_e \frac{dx_{O_2}}{dr}\right) - 4\pi r^2 S\rho_a k' x_{O_2} \nu_{O_2} \tag{2.144}$$

where the reaction rate has been expressed in terms of species mass fraction (i.e., $\bar{r}_i = k_1 p_{O_2} = k' x_{O_2}$). The mass flux at any position in the char can be evaluated from the mass continuity equation,

$$4\pi \frac{d}{dr}(r^2 \rho u) = 4\pi r^2 S\rho_a k' x_{O_2} \tag{2.145}$$

The solution to (2.144) is greatly simplified if the convective transport term is small compared to diffusive transport, whence

$$\frac{d}{dr}\left(4\pi r^2 \rho D_e \frac{dx_{O_2}}{dr}\right) = 4\pi r^2 S\rho_a k' x_{O_2} \nu_{O_2} \tag{2.146}$$

The boundary conditions for this differential equation are

$$\begin{aligned} r = 0: &\quad x_{O_2} = \text{finite} \\ r = a: &\quad x_{O_2} = x_{O_2,s} \end{aligned} \tag{2.147}$$

Solution to equations of the form of (2.146) is facilitated by substituting $x = f(r)/r$. We find

$$x = \frac{A \sinh(\phi r/a)}{r/a} + \frac{B \cosh(\phi r/a)}{r/a} \tag{2.148}$$

where

$$\phi^2 = \frac{\rho_a a^2 S k'}{\rho D_e} \tag{2.149}$$

The parameter ϕ is known as the Thiele modulus (Hill, 1977). Applying the boundary conditions, we find

$$x_{O_2} = x_{O_2,s} \frac{a \sinh(\phi r/a)}{r \sinh \phi} \tag{2.150}$$

The net diffusive flux of oxygen into the porous particle exactly equals the rate of oxygen consumption by reaction. Thus the net rate of carbon consumption is

$$\begin{aligned} \bar{R}_p &= 4\pi a^2 \rho D_e \left(\frac{dx}{dr}\right)_a \\ &= 4\pi a \rho D_e x_{O_2,s} (\phi \coth \phi - 1) \end{aligned} \tag{2.151}$$

If access to the interior surface were not limited by diffusion, the entire area would be exposed to $x_{O_2,s}$, and the net reaction rate would be

$$\bar{R}_{p,\text{ideal}} = \tfrac{4}{3} \pi a^3 \rho_a S k' x_{O_2,s} \tag{2.152}$$

The ratio of the actual reaction rate to the ideal rate gives a measure of the effectiveness of the pores in the combustion chemistry,

$$\eta \equiv \frac{\bar{R}_p}{\bar{R}_{p,\text{ideal}}} = \frac{4\pi a \rho D_e x_{O_2,s} (\phi \coth \phi - 1)}{\tfrac{4}{3} \pi a^3 \rho_a S k' x_{O_2,s}}$$

which with (2.149) yields

$$\eta = \frac{3}{\phi^2} (\phi \coth \phi - 1) \tag{2.153}$$

For fast reaction (i.e., large ϕ), (2.153) approaches

$$\eta = \frac{3}{\phi} \tag{2.154}$$

so only a small fraction of the char surface area is available for reaction, that area near the char surface. In this limit the particle will shrink, but its density will remain constant

once the pores near the char surface establish a steady-state profile of pore radius with depth. This opening of the pore mouth has been neglected in this derivation. On the other hand, in the limit of small ϕ, η tends to unity:

$$\lim_{\phi \to 0} \eta = 1 - \frac{\phi^2}{15}$$

and all of the interior surface contributes to the char oxidation. In this limit, regime 1 combustion, the pores must enlarge and the apparent density of the char must decrease during oxidation. Pulverized coal combustion corresponds most closely to the former case. Lower-temperature combustion in fluidized beds or in stokers may, however, result in a low Thiele modulus.

Coal particles are not, generally, spherical as illustrated by the scanning electron microscope photograph shown in Figure 2.27. Bird et al. (1960) suggest that a non-spherical particle be approximated as a sphere with the same ratio of apparent external surface area to volume,

$$a_{\text{nonsphere}} = \frac{3V_p}{A_p} \tag{2.155}$$

in calculating η for a variety of shapes (spheres, cylindrical, rods, flat plates, etc.). The deviations of exact results from that obtained using (2.154) are small over the range of Thiele moduli important in char combustion.

The char oxidation kinetics are not necessarily first order. The analysis can readily be carried out for reactions of arbitrary (but constant) order. The variation of the pore diffusional resistance with reaction order is relatively weak.

With this analysis it is possible to estimate the intrinsic reaction kinetics from observations of char consumption rates. Smoot et al. (1984) have shown that a single intrinsic rate expression can correlate data on a broad spectrum of coal char. Moreover,

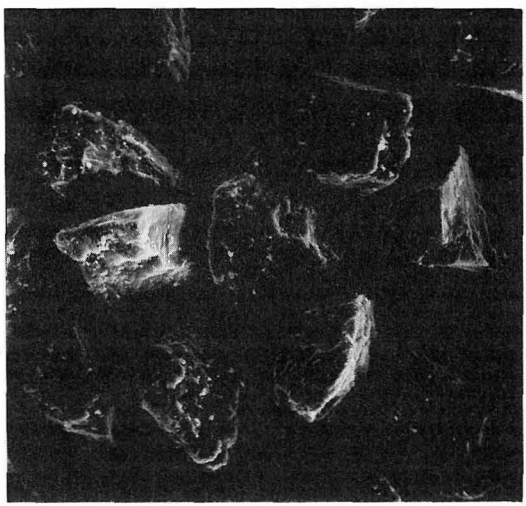

Figure 2.27 Scanning electron microscope photograph of pulverized coal particles.

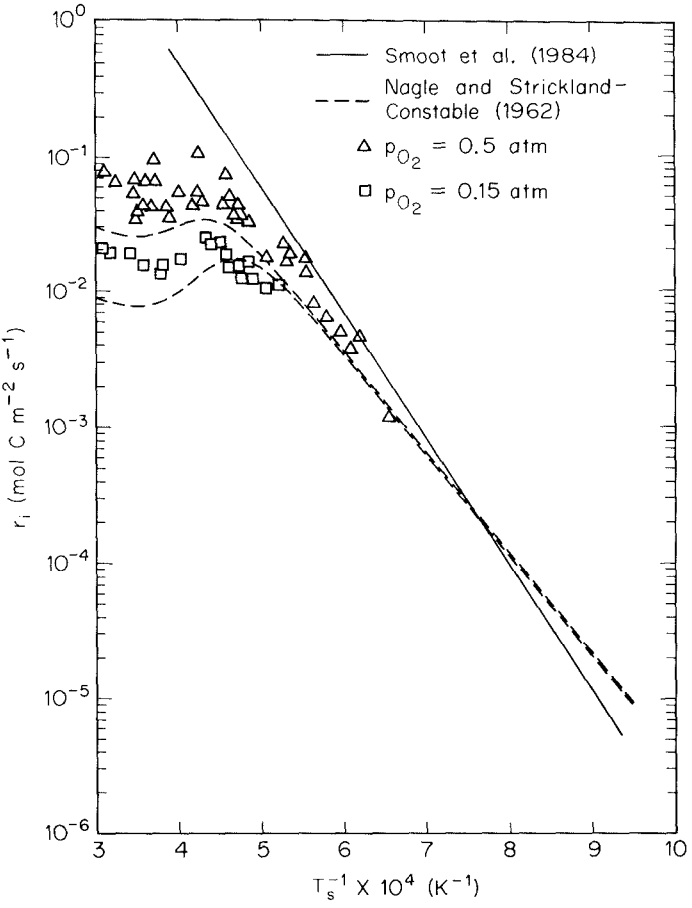

Figure 2.28 Intrinsic rate of char consumption.

this rate is well correlated with the oxidation rate for pyrolytic graphite, as illustrated in Figure 2.28. Nagle and Strickland-Constable (1962) developed a semiempirical rate expression that correlates the rate of oxidation of pyrolytic graphite for oxygen partial pressures of $10^{-5} < p_{O_2} < 1$ atm, and temperatures from 1100 to 2500 K. This rate is based on the existence of two types of sites on the carbon surface. The rate of reaction at the more reactive type *A* sites is governed by the fraction of sites not covered by surface oxides, so the reaction order varies between 0 and 1. Desorption from the less reactive type *B* sites is rapid, so the rate of reaction is first order in the oxygen concentration. Thermal rearrangement of type *A* sites into type *B* is allowed. A steady-state analysis of this mechanism yields

$$\frac{r_i}{12} = \frac{k_A p_{O_2}}{1 + k_z p_{O_2}} + k_B p_{O_2}(1 - \chi) \quad \text{mol C m}^{-2}\,\text{s}^{-1} \tag{2.156}$$

TABLE 2.11 RATE CONSTANTS FOR THE NAGLE AND STRICKLAND-CONSTABLE MODEL

$k_A = 200 \exp(-15{,}100/T)$	kg m^{-2} s^{-1} atm^{-1}
$k_B = 4.45 \times 10^{-2} \exp(-7640/T)$	kg m^{-2} s^{-1} atm^{-1}
$k_T = 1.51 \times 10^{4} \exp(-48{,}800/T)$	kg m^{-2} s^{-1}
$k_z = 21.3 \exp(2060/T)$	atm^{-1}

where χ, the fraction of the surface covered by type A sites, is

$$\chi = \left(1 + \frac{k_T}{k_B p_{O_2}}\right)^{-1}$$

The empirically determined rate constants for this model are given in Table 2.11.

According to this mechanism, the reaction is first order at low oxygen partial pressures but approaches zero order at higher p_{O_2}. At low temperatures and at fixed oxygen partial pressure, the rate increases with temperature with an activation energy corresponding to $E/R = 17{,}160$ K. Above a certain temperature, the rate begins to decrease due to the formation of unreactive type B sites by thermal rearrangement. At very high temperatures, the surface is entirely covered with type B sites and the rate becomes first order in p_{O_2}.

From the close correspondence of the char oxidation kinetics and the Nagle and Strickland-Constable rate for pyrolytic graphite, one may surmise that after processing at high temperature, carbons from a variety of sources may exhibit similar kinetics for the reaction of O_2 and, very likely, for other oxidants. Indeed, data for carbon black, soot, and some petroleum cokes are also in reasonable agreement with those from coal chars.

The model we have used to describe the porous structure is simplistic. The pores in char are not uniform in size, nor are they cylindrical in shape. Furthermore, as the char burns, the pores change shape and, in the regions near the char surface, will enlarge significantly. At high temperatures, where the surface reaction rates are high and oxygen is consumed quickly as it diffuses into the char pores, the pore mouths will enlarge until neighboring pores merge while the interior pores remain unchanged. More detailed models of the porous structure have been developed to take some of these variations into account (Gavalas, 1981; Simons, 1979, 1980). These models require more data on the pore size distribution than is commonly available at present, but may ultimately eliminate much of the remaining uncertainty in char oxidation rates.

PROBLEMS

2.1. Methanol (CH_3OH) is burned in dry air at an equivalence ratio of 0.75.

(a) Determine the fuel/air mass ratio.

(b) Determine the composition of the combustion products.

2.2. A high-volatile bituminous coal has the following characteristics:

Proximate analysis	
Fixed carbon	54.3%
Volatile matter	32.6%
Moisture	1.4%
Ash	11.7%
Ultimate analysis	
C	74.4%
H	5.1%
N	1.4%
O	6.7%
S	0.7%
Heating value	30.7×10^6 J kg^{-1}

It is burned in air at an equivalence ratio of 0.85. 500×10^6 W of electric power is produced with an overall process efficiency (based on the input heating value of the fuel) of 37%.

(a) Determine the fuel and air feed rates in kg s^{-1}.

(b) Determine the product gas composition.

(c) Sulfur dioxide is removed from the flue gases with a mean efficiency of 80% and the average output of the plant is 75% of its rated capacity. What is the SO_2 emission rate in metric tonnes (10^3 kg) per year?

2.3. A liquid fuel has the composition:

C	86.5%
H	13.0%
O	0.2%
S	0.3%

Its higher heating value is HHV = 45×10^6 J kg^{-1}. Determine an effective chemical formula and enthalpy of formation for this fuel.

2.4. Methane is burned in air at $\phi = 1$. Using the thermodynamic data of Table 2.5 and assuming complete combustion, compute the adiabatic flame temperature. The initial temperatures of the fuel and air are both 298 K.

2.5. Methanol shows promise as an alternate fuel that could reduce nitrogen oxide emissions. The reduction is attributed to lower flame temperatures. Compare the adiabatic flame temperature for combustion of pure methanol at $\phi = 1$ with that of methane (Problem 2.4). Initial fuel and air temperatures are 298 K. The enthalpy of formation of liquid methanol is Δh_f° (298 K) = $-239{,}000$ J mol^{-1}.

2.6. The bituminous coal of Problem 2.2 is burned in air that has been heated to 590 K. To estimate the maximum temperature in combustion, compute the adiabatic flame temperature for stoichiometric combustion assuming complete combustion. The specific heats of the coal carbon and ash may be taken as $\bar{c}_{pc} = 1810$ and $\bar{c}_{pa} = 1100$ J kg^{-1} K^{-1}, respectively. The ash melts at 1500 K with a latent heat of melting of $\Delta \bar{h}_m = 140$ J kg^{-1}

2.7. Kerosene (88% C, 12% H) is burned in air at an equivalence ratio of 0.8. Determine the equilibrium mole fractions of carbon monoxide and nitric oxide at $T = 2000$ K and $p = 1$ atm.

2.8. Graphite (C) is burned in dry air at $\phi = 2$ and $p = 1$ atm. Determine the equilibrium composition (mole fractions of CO, CO_2, O_2, and amount of solid carbon) of the combustion products at $T = 2500$ K.

2.9. A fuel oil containing 87% C and 13% H has a specific gravity of 0.825 and a higher heating value of 3.82×10^{10} J m^{-3}. It is injected into a combustor at 298 K and burned at atmospheric pressure in stoichiometric air at 298 K. Determine the adiabatic flame temperature and the equilibrium mole fractions of CO, CO_2, H_2, H_2O, O_2, and N_2.

2.10. For Problem 2.9, determine the equilibrium mole fractions of NO, OH, H, and O. How much is the flame temperature reduced in producing these species?

2.11. Carbon monoxide is oxidized by the following reactions:

$$\mathrm{CO + OH} \overset{1}{\rightleftharpoons} \mathrm{CO_2 + H}$$

$$\mathrm{CO + O_2} \overset{2}{\rightleftharpoons} \mathrm{CO_2 + O}$$

$$\mathrm{CO + O + M} \overset{3}{\rightleftharpoons} \mathrm{CO_2 + M}$$

$$\mathrm{CO + HO_2} \overset{4}{\rightleftharpoons} \mathrm{CO_2 + OH}$$

Rate coefficients for these reactions are given in Table 2.6.

(a) Write the full rate equation for carbon monoxide consumption.

(b) Assuming chemical equilibrium for the combustion of methane at atmospheric pressure and $\phi = 0.85$, compare the effectiveness of these reactions in terms of characteristic times for CO destruction

$$\tau_i = \frac{[\mathrm{CO}]_e}{R^e_{+i}}$$

where R^e_{+i} is the rate of reaction in the forward direction only based on equilibrium concentrations of all species. Plot the τ_is from $T = 1200$ K to $T = 2000$ K.

(c) Considering only the dominant reaction and assuming equilibrium for the minor species, derive a global rate expression for CO oxidation and CO_2 reduction in terms of CO, CO_2, O_2, and H_2O concentrations and temperature.

(d) Compare your oxidation rate with that obtained by Dryer and Glassman (1973), (2.53). Plot the two rates as a function of temperature.

2.12. An industrial process releases 500 ppm of ethane into an atmospheric pressure gas stream containing 2% oxygen at $T = 1000$ K. Use the single-step global combustion model for ethane to estimate how long the gases must be maintained at this temperature to reduce the ethane concentration below 50 ppm.

2.13. A combustor burning the fuel oil of Example 2.3 at $\phi = 1$ contains 1.5% O_2 in the combustion products. Using the data in Figure 2.6, estimate the CO level in the combustion products assuming local equilibrium.

2.14. Natural gas (assumed to be methane) is burned in atmospheric pressure air ($T_f = T_a = 300$ K) at an equivalence ratio of 0.9. For a characteristic mixing time of $\tau_m = 0.01$ s, and assuming that $B = 1$ in

$$\tau_m^{-1} = B\left(\frac{\epsilon}{l^2}\right)^{1/3}$$

compute and plot as a function of burner diameter, d, the ratio of the rate of kinetic energy dissipation in turbulence to the heat released by combustion. Assume that intense recirculation limits the volume in which the kinetic energy is dissipated to $2d^3$ and that the mean gas temperature in this volume is 2000 K. What is a reasonable maximum burner size? How many burners would be required to generate 100 MW (100×10^6 J s^{-1}) of electric power at an overall process efficiency of 40%? If the maximum burner gas velocity is limited to 30 m s^{-1}, what is the maximum burner diameter and how many burners will be needed? Suppose that we allow the mixing time to be 0.05 s. How would this influence the results?

2.15. Carbon ($\rho = 2000$ kg m^{-3}) is injected into atmospheric pressure air in a furnace that maintains both gas and walls at the same temperature. Compute and plot the particle temperature and time for complete combustion of a 50-μm diameter char particle as a function of furnace temperature over the range from 1300 to 2000 K, assuming diffusion-limited combustion. The thermodynamic properties of the carbon may be taken to be those of pure graphite. Use the following physical properties:

$$D = 1.5 \times 10^{-9} T^{1.68} \text{ m}^2 \text{ s}^{-1}$$
$$k = 3.4 \times 10^{-4} T^{0.77} \text{ W m}^{-1} \text{ K}^{-1}$$
$$\epsilon = 1$$

2.16. For the system of Problem 2.15 and a fixed wall and gas temperature of $T = 1700$ K, compute and plot the particle temperature and characteristic time for combustion of a 50-μm diameter particle as the function of the oxygen content of an O_2–N_2 mixture over the range of oxygen contents from 1 to 20.9%, assuming

(a) diffusion limited combustion.

(b) combustion according to the global rate expression of Smith (1982) for anthracite (Table 2.10).

What are the implications of these results for char burnout in pulverized coal combustion?

2.17. For the conditions of Problem 2.15 and combustion in air at 1700 K, compute and plot the particle temperature and characteristic time as a function of the char particle size over the range 1 to 200 μm.

2.18. A Millmerran subbituminous coal has the following composition:

C	72.2%
H	5.8%
N	1.4%
O	10.0%
S	1.2%
Ash	9.4%
Volatile matter	41.9%

Fixed carbon	44.5%
Moisture	4.2%

$$\rho_{\text{ash-free coal}} = 1300 \text{ kg m}^{-3}$$

$$\rho_{\text{ash}} = 2300 \text{ kg m}^{-3}$$

A 150-μm-diameter particle is injected into atmospheric pressure air in a furnace that maintains both the gas and wall temperatures at 1700 K.

(a) Assuming that the particle is instantaneously heated to the gas temperature and maintained at that temperature throughout the devolatilization process, determine the amount of volatile matter released and the quantity of char remaining. Assuming that the physical dimension of the particle has not changed, what is the final density of the particle?

(b) Oxidation begins immediately following devolatilization. Assuming quasi-steady combustion and that the particle density remains constant, and using the apparent reaction kinetics of Table 2.10, calculate the particle temperature and size throughout the combustion of the particle. Assume that the enthalpy of formation of the char is the same as that of graphite. How long does it take for the particle to burn out?

2.19. A fuel oil with composition

C	86%
H	14%

is burned in dry air. Analysis of the combustion products indicates, on a dry basis (after condensing and removing all water),

O_2	1.5%
CO	600 ppm

What is the equivalence ratio of combustion?

REFERENCES

BIRD, R. B., STEWART, W. E., and LIGHTFOOT, E. N. *Transport Phenomena*, Wiley, New York (1960).

BROWN, G. L., and ROSHKO, A. "On Density Effects and Large Structure in Turbulent Mixing Layers," *J. Fluid Mech.*, *64*, 775–816 (1974).

BURKE, S. P., and SCHUMANN, T. E. W. "Diffusion Flames," *Ind. Eng. Chem.*, *20*, 998–1004 (1928).

CHOMIAK, J. "A Possible Propagation Mechanism of Turbulent Flames at High Reynolds Numbers," *Combust. Flame*, *15*, 319–321 (1970).

CHOMIAK, J. "Application of Chemiluminescence Measurement to the Study of Turbulent Flame Structure," *Combust. Flame*, *18*, 429–433 (1972).

CORRSIN, S. "Simple Theory of an Idealized Turbulent Mixer," *AIChE J.*, *3*, 329–330 (1957).

DAMKOHLER, G. "The Effect of Turbulence on the Flame Velocities in Gas Mixtures," NACA TM 1112, *Der Einfluss der Turbolenz auf die Flammengeschwindigkeit und angewandte Gasgemischen*, *Z. Elektrochem. Angew. Phys. Chem.*, *46*, 601–626 (1940).

DENBIGH, K. *The Principles of Chemical Equilibrium*, Cambridge University Press, London (1971).

DRYER, F. L., and GLASSMAN, I. "High Temperature Oxidation of CO and CH_4," in *Fourteenth Symposium (International) on Combustion*, The Combustion Institute, Pittsburgh, PA, 987–1003 (1973).

EDELMAN, R. B., and FORTUNE, O. F. "A Quasi-global Chemical Kinetic Model for the Finite Rate Combustion of Hydrocarbon Fuels with Application to Turbulent Burning and Mixing in Hypersonic Engines and Nozzles," AIAA Paper No. 69–86, Amer. Inst. of Aero. Astro. (1969).

GAVALAS, G. R. "Analysis of Char Combustion Including the Effect of Pore Enlargement," *Combust. Sci. Technol.*, *24*, 197–210 (1981).

GAVALAS, G. R. *Coal Pyrolysis*, Elsevier, New York (1982).

GLASSMAN, I. *Combustion*, Academic Press, New York (1977).

GORDON, S., and MCBRIDE, B. J. "Computer Program for Calculation of Complex Chemical Equilibrium Compositions, Rocket Performance, Incident and Reflected Shocks, and Chapman-Jonquet Detonations," NASA Report No. SP-273 (1971).

HANSON, S. P., BEER, J. M., and SAROFIM, A. F. "Non-equilibrium Effects in the Vaporization of Multicomponent Fuel Droplets," in *Nineteenth Symposium (International) on Combustion*, The Combustion Institute, Pittsburgh, PA, 1029–1036 (1982).

HAUTMAN, D. J., DRYER, F. L., SCHUG, K. P., and GLASSMAN, I. "A Multiple-Step Overall Kinetic Mechanism for the Oxidation of Hydrocarbons," *Combust. Sci. Technol.*, *25*, 219–235 (1981).

HAWTHORNE, W. R., WEDDELL, D. S., and HOTTEL, H. C. "Mixing and Combustion in Turbulent Gas Flames," in *Third Symposium (International) on Combustion*, Combustion Institute, Pittsburgh, PA, 266–288 (1951).

HILL, C. G., JR. *An Introduction to Chemical Engineering Kinetics and Reactor Design*, Wiley, New York (1977).

KOBAYASHI, H., HOWARD, J. B., and SAROFIM, A. F. "Coal Devolatilization at High Temperatures," in *Sixteenth Symposium (International) on Combustion*, The Combustion Institute, Pittsburgh, PA, 411–425 (1977).

KOMIYAMA, K., FLAGAN, R. C., and HEYWOOD, J. B. "The Influence of Droplet Evaporation on Fuel-Air Mixing Rate in a Burner," in *Sixteenth Symposium (International) on Combustion*, The Combustion Institute, Pittsburgh, PA, 549–560 (1977).

LABOWSKY, M., and ROSNER, D. E. "Group Combustion of Droplets in Fuel Clouds: I. Quasi-steady Predictions," in *Advances in Chemistry Series No. 166: Evaporation-Combustion of Fuels*, J. T. Zung, Ed., American Chemical Society, Washington, DC, 64–79 (1978).

LAW, C. K., and LAW, H. K. "A d^2-Law for Multicomponent Droplet Vaporization and Combustion," *AIAA J.*, *20*, 522–527 (1981).

MILLER, J. A., MITCHELL, R. E., SMOOKE, M. D., and KEE, R. J. "Toward a Comprehensive Chemical Kinetic Mechanism for the Oxidation of Acetylene: Comparison of Model Predictions with Results from Flame and Shock Tube Experiments," in *Nineteenth Symposium (International) on Combustion*, The Combustion Institute, Pittsburgh, PA, 181–196 (1982).

MITCHELL, R. E., SAROFIM, A. F., and CLOMBERG, L. A. "Partial Equilibrium in the Reaction Zone of Methane-Air Diffusion Flames," *Combust. Flame*, *37*, 201–206 (1980).

MULCAHY, M. F. R., and SMITH, W. "Kinetics of Combustion of Pulverized Fuel: A Review of Theory and Experiment," *Rev. Pure Appl. Chem.*, *18*, 81–108 (1969).

NAGLE, J., and STRICKLAND-CONSTABLE, R. F. "Oxidation of Carbon between 1000–2000°C," in *Proceedings of the Fifth Carbon Conference*, *1*, 154–164 (1962).

POMPEI, F., and HEYWOOD, J. B. "The Role of Mixing in Burner-Generated Carbon Monoxide and Nitric Oxide," *Combust. Flame*, *19*, 407–418 (1972).

PRANDTL, L. *Essentials of Fluid Dynamics with Applications to Hydraulics, Aeronautics, Meteorology and Other Subjects*, Hafner (1952).

RANZ, W. E., and MARSHALL, W. R., JR. "Evaporation from Drops," *Chem. Eng. Progr.*, *48*, 141–146 and 173–180 (1952).

REYNOLDS, W. C. "STANJAN-Interactive Computer Programs for Chemical Equilibrium Analysis," Dept. of Mechanical Engineering, Stanford Univ. (1981).

SIMONS, G. A. "Char Gasification: Part I. Transport Model," *Comb. Sci. Tech.*, *20*, 107–116 (1979a).

SIMONS, G. A. "Char Gasification: Part II. Oxidation Results," *Comb. Sci. Tech.*, *20*, 117–124 (1979b).

SIMONS, G. A. "The Pore Tree Structure of Porous Char," in *Nineteenth Symposium (International) on Combustion*, The Combustion Institute, Pittsburgh, PA, 1067–1076 (1982).

SMITH, I. W. "The Combustion Rates of Coal Chars: A Review," in *Nineteenth Symposium (International) on Combustion*, The Combustion Institute, Pittsburgh, PA, 1045–1065 (1982).

SMOOT, L. D., HEDMAN, P. O., and SMITH, P. J. "Pulverized-Coal Combustion Research at Brigham Young University," *Prog. Energy Combust. Sci.*, *10*, 359–441 (1984).

STICKLER, D. B., BECKER, F. E., and UBHAYAKAR, S. K. "Combustion of Pulverized Coal at High Temperature," AIAA Paper No. 79-0298, Amer. Inst. of Aero. Astro. (1979).

STULL, D. R., and PROPHET, H. *JANAF Thermochemical Tables*, 2nd Ed., National Bureau of Standards NSRDS-NBS37 (1971).

TABACZYNSKI, R. J., FERGUSON, C. R., and RADHAKRISHNAN, K. "A Turbulent Entrainment Model for Spark-Ignition Engine Combustion," SAE Paper No. 770647, Society of Automotive Engineers, Warrendale, PA (1977).

TENNEKES, H. "Simple Model for the Small-Scale Structure of Turbulence," *Phys. Fluids*, *11*, 669–671 (1968).

VANDOOREN, J., and VAN TIGGELEN, P. J. "Experimental Investigation of Methanol Oxidation in Flames: Mechanisms and Rate Constants of Elementary Steps," in *Eighteenth Symposium (International) on Combustion*, The Combustion Institute, Pittsburgh, PA, 473–483 (1981).

VENKAT, C., BREZINSKY, K., and GLASSMAN, I. "High Temperature Oxidation of Aromatic Hydrocarbons," in *Nineteenth Symposium (International) on Combustion*, The Combustion Institute, Pittsburgh, PA, 143–152 (1982).

WARNATZ, J. "Rate Coefficients in the C/H/O System," in *Combustion Chemistry*, W. C. Gardiner, Jr., Ed., Springer-Verlag, New York, 197–360 (1984).

WESTBROOK, C. K. "Chemical Kinetics of Hydrocarbon Oxidation in Gaseous Detonations," *Combust. Flame*, *46*, 191–210 (1982).

WESTBROOK, C. K., and DRYER, F. L. "Chemical Kinetics of Modeling of Combustion Pro-

cesses," in *Eighteenth Symposium (International) on Combustion*, The Combustion Institute, Pittsburgh, PA, 749–767 (1981a).

WESTBROOK, C. K., and DRYER, F. L. "Simplified Reaction Mechanisms for the Oxidation of Hydrocarbon Fuels in Flames," *Combust. Sci. Technol.*, *27*, 31–43 (1981b).

WESTBROOK, C. K., and DRYER, F. L. "Chemical Kinetic Modeling of Hydrocarbon Combustion," *Prog. Energy Combust. Sci.*, *10*, 1–57 (1984).

WHITE, W. B., JOHNSON, W. M., and DANTZIG, G. B. "Chemical Equilibrium in Complex Mixtures," *J. Chem. Phys.*, *28*, 751–755 (1958).